

R9402070

**U.S. DEPARTMENT
OF COMMERCE**

NISTIR 5410

**TECHNOLOGY
ADMINISTRATION**

National Institute
of Standards and
Technology

**An Update
Guide for
HAZARD I
Version 1.2**

Fire Research Information Services
National Institute of Standards
and Technology
Bldg. 224, Rm. A252
Gaithersburg, MD 20899

Richard D. Peacock
Walter W. Jones
Glenn P. Forney
Rebecca W. Portier
Paul A. Reneke
Richard W. Bukowski
John H. Klote

May 1994

NIST

NISTIR 5410

An Update Guide for HAZARD I Version 1.2

Richard D. Peacock
Walter W. Jones
Glenn P. Forney
Rebecca W. Portier
Paul A. Reneke
Richard W. Bukowski
John H. Klote

Building and Fire Research Laboratory
Gaithersburg, MD 20899

May 1994

U.S. Department of Commerce
Ronald H. Brown, *Secretary*
Technology Administration
Mary L. Good, *Under Secretary for Technology*
National Institute of Standards and Technology
Arati Prabhakar, *Director*



Bibliographic Information

Abstract

A method for quantifying the hazards to occupants of buildings from fires, and the relative contribution of specific products (e.g., furniture, wire insulation) to those hazards is presented. This method, called HAZARD I, combines expert judgment and calculations to estimate the consequences of a specified fire. These procedures involve four steps: 1) defining the context, 2) defining the scenario, 3) calculating the hazard, and 4) evaluating the consequences. Steps 1, 2, and 4 are largely judgmental and depend on the expertise of the user. Step 3, which involves use of the extensive computer software, requires considerable expertise in fire safety practice. The heart of HAZARD I is a sequence of computer software procedures which calculate the development of hazardous conditions over time, calculate the time needed by building occupants to escape under those conditions, and estimate the resulting loss of life based on assumed occupant behavior and tenability criteria.

This report describes the theory and use of the latest update to the software implementing the hazard methodology. It is intended to supplement an existing Technical Reference Guide and Software User's Guide for Version 1.1 of the methodology, NIST Handbook 146. As such, it does not replace the existing documents.

Keywords

Computer models; computer programs; evacuation; fire models; fire research; hazard assessment; human behavior; toxicity

Ordering

Copies of this document are available from the National Technical Information Services, 5285 Port Royal Road, Springfield, Virginia 22161, at (800) 553-6847 or (703) 487-4650.

Contents

	Page
Nomenclature	vii
1 Introduction and Overview	1
1.1 New in HAZARD I, Version 1.2	2
1.2 The Fire Model	6
1.2.1 Fires	8
1.2.2 Plumes and Layers	8
1.2.3 Vent Flow	9
1.2.4 Heat Transfer	10
1.2.5 Species Concentration and Deposition	10
1.2.6 Assumptions and Limitations	11
1.3 Egress and Tenability Models	14
1.4 The "Residential-type Buildings" Limitation	15
2 Predictive Equations Used by the CFAST Model	17
2.1 Derivation of Equations for a Two-Layer Model	18
2.2 Equation Set Used in CFAST	22
3 Source Terms for the CFAST Model	23
3.1 The Fire	23
3.1.1 Specified Fire (Fire Types 1 and 2)	23
3.1.2 Combustion Chemistry (Fire Type 2)	24
3.2 Plumes	28
3.3 Vent Flows	30
3.3.1 Horizontal Flow Through Vertical Vents	30
3.3.2 Vertical Flow Through Horizontal Vents	33
3.3.3 Forced Flow	34
3.4 Heat Transfer	37
3.4.1 Radiation	37
3.4.2 Convection	40
3.4.3 Conduction	41
3.4.4 Ceiling Jet	43
3.5 Species Concentration and Deposition	45
3.5.1 Species Transport	45
3.5.2 HCl Deposition	45
4 Verification of the Model	47
4.1 Available Experimental Data	47
4.2 Previous Comparisons with Experimental Data	48
4.3 Model Parameters Selected for Comparison	49
4.4 Experimental Data Selected for Comparison	50
4.5 Discussion	52
4.5.1 Layer Temperature and Interface Position	52

4.5.2 Gas Species	54
4.5.3 Heat Release and Fire Pyrolysis Rate	57
4.5.4 Pressure	60
4.5.5 Flow Through Openings	62
5 Using CEdit	67
5.1 Initialization Screen	69
5.2 Overview Screen	70
5.3 Ambient Conditions Screen	71
5.4 Geometry Screen	72
5.5 Vents(doors,...) Screen	73
5.6 Vents(ceiling,...) Screen	75
5.7 Fans, Ducts,... Screen	76
5.8 Thermal Properties Screen	79
5.9 Fire Specification Screen	81
5.10 Objects Screen	83
5.11 Files,... Screen	86
5.12 Version and Settings Screen	87
5.13 Quitting CEdit	88
6 Using CFAST	91
6.1 Default Text Output	92
6.2 Reporting Options, /R:WINFST	92
6.2.1 Output for Option /R:I	93
Horizontal Natural Ventilation	94
Vertical Natural Ventilation	94
Mechanical Flow Connections	94
6.2.2 Output for Option /R:N	95
6.2.3 Output for Option /R:S	96
6.2.4 Output for Option /R:F	96
6.2.5 Output for Option /R:W	96
6.2.6 Output for Option /R:T	97
6.2.7 Sample Output	97
6.3 Default Graphical Output	104
7 Using CPlot	105
7.1 Entering Data Into CPlot	105
7.2 Generating Tables and Graphs With CPlot	108
7.3 Saving Data With CPlot	110
7.4 Changing the Default Parameters in CPlot	110
7.5 Getting Online Help in CPlot	111
7.6 Exiting CPlot	112
8 Using Exitt, Tenab, and Survival	113
9 Utility Programs	115
10 Conclusions and Future Plans	117

10.1 New phenomena	118
10.2 Limitations	119
10.3 New Technology	119
10.4 Capabilities and Processing Power	120
10.5 Summary	121
11 References	123
Appendix A: Fan-Duct Systems	129
A.1 Introduction	129
A.2 System Types	129
A.3 Network Concept of Fan-Duct System Simulation	129
A.4 Fans	130
A.4.1 Fan Performance	130
A.4.2 Computer Approximation of Fan Performance	131
A.5 Effective Resistances	132
A.6 Resistance of Ducts	133
A.7 Local Loss Resistances	134
A.8 Resistance of Junctions	135
A.9 Example	135
A.10 References	136
A.11 Nomenclature	136
Appendix B: Thermal Properties	147
Appendix C: Objects Database	149
Appendix D: Graphics Displays	151

Nomenclature

A_d	duct surface area (m^2)
A_o	area of the inlet, outlet, duct, contraction, or expansion joint, coil, damper, bend, filter, and so on in a mechanical ventilation system. (m^2)
A_{room}	floor area of a room (m^2)
A_{slab}	cross-sectional area for horizontal flow (m^2)
A_v	area of ceiling or floor vent (m^2)
A_w	wall surface area (m^2)
b_i	coefficients for adsorption and desorption of HCl
C	flow coefficient for horizontal flow of gas through a vertical vent
C_{LOL}	Lower oxygen limit coefficient, the fractional burning rate constrained by available oxygen, eq (41)
C_o	characteristic flow coefficient
C_w	wind coefficient – dot product of the wind vector and vent direction
CO/CO_2	ratio of the mass of carbon monoxide to the mass of carbon dioxide in the pyrolysis of the fuel
CO_2/C	ratio of the mass of carbon dioxide to the mass of carbon in the pyrolysis of the fuel
c_k	heat sources for the k'th wall segment (W)
c_p	heat capacity of air at constant pressure (J/kg K)
c_v	heat capacity of air at constant volume (J/kg K)
D	effective diameter of ceiling or floor vent (m)
D_e	effective duct diameter (m)
d_{HCl}	rate of deposition of HCl onto a wall surface, eq. (86) (kg/s)
E_i	internal energy in layer i (W)
F	friction factor
F_{k-j}	configuration factor
g	gravitational constant (m^3/s)
G	conductance
Gr	Grashof number
H_c	heat of combustion of the fuel (J/kg)
h_c	convective heat transfer coefficient ($J/m^2 K$)
h_i	rate of addition of enthalpy into layer i (W)
h_l	convective heat transfer coefficient in ceiling boundary layer ($J/m^2 K$)
\bar{h}	characteristic convective heat transfer coefficient
H	height of the ceiling above a fire source (m)
H/C	ratio of the mass of hydrogen to the mass of carbon in the pyrolysis of the fuel
H_2O/H	ratio of the mass of water to the mass of hydrogen in the pyrolysis of the fuel
HCl/C	ratio of the mass of hydrogen chloride to the mass of carbon in the pyrolysis of the fuel
HCl/f	ratio of the mass of hydrogen chloride to the total mass of the fuel
HCN/C	ratio of the mass of hydrogen cyanide to the mass of carbon in the pyrolysis of the fuel
HCN/f	ratio of the mass of hydrogen cyanide to the total mass of the fuel
k	mass transfer coefficients for HCl deposition
l	characteristic length for convective heat transfer (m)
m_i	total mass in layer i (kg)
$m_{i,j}$	mass flow from node i to node j in a mechanical ventilation system (kg/s)
\dot{m}_b	burning rate of the fuel (perhaps constrained by available oxygen) (kg/s)

\dot{m}_c	production rate of carbon during combustion (kg/s)
\dot{m}_d	mass flow in duct (kg/s)
\dot{m}_e	rate of entrainment of air into the fire plume (kg/s)
\dot{m}_f	pyrolysis rate of the fuel (before being constrained by available oxygen) (kg/s)
\dot{m}_i	rate of addition of mass into layer i (kg/s)
O/C	ratio of the mass of oxygen to the mass of carbon in the pyrolysis of the fuel
P	pressure (Pa)
P_{ref}	reference pressure (Pa)
Pr	Prandtl number
\dot{Q}_c	total convective heat transfer (W)
\dot{Q}_{eq}	dimensionless plume strength at layer interface
\dot{Q}_f	total heat release rate of the fire (W)
\dot{Q}_H	dimensionless plume strength at the ceiling
\dot{Q}_r	total radiative heat transfer (W)
r	radial distance from point source fire (m)
R	universal gas constant (J/kg K)
R_e	Reynolds number
S	vent shape factor for vertical flow
S/C	ratio of the mass of soot to the mass of carbon in the pyrolysis of the fuel
t	time (s)
T_{amb}	ambient temperature (K)
T_d	duct temperature (K)
T_e	temperature of gas entrainment into the fire plume (K)
T_g	gas temperature (K)
T_i	temperature of layer i (K)
T_{in}	duct inlet temperature (K)
T_k	temperature of the k'th wall segment (K)
T_{out}	duct outlet temperature (K)
T_p	temperature of the plume as it intersects the upper layer (K)
T_w	wall temperature (K)
v	gas velocity (m/s)
V_d	duct volume (m ³)
V_i	volume of layer i (m ³)
Y	mass fraction of a species in a layer
Y_{LOL}	lower oxygen limit for oxygen constrained burning, expressed as a mass fraction
z	height over which entrainment takes place (m)
Z	height (m)
α	absorption coefficient of the gas (m ⁻¹)
ΔP	pressure offset from reference pressure, $P - P_{ref}$ (Pa)
γ	ratio of c_p/c_v
ϵ_k	emissivity of the k'th wall segment
κ	thermal conductivity (J/m s K)
ν	kinematic viscosity (m ² /s)
ρ_d	density of gas in a duct (kg/m ³)
ρ_i	density of gas in layer i (kg/m ³)
σ	Stefan-Boltzman constant (5.67×10^{-8} W/m ² K ⁴)
τ	transmissivity factor

χ_c fraction of the heat release rate of the fire which goes into convection
 χ_r fraction of the heat release rate of the fire which goes into radiation

An Update Guide for HAZARD I, Version 1.2

Richard D. Peacock, Walter W. Jones, Glenn P. Forney, Rebecca W. Portier,
Paul A. Reneke, Richard W. Bukowski, and John H. Klote

Building and Fire Research Laboratory
National Institute of Standards and Technology

Abstract

A method for quantifying the hazards to occupants of buildings from fires, and the relative contribution of specific products (e.g., furniture, wire insulation) to those hazards is presented. This method, called HAZARD I, combines expert judgment and calculations to estimate the consequences of a specified fire. These procedures involve four steps: 1) defining the context, 2) defining the scenario, 3) calculating the hazard, and 4) evaluating the consequences. Steps 1, 2, and 4 are largely judgmental and depend on the expertise of the user. Step 3, which involves use of the extensive computer software, requires considerable expertise in fire safety practice. The heart of HAZARD I is a sequence of computer software procedures which calculate the development of hazardous conditions over time, calculate the time needed by building occupants to escape under those conditions, and estimate the resulting loss of life based on assumed occupant behavior and tenability criteria.

This report describes the theory and use of the latest update to the software implementing the hazard methodology. It is intended to supplement an existing Technical Reference Guide and Software User's Guide for Version 1.1 of the methodology, NIST Handbook 146. As such, it does not replace the existing documents.

1 Introduction and Overview

In June 1989, the Center for Fire Research at the National Institute of Standards and Technology released a method for quantifying the hazards to occupants of buildings from fires, and the relative contribution of specific products (e.g., furniture, wire insulation) to those hazards [1], [2]. The culmination of six years of development this method, called HAZARD I, was the first such comprehensive application of fire modeling in the world. It combined expert judgment and calculations to estimate the consequences of a specified fire. These procedures involve four steps: 1) defining the context, 2) defining the scenario, 3) calculating the hazard, and 4) evaluating the consequences. Steps 1, 2, and 4 are largely judgmental and depend on the expertise of the user. Step 3, which involves use of the extensive computer software, requires considerable expertise in fire safety practice. The heart of HAZARD I is a sequence of computer software procedures which calculate the development of hazardous conditions over time, calculate the time needed by building occupants to escape under those conditions, and estimate the resulting loss of life based on assumed occupant behavior and tenability criteria.

This report describes the theory and use of the latest update to the software implementing the hazard methodology. It is intended to supplement the existing Technical Reference Guide [3] and Software User's Guide [4] for Version 1.1 of the methodology. As such, it does not replace the existing documents.

1.1 New in HAZARD I, Version 1.2

The fire model contained in earlier versions of HAZARD I, FAST, has been replaced with the newer model CFAST. Although CFAST evolved from the FAST model, nearly all of the physics and numerics in CFAST are different from FAST. CFAST is intended to operate on many platforms, be as error free as is humanly possible, be simple to run for simple problems, yet allow complexity where needed. The code is extremely fast. It works on laptop personal computers, Unix workstations and supercomputers. It provides for extensive graphics for analysis with pre- and post-processing modules. It is extremely fast on single compartment cases, and with the data editor, there is tremendous flexibility for parameter studies, such as "what if" testing. The model is particularly well suited for doing parameter studies of changes, both subtle and large, within a single compartment. Phenomena which are now incorporated into the fire model include

- Multiple compartments (currently 15),
- Multiple fires (currently 16) - specify with "other" objects,
- Vitiated or free burn chemistry in the lower layer, the upper layer, or in the vent flow,
- Correct chemistry - consistent production and transport of species,
- Generalized species (10) transport,
- Four wall and two layer radiation to be extended for the pyrolysis model,
- Four wall conductive heat transfer through multilayered walls, ceilings and floors in each compartment,
- Convective, and radiative heat transfer applied to both inside and outside boundaries,
- Wind effects included - ASHRAE formula for wind with the NOAA integral for lapse rate of the standard atmosphere,
- Fire plume and entrainment in vent flow (doors and windows only): Fire plume is split into the entrainment in the lower layer and the upper layer,
- 3D specification of the location of the fire and non-uniform heat loss through boundaries,
- Generalized vent flow:
 - Horizontal flow (doors, windows and so on) - up to three neutral planes
 - Mixing between the upper and lower layers
 - Vertical flow (through holes in ceilings and floors),
- Separate internal and external ambient (elevation, temperature and pressure specification),
- HCL deposition, and
- Mechanical ventilation - complex building structure: 5 fans, 44 ducts, three way joints; vertical ducts interact with both layers.

There are numerous other changes to the programs in HAZARD I. The most obvious change is that we have converted most of the programs to extended memory. This has several implications for use of the package. The first is that a 386/486/P5 processor is required, and a minimum memory configuration of 4MB is needed. This has allowed us to increase the number of interior compartments to 15. There are a number of additional phenomena which have been added, based on this increased capability. We have implemented a ceiling jet algorithm which takes into account heat loss from a fire placed in an arbitrary position within a compartment. The algorithm describes the theory and implementation of the algorithm which accounts for the off-center placement of the fire and its effect on heat transfer to the room surfaces. Also, a new option has been added to the command line for ASCII type output of variables. For CFAST and ReportG, the number of variables which can be plotted is 40 and the maximum number of plot points is 100. For CPlot, the maximum number of variables which CPlot can keep is 40 and the number of points which can be plotted is 500. Vertical flow has been implemented to allow venting through a ceiling or floor vent.

A combined egress and tenability model, called SURVIVAL, is included. It is simply a combination of the existing models EXITT and TENAB. However, since tenability is judged while egress is taking place, it can have significant effects on the results of a simulation. If an occupant becomes incapacitated or dies during a simulation, their position remains fixed for the remainder of the simulation. Tenability is then judged based on the conditions in the compartment where they became incapacitated or died.

Hardware requirements: A 386 or later pc with at least 2.5 megabytes of free extended memory¹.

We now support a number of graphics displays. Changing the display adapter is done with the SETVID command, and can be done automatically by the install program.

New capability: Pressing the <f5> function key will show the current time and time step. Pressing <esc> will terminate the run.

Specific Additions to the Modeling Capability since HAZARD 1.1 (FAST)

Increase the number of rooms to 15,
Allow multiple fires, with ignition criteria for time, flux and temperature,
Four wall radiation model,
3D specification of the fire position and asymmetric heat loss based on plume position,
Distributed mechanical vents,
Vertical flow (ceiling/floor vents),
Close coupling between mechanical ventilation and normal ventilation, and
A much faster and more robust solver (about a factor of 10 faster).

Problems which have been fixed:

Over estimate lower layer entrainment: Entrainment at a vent (doors, windows, ...) into the lower layer was overestimated. We have constrained it to be in the range as predicted by Zukoski et al. in the thesis of Lim at Cal. Tech. We will explore this further.

Resizing compartments: Once two compartments are connected, it is no longer possible to change the geometry of the room so that the connecting vent would generate an impossible connection. This is not an error, but for those who assume that the data editor will automatically shut off the vents, this will appear not to be working. It is working as we intended, namely that one cannot do something which is incorrect.

Vertical flow (horizontal opening) selection rules: The selection rules in the vertical flow (horizontal vent) have been changed. Only if the incoming gas has a temperature less than the lower layer will it be deposited in that layer. The previous rule was that if the temperature of the incoming gas was lower than the upper layer, it would be deposited into the lower layer.

¹ The memory manager which CFAST uses on a PC looks first for expanded memory, then XMS memory, then unmapped EMS memory. It utilizes the first type that is available and cannot mix types. Thus, if there is expanded memory available, but not enough, the error message "insufficient memory to load EXP file" is displayed. The technique of lending (disk caches often will do this) will not work if it results in insufficient memory of a higher priority being available. The difficulty comes in that the memory extender will only grab the first available type.

Setting the height of mechanical ventilation openings: In the data editor, external nodes in the mechanical ventilation system could be set, which should not be possible. They are supposed to be tagged to the room height and vent position within the room. They are now only set as an external connection.

Reference pressure for the mechanical system: A single external pressure is used for the entire MV system. Previous versions of the model used ambient conditions from several of the compartments, which sometimes resulted in inconsistencies and difficulties in system startup.

Setting the initial values for H₂O: There was a report that the H₂O was not set correctly. It was set correctly, but we have simplified the curve used to

$$P_{S_{H_2O}} = e^{\left(23.2 - \frac{3816}{T_a - 46}\right)} \quad (1)$$

as suggested by Antoine[5]. Hydrogen chloride deposition has been turned on and has been verified with limited experimental data.

Additions and changes to the fire model:

The model now reads a file, HAZARD.TBL, which lists the breakpoint for each color change on a view or table. The values used to change the colors in the tables and views are now contained in the file HAZARD.TBL. It is read by READHZT and the colors selected from it using SELCLR. All "knots" should be in here. For example, changes for alarm systems, loudness, and similar values. The current default table is shown on the next page.

The first value indicates whether the value is increasing or decreasing. 2 is for increasing and 1 is for decreasing. The difference shows up in SELCLR which goes through the whole list for increasing values, but stops as soon as the proper interval is found. In the current instantiation, only four values are used for each variable. These correspond to the colors

Blue - no concern; Green - mental incapacitation; Yellow - physical incapacitation; Red - lethality.

These interpretations must be used loosely since there is a synergism amongst the variables, and some conditions which are interpreted as lethality do not in and of themselves cause death. Also, the state of occupants, how they are clothed and other factors influence these settings. The purpose in providing the capability to change the table is so that these values can be altered based on such considerations.

The format of the history file has been changed, together with the read/write routines, so that it is compatible across platforms. Thus, data which has been generated on a Unix platform can now be read on the PC.

The configuration files HV1.CF and CPLOT.CF have been combined. The new file format must be used. It is necessary to use `cf_set` to reset the paths if the default option is not used. For anyone with a text editor, the two lines showing the paths in the old configuration file can be inserted in place of the two blank lines in the default file.

	Type	Blue	Green	Yellow	Red
Vent	2	0.0	1.0	5.0	10.
Heat	2	0.0	100.	300.	500.
Pressure	2	0.0	100.	1000.	5000.
Wall	2	0.0	47.	66.	100.
Temperature	2	0.0	47.	66.	100.
Interface	1	1.5	1.0	0.5	0.5
N ₂	2	100.	100.	100.	100.
O ₂	1	18.	16.	14.	0.0
CO ₂	2	0.0	10000.	50000.	100000.
CO	2	0.0	1300.	2300.	4000.
HCN	2	0.0	300.	1000.	4000.
HCl	2	0.0	0.0	0.0	0.0
TUHC	2	0.0	0.0	0.0	0.0
H ₂ O	2	10000.	10000.	10000.	10000.
OD	2	0.0	0.25	0.5	1.0
CT	2	0.0	225.	450.	900.

The THERMAL.DF file has been changed. The data files which are included reflect those changes. This is an attempt to make the naming convention more rational. The old TPF file will work just fine, but prior to installation, it must be saved and copied over the distributed version if you want to continue to use the old names. The data which is now used is from Incropera and De Witt [6].

The coefficients used in the convective heat transfer have been changed. We define

$$h = kC \left(\frac{g\beta(T_s - T_g) Pr}{\alpha^2} \right)^{1/3}$$

and use the coefficients

Geometry	C
Walls	0.12
Ceilings and floors (hot surface up or cold surface down)	0.13
Ceilings and floors (cold surface up or hot surface down)	0.16

These are the accepted values from the SFPE Handbook [7].

Outstanding problems:

Other objects: The flux and temperature ignition criteria for "other objects" doesn't work. All times are currently relative to the beginning, and the flux and temperature criteria are assumed to be met initially.

Initialization of the solver: When mechanical ventilation is used, there must be at least a small opening to the outside world. This is necessary because of the way the initial solution is found. Any system without the mechanical ventilation can be closed (sealed).

Bar Graphs: There is still an inconsistency in the color value and labeling for bar graphs.

1.2 The Fire Model

Analytical models for predicting fire behavior have been evolving since the 1960's. Over the past two decades, the completeness of the models has grown. In the beginning, the focus of these efforts was to describe in mathematical language the various phenomena which were observed in fire growth and spread. These separate representations have typically described only a small part of a fire. When combined though, they can create a complex computer code intended to give an estimate of the expected course of a fire based upon given input parameters. These analytical models have progressed to the point of providing predictions of fire behavior with an accuracy suitable for most engineering applications. In a recent international survey [8], 36 actively supported models were identified. Of these, 20 predict the fire generated environment (mainly temperature) and 19 predict smoke movement in some way. Six calculate fire growth rate, nine predict fire endurance, four address detector or sprinkler response, and two calculate evacuation times. The computer models now available vary considerably in scope, complexity, and purpose. Simple "room filling" models such as the Available Safe Egress Time (ASET) model [9] run quickly on almost any computer, and provide good estimates of a few parameters of interest for a fire in a single compartment. A special purpose model can provide a single function. For example, COMPF2 [10] calculates post-flashover room temperatures and LAVENT [11] includes the interaction of ceiling jets with fusible links in a room containing ceiling vents and draft curtains. Very detailed models like the HARVARD 5 code [12] or FIRST [13] predict the burning behavior of multiple items in a room, along with the time-dependent conditions therein.

In addition to the single-room models mentioned above, there are a smaller number of multi-room models which have been developed. These include the BRI transport model [14], the HARVARD 6 code

[15] (which is a multi-room version of HARVARD 5), FAST [16], CCFM [17] and the CFAST model discussed below [18].

Although the papers are several years old, Mitler [19] and Jones [20] reviewed the underlying physics in several of the fire models in detail. The models fall into two categories: those that start with the principles of conservation of mass, momentum, and energy; the other type typically are curve fits to particular experiments or series of experiments, used in order to try and tease out the underlying relationship among some parameters. In both cases, errors arise in those instances where a mathematical short cut was taken, a simplifying assumption was made, or something important was not well enough understood to include.

Once a mathematical representation of the underlying science has been developed, the conservation equations can be re-cast into predictive equations for temperature, smoke and gas concentration, and other parameters of interest, and are coded into a computer for solution. The environment in a fire is constantly changing. Thus the equations are usually in the form of *differential equations*. A complete set of equations can compute the conditions produced by the fire at a given time in a specified volume of air. Referred to as a *control volume*, the model assumes that the predicted conditions within this volume are uniform at any time. Thus, the control volume has one temperature, smoke density, gas concentration, etc.

Different models divide the building into different numbers of control volumes depending on the desired level of detail. The most common fire model, known as a *zone model*, generally uses two control volumes to describe a room – an upper layer and a lower layer. In the room with the fire, additional control volumes for the fire plume or the ceiling jet may be included to improve the accuracy of the prediction (see Figure 1).

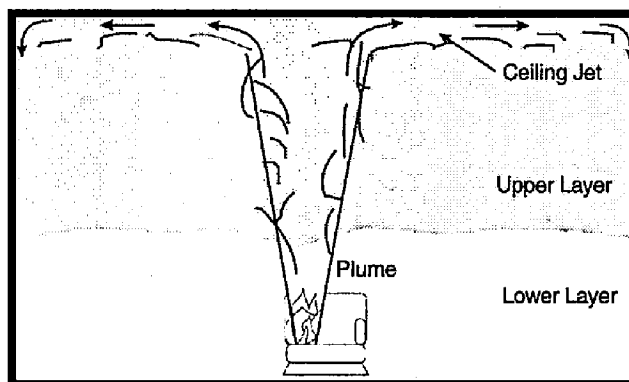


Figure 1. Zone Model Terms.

This two-layer approach has evolved from observation of such layering in real-scale fire experiments. Hot gases collect at the ceiling and fill the room from the top. While these experiments show some variation in conditions within the layer, these are small compared to the differences between the layers. Thus, the zone model can produce a fairly realistic simulation under most conditions.

Other types of models include *network models* and *field models*. The former use one element per room and are used to predict conditions in spaces far removed from the fire room, where temperatures are near ambient and layering does not occur. The field model goes to the other extreme, dividing the room into thousands or even hundreds of thousands of grid points. Such models can predict the variation in conditions within the layers, but typically require far longer run times than zone models. Thus, they are used when highly detailed calculations are essential.

CFAST is a zone model used to calculate the evolving distribution of smoke and fire gases and the temperature throughout a building during a fire. CFAST is the result of a merger of ideas that came out of the FAST [16] and the CCFM.VENTS [17] development projects. The organization of the CFAST suite of programs is thus a combination of the two models. CFAST is a member of a class of models referred to as zone or finite element models. This means that each room is divided into a small number

of volumes (called layers), each of which is assumed to be internally uniform. That is, the temperature, smoke and gas concentrations within each layer are *assumed* to be exactly the same at every point. In CFAST, each room is divided into two layers. Since these layers represent the upper and lower parts of the room, conditions within a room can only vary from floor to ceiling, and not horizontally. This assumption is based on experimental observations that in a fire, room conditions do stratify into two distinct layers. While we can measure variations in conditions within a layer, these are generally small compared to differences between the layers.

CFAST is based on solving a set of equations that predict state variables (pressure, temperature and so on) based on the enthalpy and mass flux over small increments of time. These equations are derived from the conservation equations for energy mass, and momentum, and the ideal gas law. These conservation equations are always correct, everywhere. Thus any errors which might be made by the model cannot come from these equations, but rather come from simplifying assumptions or from processes left out because we don't know how to include them. Examples of each source of error will be highlighted in the following discussion.

1.2.1 Fires

Within CFAST, a fire is a source of fuel which is released at a specified rate. This fuel is converted into enthalpy (the conversion factor is the heat of combustion) and mass (the conversion factor is the yield of a particular species) as it burns. Burning can take place in the portion of the plume in the lower layer (if any), in the upper layer, or in a door jet. For an unconstrained fire, the burning will all take place within the fire plume. For a constrained fire, burning will take place where there is sufficient oxygen. Where insufficient oxygen is entrained into the fire plume, unburned fuel will successively move into and burn in: the upper layer of the fire room, the plume in the doorway to the next room, the upper layer of the next room, the plume in the doorway to the third room, and so forth until it is consumed or gets to the outside.

This version of CFAST includes the ability to track, independently, multiple fires in one or more rooms of the building. These fires are treated as totally separate entities, i.e., with no interaction of the plumes or radiative exchange between fires in a room.

Like all current zone fire models, this version of CFAST does not include a pyrolysis model to predict fire growth. Rather pyrolysis rates for each fire modeled define the fire history. The similarity of that input to the real fire problem of interest will determine the accuracy of the resulting calculation. The user must account for any interactions between the fire and the pyrolysis rate. Planned future research should remove this limitation.

1.2.2 Plumes and Layers

Above any burning object, a plume is formed which is not considered to be a part of either layer, but which acts as a pump for enthalpy and mass from the lower layer into the upper layer (upward only). For the fire plume, CFAST does not use a point source approximation, but rather uses an empirical correlation to determine the amount of mass moved between layers by the plume.

Two sources exist for moving enthalpy and mass between the layers within and between rooms. Within the room, the fire plume provides one source. The other source of mixing between the layers occurs at vents such as doors or windows. Here, there is mixing at the boundary of the opposing flows moving into

and out of the room. The degree of mixing is based on an empirically-derived mixing relation. Both the outflow and inflow entrain air from the surrounding layers. The flow at vents is also modeled as a plume (called the door plume or jet), and uses the same equations as the fire plume, with two differences. First, an offset is calculated to account for entrainment within the doorway and second, the equations are modified to account for the rectangular geometry of vents compared to the round geometry of fire plumes. All plumes within the simulation entrain air from their surroundings according to an empirically-derived entrainment relation. Entrainment of relatively cool, non-smoke laden air adds oxygen to the plume and allows burning of the fuel. It also causes it to expand as the plume moves upward in the shape of an inverted cone. The entrainment in a vent is caused by bi-directional flow and results from a phenomenon called the Kelvin-Helmholtz instability. It is not exactly the same as a normal plume, so some error arises when this entrainment is approximated by a normal plume entrainment algorithm.

While experiments show that there is very little mixing between the layers at their interface, sources of convection such as radiators or diffusers of heating and air conditioning systems, and the downward flows of gases caused by cooling at walls, will cause such mixing. These are examples of phenomena which are not included because the theories are still under development. Also, the plumes are *assumed* not to be affected by other flows which may occur. For example, if the burning object is near the door the strong inflow of air will cause the plume axis to lean away from the door and affect entrainment of gases into the plume. Such effects are not included in the model.

As discussed above, each room is divided into two layers, the upper and lower. At the start of the simulation, the layers in each room are initialized at ambient conditions and by default, the upper layer volume set to 0.001 of the room volume (an arbitrary, small value set to avoid the potential mathematical problems associated with dividing by zero). Other values can be set. As enthalpy and mass are pumped into the upper layer by the fire plume, the upper layer expands in volume causing the lower layer to decrease in volume and the interface to move downward. If the door to the next room has a soffit, there can be no flow through the vent from the upper layer until the interface reaches the bottom of that soffit. Thus in the early stages the expanding upper layer will push down on the lower layer air and force it into the next compartment through the vent by expansion.

Once the interface reaches the soffit level, a door plume forms and flow from the fire room to the next room is initiated. As smoke flow from the fire room fills the second room, the lower layer of air in the second room is pushed down. As a result, some of this air flows into the fire room through the lower part of the connecting doorway (or vent). Thus, a vent between the fire room and connecting rooms can have simultaneous, opposing flows of air. All flows are driven by pressure differences and density differences that result from temperature differences and layer depths. Thus the key to getting the right flows is to correctly distribute the fire's mass and enthalpy between the layers.

1.2.3 Vent Flow

Flow through vents is the dominant phenomenon in a fire model because it fluctuates most rapidly and transfers the greatest amount of enthalpy on an instantaneous basis of all the source terms. Also, it is most sensitive to changes in the environment. Flow through vents comes in two varieties. The first we refer to as horizontal flow. It is the flow which is normally thought of in discussing fires. It encompasses flow through doors, windows and so on. The other is vertical flow and can occur if there is a hole in the ceiling or floor of a compartment. This latter phenomena is particularly important in two disparate situations: a ship, and the role of fire fighters doing roof venting.

Flow through normal vents is governed by the pressure difference across a vent. There are two situations which give rise to flow through vents. The first, and usually thought of in fire problems, is that of air or smoke which is driven from a compartment by buoyancy. The second type of flow is due to expansion which is particularly important when conditions in the fire environment are changing rapidly. Rather than depending entirely on density differences between the two gases, the flow is forced by volumetric expansion. The earlier version of this model did not solve this part of the problem entirely correctly. In most cases the differences are small except for rapidly changing situations. However, these small differences become very important if we wish to follow flows due to small pressure differences, such as will occur in a mechanical ventilation system. Atmospheric pressure is about 100 000 Pa, fires produce pressure changes from 1 to 1000 Pa and mechanical ventilation systems typically involve pressure differentials of about 1 to 100 Pa. In order to solve these interactions correctly, we must be able to follow pressure differences of ≈ 0.1 Pa out of 100 000 Pa for the overall problem, or 10^{-4} for adjacent compartments.

1.2.4 Heat Transfer

Heat transfer is the mechanism by which the gas layers exchange energy with their surroundings. Convective transfer occurs from the layers to the room surfaces. The enthalpy thus transferred in the simulations conducts through the wall, ceiling, or floor in the direction perpendicular to the surface only. CFAST is more advanced than most models in this field since it allows different material properties to be used for the ceiling, floor, and walls of each room (although all the walls of a room must be the same). Additionally, CFAST uniquely allows each surface to be composed of up to three distinct layers for each surface, which are treated separately in the conduction calculation. This not only produces more accurate results, but allows the user to deal naturally with the actual building construction. Material thermophysical properties are *assumed* to be constant, although we know that they actually vary with temperature. This assumption is made because data over the required temperature range is scarce even for common materials, and because the variation is relatively small for most materials. However the user should recognize that some materials may change mechanical properties with temperature. These effects are not modeled.

Radiative transfer occurs among the fire(s), gas layers and compartment surfaces (ceiling, walls and floor). This transfer is a function of the temperature differences and the emissivity of the gas layers as well as the compartment surfaces. For the fire and typical surfaces, emissivity values only vary over a small range. For the gas layers, however, the emissivity is a function of the concentration of species which are strong radiators: predominately smoke particulates, carbon dioxide, and water. Thus errors in the species concentrations can give rise to errors in the distribution of enthalpy among the layers, which results in errors in temperatures, resulting in errors in the flows. This illustrates just how tightly coupled the predictions made by CFAST can be.

1.2.5 Species Concentration and Deposition

When the layers are initialized at the start of the simulation, they are set to ambient conditions. These are the initial temperatures specified by the user, and 23 percent by mass (20.8 percent by volume) oxygen, 77 percent by mass (79 percent by volume) nitrogen, a mass concentration of water specified by the user as a relative humidity, and a zero concentration of all other species. As fuel is pyrolyzed, the various species are produced in direct relation to the mass of fuel burned (this relation is the species yield specified by the user for the fuel burning). Since oxygen is consumed rather than produced by the burning, the "yield" of oxygen is negative, and is set internally to correspond to the amount of oxygen needed to burn the fuel. Also, hydrogen cyanide and hydrogen chloride are assumed to be products of pyrolysis whereas carbon dioxide, carbon monoxide, water, and soot are products of combustion.

Each unit mass of a species produced is carried in the flow to the various rooms and accumulates in the layers. The model keeps track of the mass of each species in each layer, and knows the volume of each layer as a function of time. The mass divided by the volume is the mass concentration, which along with the molecular weight gives the concentration in volume percent or ppm as appropriate.

CFAST uses a combustion chemistry scheme different from any other model. While others compute each species concentration with an independent yield fraction, CFAST maintains a carbon-hydrogen-oxygen balance. The scheme is applied in three places. The first is burning in the portion of the plume which is in the lower layer of the room of fire origin. The second is the portion in the upper layer, also in the room of origin. The third is in the vent flow which entrains air from a lower layer into an upper layer in an adjacent compartment. This is equivalent to solving the conservation equations for each species independently.

1.2.6 Assumptions and Limitations

CFAST consists of a collection of data and computer programs which are used to *simulate* the important time-dependent phenomena involved in fires. The major functions provided include calculation of:

- the production of enthalpy and mass (smoke and gases) by one or more burning objects in one room, based on small- or large-scale measurements,
- the buoyancy-driven as well as forced transport of this energy and mass through a series of specified rooms and connections (e.g., doors, windows, cracks, ducts),
- the resulting temperatures, smoke optical densities, and gas concentrations after accounting for heat transfer to surfaces and dilution by mixing with clean air.

As can be seen from this list, fire modeling involves an interdisciplinary consideration of physics, chemistry, fluid mechanics, and heat transfer. In some areas, fundamental laws (conservation of mass, energy, and momentum) can be used, whereas in others empirical correlations or even "educated guesses" must be employed to bridge gaps in existing knowledge. The necessary approximations required by operational practicality result in the introduction of uncertainties in the results. The user should understand the inherent assumptions and limitations of the programs, and use these programs judiciously – including sensitivity analyses for the ranges of values for key parameters – in order to make estimates of these uncertainties. This section provides an overview of these assumptions and limitations.

Specified Fire Limitations: An important limitation of CFAST is the absence of a fire growth model. At the present time, it is not practical to adapt currently available fire growth models for direct inclusion in CFAST. Therefore, the system utilizes a user specified fire, expressed in terms of time specified rates of energy and mass released by the burning item(s). Such data can be obtained by measurements taken in large- and small-scale calorimeters, or from room burns. Examples of their associated limitations are as follows:

1. For a large-scale calorimeter, a product (e.g., chair, table, bookcase) is placed under a large collection hood and ignited by a 50 kW gas burner (simulating a wastebasket) placed adjacent to the item for 120 s. The combustion process then proceeds under assumed "free-burning" conditions, and the release rate data are measured. Potential sources of uncertainty here include measurement errors related to the instrumentation, and the degree to which "free-burning"

conditions are not achieved (e.g., radiation from the gases under the hood or from the hood itself, and restrictions in the air entrained by the object causing locally reduced oxygen concentrations affecting the combustion chemistry). There are limited experimental data for upholstered furniture which suggest that prior to the onset of flashover in a compartment, the influence of the compartment on the burning behavior of the item is small. The differences obtained from the use of different types or locations of ignition sources have not been explored. These factors are discussed in reference [21].

2. Where small-scale calorimeter data are used, procedures are available to extrapolate to the behavior of a full-size item. These procedures are based on empirical correlations of data which exhibit significant scatter, thus limiting their accuracy. For example, for upholstered furniture, the peak heat release rates estimated by the "triangular approximation" method averaged 91 percent (range 46 to 103 percent) of values measured for a group of 26 chairs with noncombustible frames, but only 63 percent (range 46 to 83 percent) of values measured for a group of 11 chairs with combustible frames [22]. Also, the triangle neglects the "tails" of the curve; these are the initial time from ignition to significant burning of the item, and the region of burning of the combustible frame, after the fabric and filler are consumed.
3. The provided data and procedures only relate directly to burning of items initiated by relatively large flaming sources. Little data are currently available for release rates under smoldering combustion, or for the high external flux and low oxygen conditions characteristic of post-flashover burning. While the model allows multiple items burning simultaneously, it does not account for the synergy of such multiple fires. Thus, for other ignition scenarios, multiple items burning simultaneously (which exchange energy by radiation and convection), combustible interior finish, and post-flashover conditions, the model can give estimates which are often nonconservative (the actual release rates would be *greater* than estimated). At present, the only sure way to account for all of these complex phenomena is to conduct a full-scale room burn and use the pyrolysis rates directly. Subsequent versions of the model will include detailed combustion models which can be used as the source fire.

Zone Model and Transport Limitations: The basic assumption of all zone fire models is that each room can be divided into a small number of control volumes, each of which is internally uniform in temperature and composition. In CFAST, all rooms have two zones except the fire room, which has an additional zone for the fire plume. The boundary between the two layers in a room is called the interface.

It has generally been observed that in the spaces close to the fire, buoyantly stratified layers form. While in an experiment the temperature can be seen to vary within a given layer, these variations are small compared to the temperature difference between the layers.

Beyond the basic zone assumptions, the model typically involves a mixture of established theory (e.g., conservation equations), empirical correlations where there are data but no theory (e.g., flow and entrainment coefficients), and approximations where there are neither (e.g., post-flashover combustion chemistry) or where their effect is considered secondary compared to the "cost" of inclusion. An example of a widely used assumption is that the estimated error from ignoring the variation of the thermal properties of structural materials with temperature is small. While this information would be fairly simple to add to the computer code, data are scarce over a broad range of temperatures even for the most common materials.

With a highly complex model such as CFAST, the only reasonable method of assessing impacts of assumptions and limitations is through the verification process, which is ongoing at the Building and Fire Research Laboratory (BFRL). Until the results of this process are available, the user should be aware of the general limits of zone modeling and some specific manifestations in CFAST. These include the following:

1. Burning can be constrained by the available oxygen. However, this "constrained fire" (a "type 2" fire, see page 23) is not subject to the influences of radiation to enhance its burning rate, but is influenced by the oxygen available in the room. If a large mass loss rate is entered, the model will follow this input until there is insufficient oxygen available for that quantity of fuel to burn in the room. The unburned fuel (sometimes called excess pyrolyzate) is tracked as it flows out in the door jet, where it can entrain more oxygen. If this mixture is within the user-specified flammable range, it burns in the door plume. If not, it will be tracked throughout the building until it eventually collects as unburned fuel or burns in a vent. The enthalpy released in the fire room and in each vent, as well as the total enthalpy released, is detailed in the output of the model. Since mass and enthalpy are conserved, the total will be correct. However, since combustion did not take place adjacent to the burning object, the actual mass burned could be lower than that specified by the user. The difference will be the unburned fuel.
2. An oxygen combustion chemistry scheme is employed only in constrained (type 2) fires. Here user-specified hydrocarbon ratios and species yields are used by the model to predict concentrations. A balance among hydrogen, carbon, and oxygen molecules is maintained. Under some conditions, low oxygen can change the combustion chemistry, with an attendant increase in the yields of products of incomplete combustion such as CO. Guidance is provided on how to adjust the CO/CO₂ ratio. However, not enough is known about these chemical processes to build this relationship into the model at the present time. Some data exist in reports of full-scale experiments (e.g., reference [23]) which can assist in making such determinations.
3. The entrainment coefficients are empirically determined values. Small errors in these values will have a small effect on the fire plume or the flow in the plume of gases exiting the door of that room. In a multi-compartment model such as CFAST, however, small errors in each door plume are multiplicative as the flow proceeds through many compartments, possibly resulting in a significant error in the furthest rooms. The data available from validation experiments [24] indicate that the values for entrainment coefficients currently used in most zone models produce good agreement for a three-compartment configuration. More data are needed for larger numbers of rooms to study this further.
4. In real fires, smoke and gases are introduced into the lower layer of each room primarily due to mixing at connections between rooms and from the downward flows along walls (where contact with the wall cools the gas and reduces its buoyancy). Doorway mixing has been included in CFAST, using an empirically derived mixing coefficient. However, for smoke flow along a wall, the associated theory is only now being developed and is not included in the model. This may produce an underestimate of the lower layer concentrations. The most important manifestation of this underestimate will be the temperature distribution between the upper and lower layers caused by radiation.
5. The only mechanisms provided in zone models to move enthalpy and mass into the upper layer of a room are two types of plumes: those formed by the burning item(s) in the fire room, and those formed by the jet of upper layer gases flowing through an opening. Thus, when the model calculates the flow of warm, lower layer gases through a low opening (e.g., the undercut of a "closed" door) by expansion of the smoke layer, they are assigned to the lower layer of the room

into which they flowed where they remain until the upper layer in the source room drops to the level of the undercut and the door jet forms. Thus, for a time the receiving room can show a lower layer temperature which exceeds that in the upper layer (a physically impossible condition). A better understanding of the flow within compartments in the context of a zone fire model would allow us to remove this anomaly. However, no hazard will exist during this time as the temperatures are low, and no gas species produced by the fire are carried through the opening until the upper layer drops to the height of the undercut.

1.3 Egress and Tenability Models

The EXITT model is a fairly-straightforward "node and arc" evacuation model to which an extensive series of behavioral rules has been added. The assumptions of interest are thus inherent in these rules, and the limitations are associated mostly with behavior not yet included. For example, the model does not have people re-entering the building, as they sometimes do. In addition, the current model is completely deterministic - a specific set of circumstances always results in a specific action. The data on which the rules were based sometimes identifies several potential actions (e.g., under this condition, 60% of the time they do A and 40% of the time they do B). To model such behavior properly, the program would have to employ probabilistic branching for a monte carlo type of simulation.

Within the current model, some of the rules are qualitative (e.g., a man's first action is to investigate) and some are quantitative (e.g., a woman between the ages of x and y walks at z m/min). The assumed values in quantitative rules are called parameter values, and the documentation for the model identifies each, the reason for assigning that value, and how the user can change it (allowing a sensitivity analysis to be performed on those parameters for which the user might feel that the supporting data are weak).

The impact of exposure to the occupants is evaluated in the program TENAB. Individual determinations are made for both incapacitation and lethality from temperature and toxicity, along with potential incapacitation from burns due to flux exposure. No interactions between temperature and toxicity are currently included (e.g., it is assumed but not known whether temperature exposure changes the rate of uptake of toxic species or increases the susceptibility to toxic species). The basis for the threshold values used and the derivation of the equations on which the toxicity calculation is based are provided in the Technical Reference volume in the chapter on Tenability Limits, which contains an extensive list of references. For all cases except flux exposure, the user can easily change the limit values used (and is encouraged to do so as a sensitivity test). Also, the method of presentation of the output of TENAB facilitates the observation of the sensitivity of the result to the limiting value selected.

The limiting values of temperature exposure are based on the general literature, which includes some human data. The flux criterion comes from work done with pig skin, which is generally considered to be very similar to human skin. The toxicity data, however, are from the combustion toxicology literature which is based entirely on animal exposures (primarily rodents for lethality studies and nonhuman primates for incapacitation studies). The model assumes that humans will exhibit a similar physiological response.

A toxicity parameter, Ct (concentration multiplied by exposure time, often referred to as "exposure dose"), is used to indicate the toxic impact of the smoke without differentiating the constituent gases or the possibility of diminished oxygen. This is a broad assumption. Another toxicity parameter, the fractional exposure dose (FED), is also introduced. This represents the fraction of the lethal concentration that an individual has been exposed to over time. The FED parameter combines the effects and interactions of the gases CO, CO₂, and HCN along with the effect of diminished oxygen. The model on which the FED

calculation is based, referred to as the N-Gas model [25], is under continuing development, and additional gases will be added as the data are obtained.

1.4 The "Residential-type Buildings" Limitation

In the initial release of HAZARD I, a limitation in scope to one- and two-family residential structures was carried over to version 1.1. Some have used this statement to imply that HAZARD I and its component models are less capable than other models (including some developed here) that have not carried such a conservative warning. Thus, the authors wanted to expand on this limitation to set the record straight.

As discussed in the previous sections, the models which make up HAZARD I are based on the best technical understanding of the underlying science supplemented by experimental data and expert judgement. Every attempt to verify the applicability of the models has been made, and is an ongoing activity. But data on fires in large buildings or spaces is scarce, so most of the verification studies have been done in smaller compartments constructed of "typical" materials.

For these reasons HAZARD I, and **all zone models**, can be shown to be applicable to "normal" sized compartments constructed of "typical" materials. In larger spaces it is not that we know that these models are wrong, it is that we cannot say for sure that they are right. Recent opportunities to run tests in large aircraft hangers and to compare zone models with CFD models in large spaces have given us more confidence that the zone concept is applicable in large spaces [26]. However, the conscientious engineer will still utilize sensitivity analysis or other techniques to increase confidence in such calculations, especially where the results are critical to public safety.

Where the residential limitation should still be honored is with EXITT. Here, the behavioral rules incorporated in the model are applicable only for family groups, since this altruism is not generally observed in populations who are unacquainted. The toxicity determinations of TENAB have never been subject to any such limitations.

2 Predictive Equations Used by the CFAST Model

This section presents a derivation of the predictive equations for zone fire models and explains in detail the ones used in CFAST [16], [18]. All current zone fire models take the mathematical form of an initial value problem for a mixed system of differential and algebraic equations. These equations are derived from the conservation of mass, energy and momentum. Subsidiary equations are the ideal gas law, and definitions of density and internal energy (for example, see [27]). These conservation laws are invoked for each zone or control volume. For further information on the numerical implications of these choices please see reference [28].

The basic element of the model is a zone. The basic assumption of a zone model is that properties such as temperature can be approximated throughout the zone by some uniform function. The usual approximation is that temperature, density and so on are uniform within a zone. This is not a necessary approximation. For example, a temperature which increases monotonically from the bottom of the zone to the top uniformly would, perhaps, improve the precision somewhat. However, the assumption of uniform properties is reasonable and yields good agreement with experiment. In general, these zones are grouped within compartments. The usual grouping is two gas layers per compartment. Once again, more could be utilized with a concomitant increase in computing time, but little improvement in accuracy.

There are two reasonable conjectures which dramatically improve the ease of solving these equations. Momentum is ignored within a compartment. The momentum of the interface has no significance in the present context. However, at boundaries such as windows, doors and so on, the Euler equation is integrated explicitly to yield the Bernoulli equation. This is solved implicitly in the equations which are discussed below. This stratagem avoids the short time step imposed by acoustic waves (Courant condition), which couple the pressure equation and the momentum equation. The other approximation is that the pressure is approximately uniform within a compartment. The argument is that a change in pressure of a few tens of Pascals over the height of the compartment is negligible in comparison with atmospheric pressure. Once again, this is applied to the basic conservation equations. This is consistent with the point source view of finite element models. Volume is merely one of the dependent variables. However, the hydrostatic variation in pressure is taken into account in calculating pressure differences between compartments. This might be viewed as analogous to the Boussinesque approximation in plume dynamics.

Many formulations based upon these assumptions can be derived. Several of these are discussed later. One formulation can be converted into another using the definitions of density, internal energy and the ideal gas law. Though equivalent analytically, these formulations differ in their numerical properties. Also, until the development of FAST [16], all models of this type assumed that the pressure equilibrated instantaneously, and thus the dP/dt term could be set to zero. However, as has been shown [29], it is better to solve these equations in the differential rather than the algebraic form if the proper solver is used.

As discussed in references [28] and [30], the zone fire modeling differential equations (ODE's) are stiff. Physically, the equations are stiff because of the presence of multiple time scales. Pressures adjust to changing conditions much quicker than other quantities such as layer temperatures or interface heights. Special solvers are required in general to solve zone fire modeling ODE's because of this stiffness. Runge-Kutta methods or predictor-corrector methods such as Adams-Bashforth require prohibitively small time steps in order to track the short-time scale phenomena (pressure in our case). Methods that calculate the Jacobian (or at least approximate it) have a much larger stability region for stiff problems and are thus more successful at their solution.

Each formulation can be expressed in terms of mass and enthalpy flow. These rates represent the exchange of mass and enthalpy between zones due to physical phenomena such as plumes, natural and forced ventilation, convective and radiative heat transfer, and so on. For example, a vent exchanges mass and enthalpy between zones in connected rooms, a fire plume typically adds heat to the upper layer and transfers entrained mass and enthalpy from the lower to the upper layer, and convection transfers enthalpy from the gas layers to the surrounding walls.

We use the formalism that the mass flow to the upper and lower layers is denoted \dot{m}_U and \dot{m}_L and the enthalpy flow to the upper and lower layers is denoted \dot{s}_U and \dot{s}_L . It is tacitly assumed that these rates may be computed in terms of zone properties such as temperature and density. These rates represent the net sum of all possible sources of mass and enthalpy due to phenomena such as those listed above. The numerical characteristics of the various formulations are easier to identify if the underlying physical phenomena are decoupled in this way.

Many approximations are necessary when developing physical sub-models for the mass and enthalpy terms. For example, most fire models assume that 1) the specific heat terms c_p and c_v are constant even though they depend upon temperature, 2) hydrostatic terms can be ignored in the equation of state (the ideal gas law) relating density of a layer with its temperature. However, the derivations which follow are all based on the basic conservation laws.

2.1 Derivation of Equations for a Two-Layer Model

A compartment is divided into two control volumes, a relatively hot upper layer and a relatively cooler lower layer, as illustrated in Figure 2. The gas in each layer has attributes of mass, internal energy, density, temperature, and volume denoted respectively by m_i , E_i , ρ_i , T_i , and V_i where $i=L$ for the lower layer and $i=U$ for the upper layer. The compartment as a whole has the attribute of pressure P . These 11 variables are related by means of the following seven constraints

$$\rho_i = \frac{m_i}{V_i} \quad (\text{density}) \quad (3)$$

$$E_i = c_v m_i T_i \quad (\text{internal energy}) \quad (4)$$

$$P = R \rho_i T_i \quad (\text{ideal gas law}) \quad (5)$$

$$V = V_L + V_U \quad (\text{total volume}) \quad (6)$$

We get seven by counting density, internal energy and the ideal gas law twice (once for each layer). The specific heat at constant volume and at constant pressure c_v and c_p , the universal gas constant, R , and the ratio of specific heats, γ , are related by $\gamma = c_p / c_v$ and $R = c_p - c_v$. For air, $c_p \approx 1000$ kJ/kg K and $\gamma = 1.4$. This leaves four unconstrained, or independent, variables. So we require four equations for a unique solution. The four are the conservation of mass and enthalpy for each layer.

The differential equations for mass in each layer are trivially

$$\begin{aligned}\frac{dm_L}{dt} &= \dot{m}_L \\ \frac{dm_U}{dt} &= \dot{m}_U\end{aligned}\quad (7)$$

The first law of thermodynamics states that the rate of increase of internal energy plus the rate at which the layer does work by expansion is equal to the rate at which enthalpy is added to the gas. In differential form this is

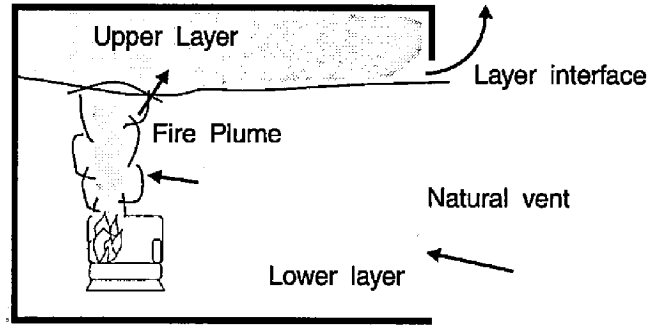


Figure 2. Schematic of control volumes in a two-layer zone model.

$$\begin{aligned}\text{internal energy} + \text{work} &= \text{enthalpy} \\ \underbrace{\frac{dE_i}{dt}} + \underbrace{P \frac{dV_i}{dt}} &= \underbrace{\dot{h}_i}\end{aligned}\quad (8)$$

A differential equation for pressure can be derived by adding the upper and lower layer versions of eq (8), noting that $dV_U/dt = -dV_L/dt$, and substituting the differential form of eq (4) to yield

$$\frac{dP}{dt} = \frac{\gamma - 1}{V} (\dot{h}_L + \dot{h}_U). \quad (9)$$

Differential equations for the layer volumes can be obtained by substituting the differential form of eq (4) into eq (8) to obtain

$$\frac{dV_i}{dt} = \frac{1}{P\gamma} \left((\gamma - 1) \dot{h}_i - V_i \frac{dP}{dt} \right) \quad (10)$$

Equation (8) can be rewritten using eq (10) to eliminate dV/dt to obtain

$$\frac{dE_i}{dt} = \frac{1}{\gamma} \left(\dot{h}_i + V_i \frac{dP}{dt} \right). \quad (11)$$

A differential equation for density can be derived by applying the quotient rule to $\frac{dp_i}{dt} = \frac{d}{dt} \left(\frac{m_i}{V_i} \right)$ and using eq (10) to eliminate dV/dt to obtain

$$\frac{d\rho_i}{dt} = -\frac{1}{c_p T_i V_i} \left(\dot{h}_i - c_p \dot{m}_i T_i \right) - \frac{V_i}{\gamma - 1} \frac{dP}{dt} \quad (12)$$

Temperature differential equations can be obtained from the equation of state by applying the quotient rule to $\frac{dT_i}{dt} = \frac{d}{dt} \left(\frac{P}{R\rho_i} \right)$ and using eq (12) to eliminate $d\rho/dt$ to obtain

$$\frac{dT_i}{dt} = \frac{1}{c_p \rho_i V_i} \left(\dot{h}_i - c_p \dot{m}_i T_i \right) + V_i \frac{dP}{dt} \quad (13)$$

These equations for each of the eleven variables are summarized in Table 3. The time evolution of these solution variables can be computed by solving the corresponding differential equations together with appropriate initial conditions. The remaining seven variables can be determined from the four independent solution variables using eqs (3) to (6).

There are, however, many possible differential equation formulations. Indeed, there are 330 different ways to select four variables from eleven. Many of these systems are incomplete due to the relationships that exist between the variables given in eqs (3) to (6). For example the variables, ρ_U , V_U , m_U , and P form a dependent set since $\rho_U = m_U / V_U$. Table 4 shows the solution variable selection made by several zone fire models.

The number of differential equation formulations can be considerably reduced by not mixing variable types between layers; that is, if upper layer mass is chosen as a solution variable, then lower layer mass must also be chosen. For example, for two of the solution variables choose m_L and m_U , or ρ_L and ρ_U , or T_L and T_U . For the other two solution variables pick E_L and E_U or P and V_L or P and V_U . This reduces the number of distinct formulations to nine. Since the numerical properties of the upper layer volume equation are the same as a lower layer one, the number of distinct formulations can be reduced to six.

Table 3. Conservative Zone Modeling Differential Equations

Equation Type	Differential Equation
i'th layer mass	$\frac{dm_i}{dt} = \dot{m}_i$
pressure	$\frac{dP}{dt} = \frac{\gamma-1}{V} (\dot{h}_L + \dot{h}_U)$
i'th layer energy	$\frac{dE_i}{dt} = \frac{1}{\gamma} \left(\dot{h}_i + V_i \frac{dP}{dt} \right)$
i'th layer volume	$\frac{dV_i}{dt} = \frac{1}{\gamma P} \left((\gamma - 1) \dot{h}_i - V_i \frac{dP}{dt} \right)$
i'th layer density	$\frac{d\rho_i}{dt} = -\frac{1}{c_p T_i V_i} \left(\dot{h}_i - c_p \dot{m}_i T_i \right) - \frac{V_i}{\gamma-1} \frac{dP}{dt}$
i'th layer temperature	$\frac{dT_i}{dt} = \frac{1}{c_p \rho_i V_i} \left(\dot{h}_i - c_p \dot{m}_i T_i \right) + V_i \frac{dP}{dt}$

Table 4. Conservative Zone Model Equation Selections

Zone Fire Model	Equations	Substitutions
FAST	$\frac{d\Delta P}{dt}, \frac{dV_L}{dt}, \frac{dT_U}{dt}, \frac{dT_L}{dt}$	$\Delta P = P - P_{ref}$
CCFM.HOLE	$\frac{d\Delta P}{dt}, \frac{dy}{dt}, \frac{d\rho_U}{dt}, \frac{d\rho_L}{dt}$	$\Delta P = P - P_{ref}$ $y = V_L / A_{room}$
CCFM.VENTS	$\frac{d\Delta P}{dt}, \frac{dy}{dt}, \frac{dm_U}{dt}, \frac{dm_L}{dt}$	$\Delta P = P - P_{ref}$ $y = V_L / A_{room}$
FIRST, HARVARD	$\frac{dE_U}{dt}, \frac{dE_L}{dt}, \frac{dm_U}{dt}, \frac{dm_L}{dt}$	

2.2 Equation Set Used in CFAST

The current version of CFAST is set up to use the equation set for layer temperature, layer volume, and pressure as shown below. However, the internal structure of the model is such that it will allow any of the formulations above to be substituted with minimal effort.

$$P = P_{ref} + \Delta P \quad (14)$$

$$\frac{dP}{dt} = \frac{\gamma-1}{V}(\dot{h}_L + \dot{h}_U) \quad (15)$$

$$\frac{dV_U}{dt} = \frac{1}{\gamma P} \left((\gamma - 1)\dot{h}_U - V_U \frac{dP}{dt} \right) \quad (16)$$

$$\frac{dT_U}{dt} = \frac{1}{c_p \rho_U V_U} \left((\dot{h}_U - c_p \dot{m}_U T_U) + V_U \frac{dP}{dt} \right) \quad (17)$$

$$\frac{dT_L}{dt} = \frac{1}{c_p \rho_L V_L} \left((\dot{h}_L - c_p \dot{m}_L T_L) + V_L \frac{dP}{dt} \right) \quad (18)$$

3 Source Terms for the CFAST Model

The conserved quantities in each compartment are described by the set of predictive equations shown above. The form of the equations is such that the physical phenomena are source terms on the right-hand-side of these equations. Such a formulation makes the addition and deletion of physical phenomena and changing the form of algorithms a *relatively* simple matter. For each of the phenomena discussed below, the physical basis for the model is discussed first, followed by a brief presentation of the implementation within CFAST. For all of the phenomena, there are basically two parts to the implementation: the physical interface routine (which is the interface between the CFAST model and the algorithm) and the actual physical routine(s) which implement the physics. This implementation allows the physics to remain independent of the structure of CFAST and allows easier insertion of new phenomena.

3.1 The Fire

3.1.1 Specified Fire (Fire Types 1 and 2)

A specified fire is one for which the time dependent characteristics are specified as a function of time. The specified fire can be unconstrained or constrained. These fires are later referred to as type 1 and type 2, respectively. The meaning of this assignment will become clearer in the discussion of the data file structure. For the constrained fire, the constraint is based on the minimum of the fuel and oxygen available for combustion. For either, the pyrolysis rate is specified as \dot{m}_p , the burning rate as \dot{m}_b , and the heat of combustion as H_c so that the nominal heat release rate is

$$\dot{Q}_f = H_c \dot{m}_b - c_p (T_u - T_v) \dot{m}_b . \quad (19)$$

For the unconstrained fire, $\dot{m}_b = \dot{m}_p$ whereas for the constrained fire, the burning rate may be less than the pyrolysis rate. Models of specified fires generally use an effective heat of combustion which is obtained from an experimental apparatus such as the Cone Calorimeter [31]. The shortcoming of this approach is that the pyrolysis rate is not connected to radiative feedback from the flame or compartment. In an actual fire, this is an important consideration, and the specification used should match the experimental conditions as closely as possible.

The enthalpy which is released goes into radiation and convection

$$\begin{aligned} \dot{Q}_r(\text{fire}) &= \chi_R \dot{Q}_f \\ \dot{Q}_c(\text{fire}) &= (1 - \chi_r) \dot{Q}_f . \end{aligned} \quad (20)$$

The term $\dot{Q}_c(\text{fire})$ then becomes the driving term in the plume flow. In the actual implementation, these formulae are modified to be compatible with the two-zone nature of the model. For a specified fire there is radiation to both the upper and lower layers, whereas the convective part contributes only to the upper layer. In addition, a view factor must be calculated for the radiative portion.

3.1.2 Combustion Chemistry (Fire Type 2)

For a type 2 fire, the products of combustion are calculated via a species balance consistent with the constraint on available oxygen. The scheme is applied in three places. The first is burning in the portion of the plume which is in the lower layer of the room of fire origin (region #1). The second is the portion in the upper layer, also in the room of origin (region #2). The third is in the vent flow which entrains air from a lower layer into an upper layer in an adjacent compartment (region #3). Figure 3 is a schematic of the concept of division of burning regions.

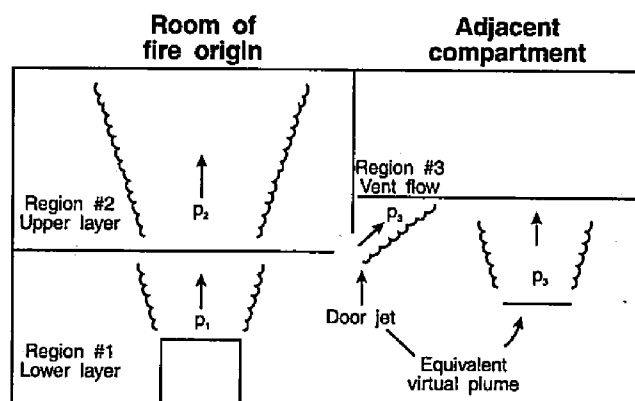


Figure 3. Schematic of entrainment and burning regions.

The simplest form of enthalpy release is made by specifying a heat release rate, together with a consistent pyrolysis rate. This would simulate the fire that occurs in an unconfined area. This is the form that all zone models have used until now. As soon as one is constrained by the confines of a compartment, then the nature of the fire changes. In particular, the available oxygen may not be sufficient to allow complete combustion. It is not sufficient to account for the oxygen alone, however. A consistent prescription for the combustion chemistry is required. In CFAST, we calculate a chemical balance for a simplified combustion reaction in terms of the ratios of species to carbon dioxide, the primary product of combustion. We allow for a realistic fuel composition, including oxygen, carbon, hydrogen, and chlorine as part of the fuel. Carbon monoxide, carbon dioxide, soot, water, hydrogen cyanide and hydrogen chloride are the products of combustion. Infinite rate kinetics is assumed. Further, we do not calculate backwards reactions.

The fuel burning rate in terms of the carbon production is

$$\dot{m}_f = \{-\} \times \dot{m}_c \quad (21)$$

where $\{-\}$ is the multiplier in the fuel production

$$\{-\} = \left(1 + \frac{H}{C} + \frac{HCl}{C} + \frac{HCN}{C} + \frac{O}{C} \right) \equiv f/C. \quad (22)$$

The following definitions are for the heat release rate as a function of the fuel burning rate, and the heat release rate based on oxygen consumption. H/C , HCl/C , HCN/C and O/C are the ratio of mass of that species to carbon in the fuel. Thus H/C is for the mass of hydrogen to the mass of carbon produced in pyrolysis. This is a very useful way to characterize the fuel. This is in terms of the elemental composition of the fuel, and not elemental molecules, such as H_2 . These are the ratios for the fuel, and the material which comes from it. For the products of the combustion process, we have CO_2/C , CO/C , H_2O/C and S/C . These ratios are in terms of free molecules, generally gaseous. Note that the "S" is used to designate soot, and we assume it consists primarily of carbon.

The first step is to limit the actual burning which takes place in the combustion zone. In each combustion zone, there is a quantity of fuel available. At the source this results from the pyrolysis of the material. In other situations such as a plume or door jet, it is the net unburned fuel available. At the source we

refer to \dot{m}_p , but in the other regions we use a catch-all, \dot{m}_{TUHC} (for total unburned hydrocarbons). In each case, the fuel which is available but not burned is then deposited into this category. This provides a consistent notation. In the discussion below, we will speak of the \dot{m}_f as the amount burned. The understanding is that in the iterative scheme discussed, this value is initialized to the available fuel, and then possibly reduced by the algorithm discussed. Subsequently, the available fuel, \dot{m}_{TUHC} , is reduced by the final value of \dot{m}_f . Thus we have a consistent description in each burning region, with an algorithm that can be invoked independent of the region being analyzed. The energy released by the available fuel if there were no constraint (free burn) is

$$\dot{Q} = \dot{m}_f \times H_c, \quad (23)$$

with the mass of oxygen required to achieve this energy release rate (based on the oxygen consumption principle [32]) of

$$\dot{m}_O = \frac{\dot{Q}}{1.32 \times 10^7} = \dot{m}_f \times \frac{H_c}{1.32 \times 10^7}. \quad (24)$$

If the fuel contains oxygen, the oxygen needed to achieve full combustion is less than this value

$$\dot{m}_O(\text{needed}) = \dot{m}_O - \dot{m}_O(\text{in the fuel}) \quad (25)$$

If sufficient oxygen is available, then it is fully burned. However, if the oxygen concentration is low enough, it will constrain the burning and impose a limit on the the amount of fuel actually burned, as opposed to the amount pyrolyzed. The actual limitation is discussed below and is presented as eq (40).

$$\dot{m}_O(\text{actual}) = \text{minimum of } \{ \dot{m}_O(\text{available}), \dot{m}_O(\text{needed}) \}, \quad (26)$$

$$\dot{m}_f(\text{actual}) = \dot{m}_O(\text{actual}) \times \frac{1.32 \times 10^7}{H_c} \quad (27)$$

Essentially, we limit the amount of fuel that is burned, as opposed to the amount that is pyrolyzed, to the lesser of the amount pyrolyzed and that required to consume the *available* oxygen. The $\dot{m}_O(\text{actual})$ and $\dot{m}_f(\text{actual})$ are the quantities used below.

We begin with the mass balance equation. The mass consumed as pyrolyzate plus oxygen must reappear as product.

$$\begin{aligned} \dot{m}_f + \dot{m}_O &= \dot{m}_f + \dot{m}_f \times \frac{H_c}{1.32 \times 10^7} - \frac{\dot{m}_f}{\{-\}} \times \left(\frac{O}{C} \right) \\ &= \dot{m}_{CO_2} + \dot{m}_{CO} + \dot{m}_S + \dot{m}_{H_2O} + \dot{m}_{HCl} + \dot{m}_{HCN} \end{aligned} \quad (28)$$

We then substitute the following definitions of mass produced of each species based on the amount of carbon consumed as

$$\dot{m}_{HCl} = \left(\frac{HCl}{C} \right) \times \dot{m}_C \rightarrow \left(\frac{HCl}{f} \right) \times \dot{m}_f \quad (29)$$

$$\dot{m}_{HCN} = \left(\frac{HCN}{C} \right) \times \dot{m}_C \rightarrow \left(\frac{HCN}{f} \right) \times \dot{m}_f \quad (30)$$

$$\dot{m}_{H_2O} = \frac{1}{2} \left(\frac{H_2O}{H} \right) \times \left(\frac{H}{C} \right) \times \dot{m}_C = 9 \times \left(\frac{H}{C} \right) \times \dot{m}_C \rightarrow 9 \times \left(\frac{H}{C} \right) \times \frac{\dot{m}_f}{\{-\}} \quad (31)$$

$$\dot{m}_{CO_2} = \left(\frac{CO_2}{C} \right) \times \dot{m}_C \quad (32)$$

$$\dot{m}_S = \left(\frac{S}{C} \right) \times \dot{m}_C = \left(\frac{CO_2}{C} \right) \times \left(\frac{S}{CO_2} \right) \times \dot{m}_C \rightarrow \left(\frac{S}{CO_2} \right) \times \dot{m}_{CO_2} \quad (33)$$

$$\dot{m}_{CO} = \left(\frac{CO}{C} \right) \times \dot{m}_C = \left(\frac{CO_2}{C} \right) \times \left(\frac{CO}{CO_2} \right) \times \dot{m}_C \rightarrow \left(\frac{CO}{CO_2} \right) \times \dot{m}_{CO_2} \quad (34)$$

Substituting the above definitions into the mass balance equation yields:

$$\left(\frac{CO_2}{C} \right) = \frac{\{-\} \times \left(1 + \frac{H_c}{1.32 \times 10^7} - \frac{O/C}{\{-\}} \right) - \left(\frac{HCl}{C} + \frac{HCN}{C} + \frac{H}{C} \right)}{\left(1 + \frac{S}{CO_2} + \frac{CO}{CO_2} \right)} \quad (35)$$

With this definition, we can substitute back into the equation for carbon dioxide production, which yields

$$\dot{m}_{CO_2} = \dot{m}_f \times \frac{\left(1 + \frac{h_c}{1.32 \times 10^7} - \frac{O/C}{\{-\}} \right) - \left(\frac{HCl}{C} + \frac{HCN}{C} + \frac{H}{C} \right)}{\left(1 + \frac{S}{CO_2} + \frac{CO}{CO_2} \right)} \quad (36)$$

The form in which we cast these equations evolves naturally from the properties of combustion. Hydrogen, carbon and bound oxygen are properties of the fuel. They can be measured experimentally independent of the combustion process. Thus we use these ratios as the basis of the scheme. In a similar sense, hydrogen chloride and hydrogen cyanide are properties of the pyrolysis process. So hydrogen

chlorine and hydrogen cyanide production are specified with respect to the fuel pyrolysis. Normally this is how they are measured, for example with the cone calorimeter, so we can use the measured quantities directly. Other than the cyanide, chloride and water production, hydrogen does not play a role. In general, hydrogen has much more of an affinity for oxygen than for carbon, so almost all of the hydrogen will go toward production of water. This dictates the next choice, which is that soot is essentially all carbon. On a mass basis this is certainly true. On a molecular basis, however, it may consist of molecules which vary greatly in size. Carbon dioxide is a direct product of combustion, and the assumption is that most carbon will end up here. Thus, in this model, carbon monoxide and soot are functions of incomplete combustion. They are assumed not to be a function of the pyrolysis process itself. (Although carbon monoxide can be produced directly, it is presumed such production will be negligible when compared to its generation during incomplete combustion.) Thus they depend on the environment in which the burning takes place. Thus the production of these products are specified with respect to the carbon dioxide. At present, we must rely on measured ratios, but this is beginning to change as we gain a better understanding of the combustion process. So, in the present model, carbon goes to one of three final species, carbon dioxide, carbon monoxide or soot (carbon), with the particular branching ratio depending on the chemistry active at the time.

Equations (31) through (36) are used in terms of the carbon production. We now need to recast HCl and HCN in terms of fuel production rather than carbon production, since that is how they are measured. Since HCl and HCN are similar, we will just make the argument for one, and then assume that the derivation is the same. One simplification will be possible for the HCN though, and that is that its production rate is *always* much less than the pyrolysis rate.

Since {—} is just f/C ,

$$\left(\frac{HCl}{C}\right) = \left(\frac{HCl}{f}\right) \times \left(1 + \frac{H}{C} + \frac{HCl}{C} + \frac{HCN}{C} + \frac{O}{C}\right) \quad (37)$$

Therefore

$$\left(\frac{HCl}{C}\right) = \left(\frac{HCl}{f}\right) \times \frac{1 + \frac{H}{C} + \frac{O}{C}}{1 - \left(\frac{HCl}{f}\right)} \quad (38)$$

and for hydrogen cyanide we have

$$\left(\frac{HCN}{C}\right) = \left(\frac{HCN}{f}\right) \times \left(1 + \frac{H}{C} + \frac{HCl}{C} + \frac{O}{C}\right) \quad (39)$$

In this latter case, we assume that the cyanide ratio (HCN/C) is small compared to unity. It is the HCl/C and HCN/C ratios which are used by the model.

The relationship between oxygen and fuel concentration defines a range where burning will take place. The rich limit is where, for a given ratio of O_2 to N_2 (generally the ratio in air), there is too much fuel for combustion. At the other end, there is the lean flammability limit, where there is too little fuel for combustion. In the CFAST model, the rich limit is incorporated by limiting the burning rate as the oxygen level decreases until a "lower oxygen limit" is reached. The lower oxygen limit is incorporated through a smooth decrease in the burning rate near the limit:

$$\dot{m}_o(\text{available}) = \dot{m}_e Y_{O_2} C_{LOL} \quad (40)$$

The lower oxygen limit coefficient, C_{LOL} , is the fraction of the available fuel which can be burned with the available oxygen and varies from 0 at the limit to 1 above the limit. The functional form provides a smooth cutoff of the burning over a narrow range above the limit.

$$C_{LOL} = \frac{\tanh\left(800(Y_{O_2} - Y_{LOL}) - 4\right) + 1}{2} \quad (41)$$

For the lean flammability limit, an ignition temperature criterion is included, below which no burning takes place.

In summary, the formation of some of the products of combustion, carbon dioxide, carbon monoxide, soot, water, hydrogen cyanide, and hydrogen chloride can be predicted given the branching ratios CO/CO_2 , $S(\text{soot})/CO_2$, the composition of the fuel, H/C , O/C , HCl/f and HCN/f and the flammability limit. In principle, the flammability limit comes from theory. At present, in practice we use experimental values, such as those from Morehart et al. [33]. The composition of the fuel is a measurable quantity, although it is complicated somewhat by physical effects. The complication arises in that materials such as wood will yield methane in the early stages of burning, and carbon rich products at later times. Thus the H/C and O/C ratios are functions of time. Finally, the production ratios of CO/CO_2 , $S(\text{soot})/CO_2$ are based on the kinetics which in turn is a function of the ambient environment.

3.2 Plumes

Buoyancy generated by the combustion processes in a fire causes the formation of a plume. Such a plume can transport mass and enthalpy from the fire into the lower or upper layer of a compartment. In the present implementation, we assume that both mass and enthalpy from the fire are deposited only into the upper layer. In addition the plume entrains mass from the lower layer and transports it into the upper layer. This yields a net enthalpy flux between the two layers. Actually, the flame and plume will generally radiate somewhat into the lower layer, at least if it is not diathermous. So our approximation causes the upper layer to be somewhat hotter, and the lower layer somewhat cooler than is the case, at least in a well developed fire. For normal fires and door jet fires, plume entrainment is implemented as part of the fire calculation detailed in section ?.

A fire generates energy at a rate \dot{Q} . Some fraction, χ_R , will exit the fire as radiation. The remainder, χ_O , will then be deposited in the layers as convective energy or heat additional fuel so that it pyrolyses. Defining this quantity ($C_p \dot{m}_e (T_u - T_e)$) to be the convective heat release rate, we can use the work of McCaffrey [34] to estimate the mass flux from the fire into the upper layer. This correlation divides the flame/plume into three regions as shown below. This prescription agrees with the work of Cetegen

et al. [35] in the intermittent regions but yields greater entrainment in the other two regions. This difference is particularly important for the initial fire since the upper layer is far removed from the fire.

$$\begin{array}{lll}
 \text{flaming:} & \frac{\dot{m}_e}{\dot{Q}} = 0.011 \left(\frac{Z}{\dot{Q}^{2/5}} \right)^{0.566} & 0.00 \leq \left(\frac{Z}{\dot{Q}^{2/5}} \right) < 0.08 \\
 \text{intermittent:} & \frac{\dot{m}_e}{\dot{Q}} = 0.026 \left(\frac{Z}{\dot{Q}^{2/5}} \right)^{0.909} & 0.08 \leq \left(\frac{Z}{\dot{Q}^{2/5}} \right) < 0.20 \\
 \text{plume:} & \frac{\dot{m}_e}{\dot{Q}} = 0.124 \left(\frac{Z}{\dot{Q}^{2/5}} \right)^{1.895} & 0.20 \leq \left(\frac{Z}{\dot{Q}^{2/5}} \right)
 \end{array} \quad (42)$$

McCaffrey's correlation is an extension of the common point source plume model, with a different set of coefficients for each region. These coefficients are experimental correlations, and are not based on theory. The theory appears only in the form of the fitted function. The binding to the point source plume model is for the value for Z where the mode changes, namely from flaming to intermittent to plume.

Within CFAST, the radiative fraction defaults to 0.15; i.e., 15 percent of the fire's energy is released via radiation. This value is consistent with typical methane flames. For other fuels, the work of Tewarson [36], McCaffrey [37], or Koseki [38] is available for reference. These place the typical range for the radiative fraction at a maximum of about 0.4 to 0.6.

In CFAST, there is a constraint on the quantity of gas which can be entrained by a plume arising from a fire. The constraint arises from the physical fact that a plume can rise only so high for a given size of a heat source. In the earlier versions of this model (FAST version 17 and earlier), the plume was not treated as a separate zone. Rather we assumed that the upper layer was connected immediately to the fire by the plume. The implication is that the plume is formed instantaneously and stretches from the fire to the upper layer or ceiling. Consequently, early in a fire, when the energy flux was very small and the plume length very long, the entrainment was over predicted. This resulted in the interface falling more rapidly than was seen in experiments. Also the initial temperature was too low and the rate of rise too fast, whereas the asymptotic temperature was correct. The latter occurred when these early effects were no longer important.

The correct sequence of events is for a small fire to generate a plume which does not reach the ceiling or upper layer initially. The plume entrains enough cool gas to decrease the buoyancy to the point where it no longer rises. When there is sufficient energy present in the plume, it will penetrate the upper layer. The effect is two-fold: first, the interface will take longer to fall and second, the rate of rise of the upper layer temperature will not be as great. To this end the following prescription has been incorporated: for a given size fire, a limit is placed on the amount of mass which can be entrained, such that no more is entrained than would allow the plume to reach the layer interface. The result is that the interface falls at about the correct rate, although it starts a little too soon, and the upper layer temperature is over predicted, but follows experimental data after the initial phase (see sec. 4).

For a section (segment) of the plume to penetrate the inversion formed by a hot layer at T_u over a cool layer T_l , the density of the gas in the plume at the point of intersection must be less than the density of the gas in the upper layer, that is $\rho_p < \rho_u$. The subscript "v" is the virtual point at which mass is coming off the fire, "q" the state at which this same mass would be if there were no cooling from the entrained

gases and "p" the plume at the point at which it intersects the upper layer. The "l" refers to the lower layer, and the "u" to the upper layer. The temperature rise in the plume is given by

$$(T_q - T_v) C_p \dot{m}_v = \dot{Q}. \quad (43)$$

From conservation of mass we have

$$\dot{m}_p = \dot{m}_e + \dot{m}_q. \quad (44)$$

And from conservation of enthalpy we have

$$\dot{m}_p T_p = \dot{m}_e T_l + \dot{m}_v T_v. \quad (45)$$

The criterion that the density in the plume region must be lower than the upper layer implies

$$T_u < T_p. \quad (46)$$

By substituting the equation for temperature rise, eq (43), and the conservation of mass, eq (44), into eq (45)

$$\dot{m}_e < \frac{\dot{Q}}{C_p(T_u - T_l)} - \left(\frac{T_u - T_v}{T_u - T_l} \right) \dot{m}_v. \quad (47)$$

The right most term is negligible in the cases under consideration so we will ignore it. In the case where it is of the same order as the first term, there are other constraints on the entrainment. Thus we are left with the maximum for \dot{m}_e of

$$\dot{m}_e < \frac{\dot{Q}}{c_p(T_u - T_l)} \quad (48)$$

which is incorporated into the model. It should be noted that both the plume and layers are assumed to be well mixed with negligible mixing and transport time for the plume and layers.

3.3 Vent Flows

Mass flow (in the remainder of this section, the term "flow" will be used to mean mass flow) is the dominant source term for the predictive equations because it fluctuates most rapidly and transfers the greatest amount of enthalpy on an instantaneous basis of all the source terms. Also, it is most sensitive to changes in the environment. Flow through vents comes in two varieties. The first is horizontal flow. It is the flow which is normally thought of in discussing fires. It encompasses flow through doors, windows and so on. The other is vertical flow and can occur if there is a hole in the ceiling or floor of a compartment. This latter phenomena is particularly important in two disparate situations: a ship, and the role of fire fighters doing roof venting. Vertical flow is discussed in section 3.3.2.

3.3.1 Horizontal Flow Through Vertical Vents

Flow through normal vents is governed by the pressure difference across a vent. A momentum equation for the zone boundaries is not solved directly. Instead momentum transfer at the zone boundaries is included by using an integrated form of Euler's equation, namely Bernoulli's solution for the velocity

equation. This solution is augmented for restricted openings by using flow coefficients [39] to allow for constriction from finite size doors. The flow (or orifice) coefficient is an empirical term which addresses the problem of constriction of velocity streamlines at an orifice.

Bernoulli's equation is the integral of the Euler equation and applies to general initial and final velocities and pressures. The implication of using this equation for a zone model is that the initial velocity in the doorway is the quantity sought, and the final velocity in the target compartment vanishes. That is, the flow velocity vanishes where the final pressure is measured. Thus, the pressure at a stagnation point is used. This is consonant with the concept of uniform zones which are completely mixed and have no internal flow. The general form for the velocity of the mass flow is given by

$$v = C \left(\frac{2\delta P}{\rho} \right)^{1/2} \quad (49)$$

where C is the constriction (or flow) coefficient (≈ 0.7), ρ is the gas density on the source side, and δP is the pressure across the interface. (Note: at present we use a constant C for all gas temperatures) We apply the above equation to rectangular openings which allows us to remove the width from the mass flux integral. That is

$$\text{mass flux} = \int_{\text{width}} \int_{\text{height}} \rho v dz dw \rightarrow \text{width} \int_{z_1}^{z_2} \rho v dz \quad (50)$$

The simplest means to define the limits of integration is with neutral planes, that is the height at which flow reversal occurs, and physical boundaries such as sills and soffits. By breaking the integral into intervals defined by flow reversal, a soffit, a sill, or a zone interface, the flow equation can be integrated piecewise analytically and then summed.

The approach to calculating the flow field is of some interest. The flow calculations are performed as follows. The vent opening is partitioned into at most six slabs where each slab is bounded by a layer height, neutral plane, or vent boundary such as a soffit or sill. The most general case is illustrated in Figure 4.

The mass flow for each slab can be determined from

$$\dot{m}_{i \rightarrow o} = \frac{1}{3} C (8\rho) A_{\text{slab}} \left(\frac{x^2 + xy + y^2}{x+y} \right) \quad (51)$$

where $x = |P_t|^{1/2}$, and $y = |P_b|^{1/2}$. P_t and P_b are the cross-vent pressure differential at the top and bottom of the slab respectively and A_{slab} is the cross-sectional area of the slab. The value of the density, ρ , is taken from the source compartment.

A mixing phenomenon occurs at vents which is similar to entrainment in plumes. As hot gases from one compartment leave that compartment and flow into an adjacent compartment a door jet can exist which is analogous to a normal plume. Mixing of this type occurs for $\dot{m}_{13} > 0$ as shown in Figure 5. To calculate the entrainment (\dot{m}_{43} in this example), once again we use a plume description, but with an extended source point. The estimate for the point source extension is given by Cetegen et al. [35]. This virtual point source is chosen so that the flow at the door opening would correspond to a plume with the heating (with respect to the lower layer) given by

$$\dot{Q}_{eq} = c_p(T_1 - T_4)\dot{m}_{13} \quad (52)$$

The concept of the virtual source is that the enthalpy flux from the virtual point source should equal the actual enthalpy flux in the door jet at the point of exit from the vent using the same prescription. Thus the entrainment is calculated the same way as was done for a normal plume. The height, z_n , of the plume is

$$z_p = \frac{z_{13}}{\dot{Q}_{eq}^{2/5}} + v_p \quad (53)$$

where v_p , the virtual source point, is defined by inverting the entrainment process to yield

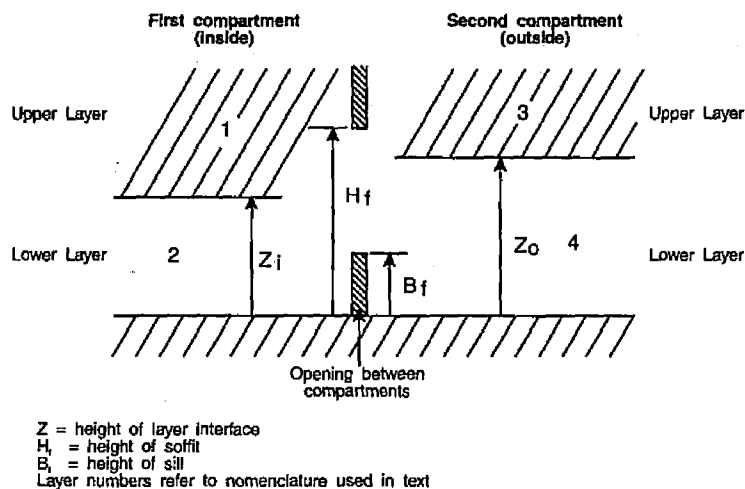


Figure 4. Notation conventions for two-layer model in two rooms with a connecting vent.

$$\begin{aligned} v_p &= \left(\frac{90.9\dot{m}}{\dot{Q}_{eq}} \right)^{1.76} & \text{if } 0.00 < v_p \leq 0.08 \\ v_p &= \left(\frac{38.5\dot{m}}{\dot{Q}_{eq}} \right)^{1.001} & \text{if } 0.08 < v_p \leq 0.20 \\ v_p &= \left(\frac{8.10\dot{m}}{\dot{Q}_{eq}} \right)^{0.528} & \text{if } 0.20 < v_p \end{aligned} \quad (54)$$

The units of this height, z_p and of v_p , are not length, but rather the reduced notation of McCaffrey [34]. That is, the z_p defined here is the term $z/Q^{2/5}$ used earlier. Although outside of the normal range of validity of the plume model, a level of agreement with experiment is apparent (see sec. 4). Since a door jet forms a flat plume whereas a normal fire plume will be approximately circular, strong agreement is not expected.

The other type of mixing is much like an inverse plume and causes contamination of the lower layer. It occurs when there is flow of the type $\dot{m}_{42} > 0$. The shear flow causes vortex shedding into the lower layer and thus some of the particulates end up in the lower layer. The actual amount of mass or energy transferred is usually not large, but its effect can be large. For example, even minute amounts of carbon can change the radiative properties of the gas layer, from negligible to something finite. It changes the rate of radiation absorption by orders of magnitude which invalidates the notion of a diathermous lower layer. This term is predicated on the Kelvin-Helmholz flow instability and requires shear flow between two separate fluids. The mixing is enhanced for greater density differences between the two layers. However, the amount of mixing has never been well characterized. Quintiere et al. discuss this phenomena for the case of crib fires in a single room, but their correlation does not yield good agreement with experimental data in the general case [40]. In the CFAST model, it is assumed that the incoming

cold plume behaves like the inverse of the usual door jet between adjacent hot layers; thus we have a descending plume. It is possible that the entrainment is overestimated in this case, since buoyancy, which is the driving force, is not nearly as strong as for the usually upright plume.

3.3.2 Vertical Flow Through Horizontal Vents

Flow through a ceiling or floor vent can be somewhat more complicated than through door or window vents. The simplest form is uni-directional flow, driven solely by a pressure difference. This is analogous to flow in the horizontal direction driven by a piston effect of expanding gases. Once again, it can be calculated based on the Bernoulli equation, and presents little difficulty. However, in general we must deal with more complex situations that must be modeled in order to have a proper understanding of smoke movement. The first is an occurrence of puffing. When a fire exists in a compartment in which there is only a hole in the ceiling, the fire will burn until the oxygen has been depleted, pushing gas out the hole. Eventually the fire will die down. At this point ambient air will rush back in, enable combustion to increase, and the process will be repeated. Combustion is thus tightly coupled to the flow. The other case is exchange flow which occurs when the fluid configuration across the vent is unstable (such as a hotter gas layer underneath a cooler gas layer). Both of these pressure regimes require a calculation of the onset of the flow reversal mechanism.

Normally a non-zero cross vent pressure difference tends to drive unidirectional flow from the higher to the lower pressure side. An unstable fluid density configuration occurs when the pressure alone would dictate stable stratification, but the fluid densities are reversed. That is, the hotter gas is underneath the cooler gas. Flow induced by such an unstable fluid density configuration tends to lead to bi-directional flow, with the fluid in the lower compartment rising into the upper compartment. This situation might arise in a real fire if the room of origin suddenly had a hole punched in the ceiling. We make no pretense of being able to do this instability calculation analytically. We use Coopers's algorithm [41] for computing mass flow through ceiling and floor vents. It is based on correlations to model the unsteady component of the flow. What is surprising is that we can find a correlation at all for such a complex phenomenon. There are two components to the flow. The first is a net flow dictated by a pressure difference. The second is an exchange flow based on the relative densities of the gases. The overall flow is given by [41]

$$\dot{m} = Cf(\gamma, \epsilon) \left(\frac{\delta P}{\bar{\rho}} \right)^{1/2} A_v \quad (55)$$

where

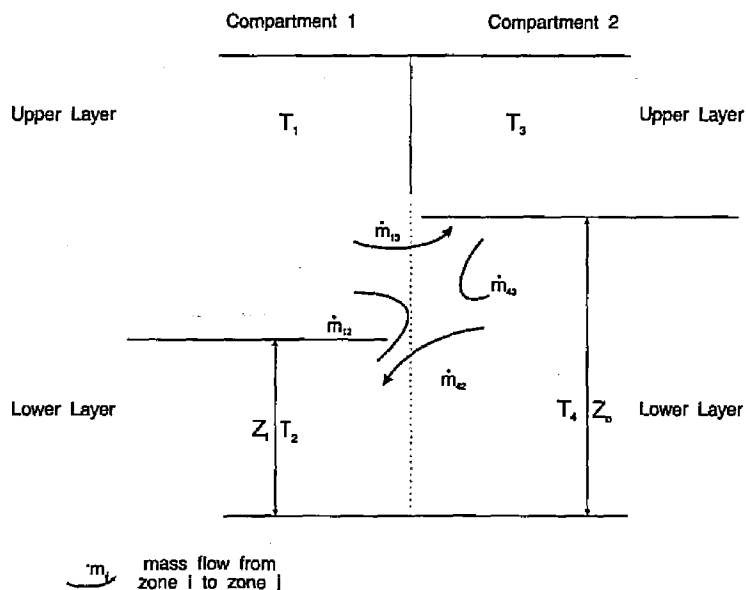


Figure 5. Example of a possible flow pattern and layer numbering convention.

$$C = 0.68 + 0.17\varepsilon, \quad (56)$$

$$\varepsilon = \frac{\delta P}{P}, \quad (57)$$

and f is a weak function of both γ and ε . In the situation where we have an instability, we use Cooper's correlations. The algorithm for this exchange flow is given by

$$\dot{m}_{ex} = 0.1 \left(\frac{g \delta \rho A_v^{5/2}}{\rho_{av}} \right) \left(1.0 - \frac{2 A_v^2 \delta \rho}{S^2 g \delta \rho D^5} \right) \quad (58)$$

where

$$D = 2 \sqrt{\frac{A_v}{\pi}} \quad (59)$$

and S is 0.754 or 0.942 for round or square openings, respectively.

A simple example of the effect of this exchange flow can be shown with the following example. Consider two closed compartments, each 10 m in height, one on top of the other, connected by a one meter diameter round hole. Given hydrostatic equilibrium, there will be no flow between the compartments. Varying the pressure and density of the gas in the lower compartment very slightly from initial values of 1.2 kg/m³ and 117.6 N/m² respectively, we calculate the flow between the compartments, as shown in Figure 6.

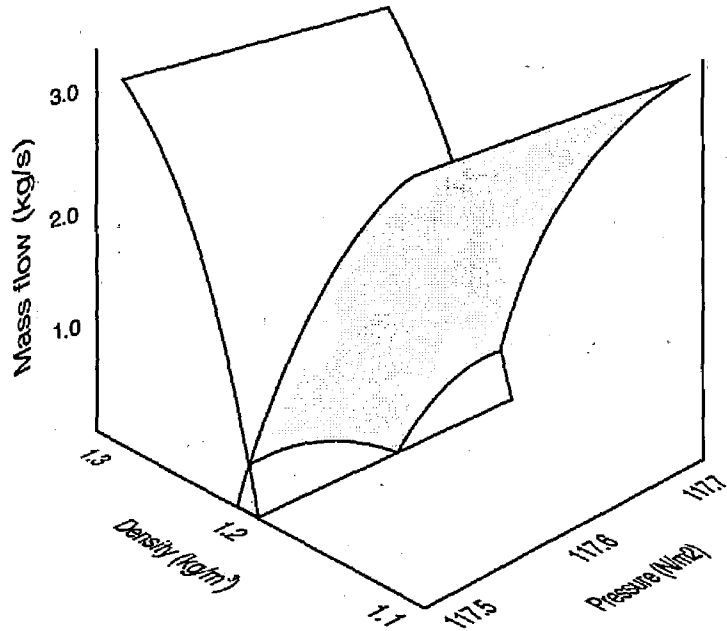


Figure 6. An example of vertical flow between two compartments.

3.3.3 Forced Flow

The model for mechanical ventilation is based on the theory of networks and is based on the model developed by Klotz [42]. This is a simplified form of Kirchoff's law which says that flow into a node must be balanced by flow out of the node. There is a close analog to electrical networks for which the flow consists of electrons. In the case of ventilation, the flow is formed by molecules of air. The conservation equation differs slightly from that of an electrical system, but the basic ideas carry over. For the former case, we have:

$$\text{voltage} = \text{current} \times \text{resistance}.$$

In the present case we have

$$\text{pressure change} = \text{mass flow} \times \text{resistance} .$$

So the application of network theory is used, although the circuit laws are slightly different. In practice, as with the electrical analog, one solves the problem by summing all of the equations for the nodes, and requires that the mass be conserved at each node. Thus we turn the equation around and put it into the form

$$\text{mass flow} = \text{conductance} \times (\text{pressure drop across a resistance})^{1/2} .$$

For each node, this flow must sum to zero. There are several assumptions which are made in computing this flow in ducts, fans, elbow, *etc.* First, we assume unidirectional flow. Given the usual size of ducts, and the nominal presence of fans, this is quite reasonable. Also, the particular implementation used here [42] does not allow for reverse flow in the duct system. The difficulty lies in describing how a fan behaves in such a case.

Given that we can describe mass flow in terms of pressure differences and conductance, the conservation equation for each node is

$$\sum_j \dot{m}_{ij} = 0. \quad (60)$$

The index "j" is a summation over connections to a node, and there is an equation "i" for each node. The remaining problem is to specify the boundary conditions. At each connection to a compartment, the pressure is specified. Then, given that flow at each connection is unidirectional (at a given instant of time, the flow is either all into or all out of a given connection), the mass and enthalpy flow into or out of a room can be calculated explicitly. Thus we end up with a set of equations of the form

$$\begin{aligned} f_1(P_1, P_2, \dots) &= 0 \\ &\vdots \\ f_i(P_1, P_2, \dots) &= 0 \\ &\vdots \\ f_n(P_1, P_2, \dots) &= 0. \end{aligned} \quad (61)$$

This is an algebraic set of equations that is solved simultaneously with the equations for flow in the compartments.

The equations describe the relationship between the pressure drop across a duct, the resistance of a duct, and the mass flow. The pressure can be changed by conditions in a compartment, or a fan in line in the duct system. Resistance arises from the finite size of ducts, roughness on surfaces, bends and joints. To carry the electrical analog a little further, fans act like constant voltage sources. The analogy breaks down, however, in that the voltage, current and resistance are related by the square of the current, rather than being linearly proportional. Since we are using the current form of the conservation equation to balance the system, the flow can be recast in terms of a conductance

$$\dot{m} = G\sqrt{\Delta P} . \quad (62)$$

The conductance can be expressed generally as

$$G = \sqrt{\frac{2p}{C_0}} A_0 \quad (63)$$

where C_0 is the flow coefficient, and A_0 is the area of the inlet, outlet, duct, contraction or expansion joint, coil, damper, bend, filter, and so on. Their values for the most common of these items are tabulated in the ASHRAE Handbook [43].

Ducts are long pipes through which gases can flow. They have been studied much more extensively than other types of connections. For this reason, eq (63) can be put into a form which allows one to characterize the conductance in more detail, depending on the type of duct (e.g., oval, round, or square). The form derives from the Darcy equation and is

$$G = \sqrt{\frac{FL}{2\rho D_e A_0^2}} \quad (64)$$

where F is the friction factor and can be calculated from

$$\frac{1}{\sqrt{F}} = -2 \log \left(\frac{\epsilon}{3.7 D_e} + \frac{2.51}{R_e \sqrt{F}} \right) \quad (65)$$

For each node in the system, one has an entry of the form of eq (63).

The temperature for each duct d is determined using the following differential equation

accumulated heat = (heat in - heat out) - convective losses through duct walls

$$c_v \rho_d V_d \frac{dT_d}{dt} = c_p m_d (T_{in} - T_{out}) - h_d A_d (T_d - T_{amb}) \quad (66)$$

where c_v , c_p are the specific heats at constant volume, pressure; V_d is the duct volume, ρ_d is the duct gas density, dT_d/dt is the time rate of change of the duct gas temperature, m_d is the mass flow rate, T_{in} and T_{out} are the gas temperatures going into and out of the duct, c_d , A_d are the convective heat transfer coefficient and surface area for duct d and T_{amb} is the ambient temperature. The first term on the right hand side of eq (66) represents the net gain of energy due to gas transported into or out of the duct. The second term represents heat transferred to the duct walls due to convection. In version 1.6, the loss coefficient is set to zero. We retain the form for future work. The differential and algebraic (DAE) solver used by CFAST solves eq (66) exactly as written. A normal ordinary differential equation solver would require that this equation be solved for dT/dt . By writing it this way, the duct volumes can be zero which is the case for fans.

The mechanical ventilation system is partitioned into one or more independent systems. Differential equations for species for each of these systems are derived by lumping all ducts in a system into one

pseudo tank. The equations for each tank are solved using time splitting similar to how the gas layer species are computed.

This set of equations is then solved at each time step. Previously the mechanical ventilation computations in CFAST were performed as a side calculation using time splitting. This could cause problems since time-splitting methods require that the split phenomenon (the pressures and temperatures in this case) change slowly compared to other phenomenon such as room pressures, layer heights etc. The pressures at each internal node and the temperatures in each branch (duct, fan) are now determined explicitly by the solver once again using conservation of mass and energy.

3.4 Heat Transfer

3.4.1 Radiation

Objects such as walls, gases and fires radiate as well as absorb radiation. Each object has its own properties, such as temperature and emissivity. As we are solving the enthalpy equation for the gas temperature, the primary focus is in finding out how much enthalpy is gained or lost by the gas layers due to radiation. To calculate the radiation absorbed in a zone, a heat balance must be done which includes all surfaces which radiate to and absorb radiation from a zone. The form of the terms which contribute heat to an absorbing layer are the same for all layers. Essentially we assume that all zones in these models are similar so we can discuss them in terms of a general layer contribution. For this calculation to be done in a time commensurate with the other sources, some approximations are necessary.

Radiation can leave a layer by going to another layer, by going to the walls, by exiting through a vent, by heating an object, or by changing the pyrolysis rate of the fuel source. Similarly, a layer can be heated by absorption of radiation from these surfaces and objects as well as from the fire itself. The formalism which we employ for the geometry and view factor calculation is that of Siegel and Howell [45]. Although the radiation could be done with a great deal of generality, we have assumed that the zones and surfaces radiate and absorb like a grey body.

Radiation is an important mechanism for heat exchange in compartments subject to fires. It is important in the present application because it can affect the temperature distribution within a compartment, and thus the buoyancy forces. In the present implementation the fire is assumed to be a point source; it is assumed that plumes do not radiate. We use a simplified geometrical equivalent of the compartment in order to calculate the radiative transfer between the ceiling, floor and layer(s). The original paper which described FAST pointed out that there was an inconsistency in the interaction between the walls and the radiation from and to the gas layers. This modification fixes that problem. A radiative heat transfer calculation could easily dominate the computation in any fire model. This is because radiation exchange is a global phenomena. Each portion of an enclosure interacts radiatively with every other portion that it "sees." Therefore, it is important to construct algorithms for radiative heat transfer that are both accurate and efficient [44].

This is a "next step" algorithm for computing radiative heat transfer between the bounding surfaces of a compartment containing upper and lower layer gasses and point source fires. The two-wall radiation model used has been enhanced to treat lower layer heating and to treat radiative heat exchange with the upper and lower walls independently of the floor and ceiling. We refer to this as the four wall model.

The original radiation algorithm used the extended floor and ceiling concept for computing radiative heat exchange. For the purposes of this calculation, the room is assumed to consist of two wall segments: an

extended ceiling and an extended floor. The extended ceiling consisted of the ceiling plus the upper wall segments. Similarly, the extended floor consisted of the floor plus the lower wall segments. The upper layer was modeled as a sphere equal in volume to the volume of the upper layer. Radiative heat transfer to and from the lower layer was ignored. This algorithm is inconsistent with the way heat conduction is handled, since we solve up to four heat conduction problems for each room: the ceiling, the upper wall, the lower wall and the floor. The purpose of the new radiation algorithm then is to enhance the radiative module to allow the ceiling, the upper wall segments, the lower wall segments and the floor to transfer radiant heat independently and consistently.

The four wall algorithm for computing radiative heat exchange is based upon the equations developed in Siegel and Howell [45] which in turn is based on the work of Hottel [46]. Siegel and Howell model an enclosure with N wall segments and an interior gas. A radiation algorithm for a two layer zone fire model requires treatment of an enclosure with two uniform gases. Hottel and Cohen [47] developed a method where the enclosure is divided into a number of wall and gas volume elements. An energy balance is written for each element. Each balance includes interactions with all other elements. Treatment of the fire and the interaction of the fire and gas layers with the walls is based upon the work of Yamada and Cooper [48]. They model fires as point heat sources radiating uniformly in all directions and use the Lambert-Beer law to model the interaction between heat emitting elements (fires, walls, gas layers) and the gas layers. The original formulation is for an N -wall configuration. Although this approach would allow arbitrary specification of compartment surfaces (glass window walls, for example), the computational requirements are significant.

Even the more modest approach of a four wall configuration for computing radiative heat transfer is more sophisticated than was used previously. By implementing a four wall rather than an N wall model, significant algorithmic speed increases were achieved. This was done by exploiting the simpler structure and symmetry of the four wall problem.

The radiation exchange at the k 'th surface is shown schematically in Figure 7. For each wall segment k from 1 to N we must find a net heat flux, Δq_k , such that

$$A_k \epsilon_k \sigma T_k^4 + (1 - \epsilon_k) q_k^{in} = q_k^{in} + A_k \Delta q_k \quad (k=1, \dots, N). \quad (67)$$

Radiation exchange at each wall segment has emitted, reflected, incoming and net radiation terms. Equation (67) then represents a system of linear equations that must be solved for Δq_k to determine the net fluxes given off by each surface. The setup and solution of this linear system is the bulk of the work required to implement the net radiation method of Siegel and Howell. Equation (68) derived by Siegel and Howell [45] and listed there as eqs 17 to 20, is called the **net radiation equation**,

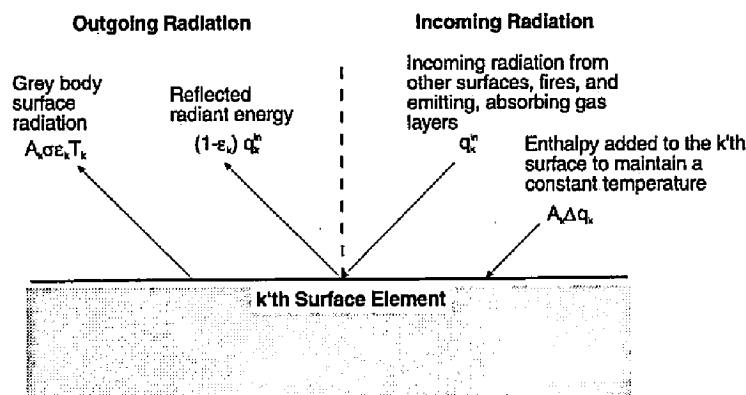


Figure 7. Radiation exchange in a two-zone fire model.

$$\frac{\Delta q_k''}{\epsilon_k} - \sum_{j=1}^N \frac{1-\epsilon_j}{\epsilon_j} \Delta q_j'' F_{k-j} \tau_{j-k} = \sigma T_k^4 - \sum_{j=1}^N \sigma T_j^4 F_{k-j} \tau_{j-k} - \frac{c_k}{A_k} \quad (68)$$

where σ is the Stefan-Boltzman constant, ϵ_k is the emissivity of the k 'th wall segment, T_k is the temperature of the k 'th wall segment, F_{k-j} a configuration factor, and τ is a transmissivity factor. This latter is the fraction of energy passing unimpeded through a gas along a path from surface j to k . The parameters c_k represent the various sources of heat, namely the fire itself and the gas layers. In the form shown, the view factor of the k 'th element is included in the parameter c .

The actual implementation uses a slightly modified form of eq (68), namely

$$\Delta \hat{q}_k'' - \sum_{j=1}^N (1-\epsilon_j) \Delta \hat{q}_j'' F_{k-j} \tau_{j-k} = \sigma T_j^4 - \sum_{j=1}^N \sigma T_j^4 F_{k-j} \tau_{j-k} - \frac{c_k}{A_k}, \text{ where} \quad (69)$$

$$\Delta q_k'' = \epsilon_k \Delta \hat{q}_k'' \quad (70)$$

There are two reasons for solving eq (69) rather than eq (68). First, since ϵ_k does not occur in the denominator, radiation exchange can be calculated when some of the wall segments have zero emissivity. Second and more importantly, the matrix corresponding to the linear system of eq (70) is diagonally dominant [44]. Iterative algorithms can be used to solve such systems more efficiently than direct methods such as Gaussian elimination. The more diagonally dominant a matrix (the closer the emissivities are to unity), the quicker the convergence when using iterative methods. Typical values of the emissivity for walls subject to a fire environment are in the range of $0.85 < \epsilon < 0.95$, so this is a reasonable approximation. The computation of, F_{k-j} , τ_{j-k} and c_k is discussed by Forney [44]. It is shown how it is possible to use the symmetries present in the four wall segment problem to minimize the number of direct configuration factor calculations required.

For rooms containing a fire, CFAST models the temperature of four wall segments independently. A two wall model for radiation exchange can break down when the temperatures of the ceiling and upper walls differ significantly. This typically happens in the room of fire origin when different wall materials are used as boundaries for the ceiling, walls and floor. To demonstrate this consider the following example.

To simplify the comparison between the two and four wall segment models, assume that the wall segments are black bodies (the emissivities of all wall segments are one) and the gas layers are transparent (the gas absorptivities are zero). This is legitimate since for this example we are only interested in comparing how a two wall and a four wall radiation algorithm transfer heat to the wall segments. Let the room dimensions be $4 \times 4 \times 4$ [m], the temperature of the floor and the lower and upper walls be 300 K. Let the ceiling temperature vary from 300 to 600 K.

Figure 8 shows a plot of the heat flux to the ceiling and upper wall as a function of the ceiling temperature [44], [49]. The two wall model predicts that the extended ceiling (a surface formed by combining the ceiling and upper wall into one wall segment) cools, while the four wall model predicts that the ceiling cools and the upper wall warms. The four-wall model moderates temperature differences that may exist between the ceiling and upper wall (or floor and lower wall) by allowing heat transfer to occur between the ceiling and upper wall. The two wall model is unable to predict heat transfer between the ceiling and the upper wall since it models them both as one wall segment.

3.4.2 Convection

Convection is one of the mechanisms by which the gas layers lose or gain energy to walls, objects or through openings. Conduction is a process which is intimately associated with convection; but as it does not show up directly as a term for heat gain or loss, it will be discussed separately. Convective heating describes the energy transfer between solids and gases. The enthalpy transfer associated with flow through openings will be discussed in the section on flow through vents.

Convective heat flow is enthalpy transfer across a thin boundary layer. The thickness of this layer is determined by the temperature difference between the gas zone and the wall or object being heated [50]. We can write the heat flux term as

$$\dot{Q}_c = h_c (T_g - T_w) A_w \quad (71)$$

where the transfer coefficient (assuming natural convection) can be written as

$$h_c = \frac{\kappa}{l} C_o (Gr Pr)^{1/3}$$

$$Gr = \frac{gl^3 |T_g - T_w|}{\nu^2 T_g}$$

$$\kappa = 2.72 \times 10^{-4} \left(\frac{T_g + T_w}{2} \right)^{4/5}$$

$$\nu = 7.18 \times 10^{-10} \left(\frac{T_g + T_w}{2} \right)^{7/4} \quad (72)$$

and T_g and T_w are the temperatures of the gas layer and the wall respectively, A_w is the area of surfaces in contact with the zone, Pr is the Prandtl number (0.72), l is a characteristic length scale $\approx (A_w)^{1/2}$, and C_o is a coefficient which depends on orientation [50].

For the cases of interest we use the coefficients shown below. The coefficients for horizontal surfaces apply to a slab over a zone, such as ceiling surfaces. For a floor, the conditions (T_g and T_w) are reversed. For the outside boundary, the condition is reversed, at least for the ceiling and floor. Physically, outside a compartment, the ceiling of a compartment will behave as if it were the floor of a compartment over it, and similarly for the floor of a compartment. Thus, we use the floor boundary coefficient for the

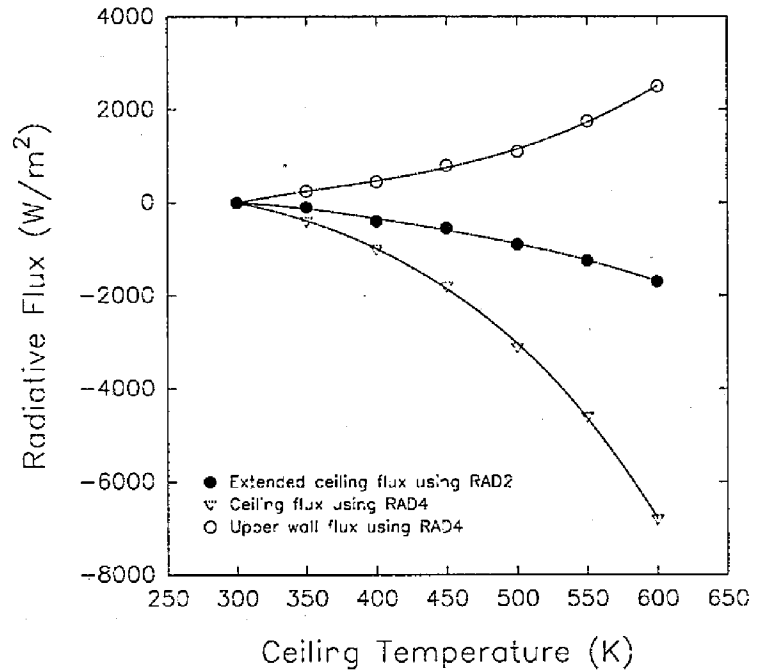


Figure 8. An example of two-wall and four-wall calculations for radiation exchange on a ceiling and wall surface.

outside boundary of the ceiling and the ceiling coefficient for the outside boundary of a compartment floor. For vertical boundaries, the coefficient remains the same on the interior and exterior.

Orientation	Coefficient[C _o]	Condition
Vertical	0.12	all
Horizontal	0.13	$T_g > T_w$
Horizontal	0.16	$T_g < T_w$

These coefficients are for turbulent boundary layer flow. They overestimate the heat transfer which can occur in a quiescent compartment.

The boundary condition which connects the interior of the wall to the zone is fairly straightforward. This convective heating generates a flux from the gas layer which becomes a derivative boundary condition for the conduction algorithm. A similar boundary condition must be applied on the exterior of the walls. The assumption made is that the exterior portion of a wall is truly facing the ambient. This precludes a fire in one compartment heating a connected compartment through conduction. The omission is due to the difficulty of specifying how compartment walls are connected and not to the difficulty of specifying the boundary conditions or solving the equations. So the boundary condition for the exterior of a wall is similar to the interior, except that the exterior surface is assumed to be convecting and radiating to the ambient. With this caveat in mind, we can use the convection routine to calculate the boundary condition for the exterior wall also.

The current model allows for a ceiling, floor and two walls. Actually the two walls are the same material, but a separate temperature profile is maintained for the wall in contact with the upper and lower zones respectively. Therefore we have four components for convective heat transfer.

3.4.3 Conduction

Conduction of heat through solids is not a source term in the sense discussed earlier. That is, loss or gain of energy from solids occurs by convective heating, which in turn is influenced by subsequent gain or loss through the solids. However, as much of the net heat loss from a compartment occurs through loss to the walls and heating of interior objects and thus provides the boundary conditions for the other source terms discussed above.

The equation which governs the heat transfer in solids is

$$\frac{\partial T}{\partial t} = \frac{k}{\rho c} \nabla^2 T \quad (73)$$

and is a linear parabolic equation. As such it must be solved by a different technique than is used for the ordinary differential equations which describe mass and enthalpy flux. The equation is linear only if the coefficients k , ρ and c are independent of temperature throughout the material. This may not be the case, especially for some materials such as gypsum for which the value of k may vary by a factor of two or more. However, to the accuracy that we know most of the thermal properties, it is a reasonable approximation. Procedures for solving 1-d heat conduction problems are well known. For finite difference methods such as backward difference (fully implicit), forward difference (fully explicit) or Crank-Nicolson, see [51]. For finite element methods see [52].

To advance the solution for the wall temperature profile, a finite difference approach [53] is used. A graded (non-uniform) mesh with n_x breakpoints was introduced for the spatial variable x . The second spatial derivative in the heat equation was replaced by a second divided (finite) difference approximation. This produces a system of n_{x-2} ODE's for the n_{x-2} unknown temperatures at the interior breakpoints. The conduction is tightly coupled to the room conditions from temperatures at the interior boundary supplied by the differential equation solver. The exterior boundary conditions (constant flux, insulated, or constant temperature) is specified in the configuration of CFAST. This system was solved by one step of the backward Euler method. Crank-Nicholson was also tried but produced spurious oscillations in the temperature profiles at the beginning of the simulation; backward Euler does not suffer from this defect which is related to the non-uniform mesh being used. The solution at time $t + \delta t$ can be found by solving a tridiagonal system of linear equations. The temperature gradient at $x=0$ and time $t + \delta t$ was approximated by computing a derivative difference using the first two temperatures.

A graded mesh scheme was chosen to allow breakpoints to cluster near the interior and exterior wall segment surfaces. This is where the temperature gradients are the steepest. A breakpoint x_b was defined by $x_b = \text{MIN}(x_p, W/2)$, where $x_p = 2(\alpha t_{final})^{1/2} \text{erfc}^{-1}(0.05)$ and erfc^{-1} denotes the inverse of the complementary error function. The value x_p is the location in a semi-infinite wall where the temperature rise is 5 percent after t_{final} seconds and is sometimes called the penetration depth. Eighty percent of the breakpoints were placed on the interior side of x_b and the remaining 20 percent were placed on the exterior side.

In this version of the model, we use a new strategy for coupling the 1-d heat conduction problem with the ODE's for the gas solution variables based on the work of Moss and Forney [53]. This method couples the wall segment surface temperatures, rather than the entire wall segment temperature profile, with the gas solution variables by requiring that the wall segment surface temperature gradient, $\partial u(x,t)/\partial x$, and the incident heat flux (sum of convective and net radiative flux), q'' satisfy Fourier's law

$$q'' = -\kappa \frac{\partial u(x,t)}{\partial x} \quad (74)$$

at the wall boundary $x=0$ where K is the thermal conductivity of the wall material. This solution strategy requires a DAE solver that can simultaneously solve both differential (gas ODE's) and algebraic equations (Fourier's law). With this method, only one or two extra equations are required per wall segment (two if both the interior and exterior wall segment surface temperatures are computed). This solution strategy is more efficient than the method of lines since fewer equations need to be solved. Wall segment temperature profiles, however, still have to be stored so there is no decrease in storage requirements.

To illustrate the method, consider a one room case with one active wall. There will be four gas equations (pressure, upper layer volume, upper layer temperature, and lower layer temperature) and one wall temperature equation. Implementation of the gradient matching method requires that storage be allocated for the temperature profile at the previous time, t , and at the next time, $t + \delta t$. Given the profile at time t and values for the five unknowns at time $t + \delta t$ (initial guess by the solver), the temperature profile is advanced from time t to time $t + \delta t$. The temperature profile gradient at $x = 0$ is computed followed by the residuals for the five equations. The DAE solver adjusts the solution variables and the time step until the residuals for all the equations are below an error tolerance. Once the solver has completed the step, the array storing the temperature profile for the previous time is updated, and the DAE solver is ready to take its next step.

One limitation of our implementation of conduction is that it serves only as a loss term for enthalpy. Heat lost from a compartment by conduction is assumed to be lost to the outside ambient. In reality, compartments adjacent to the room which contains the fire can be heated, possibly catastrophically, by conducted energy not accounted for in the model. Although solving the conduction equations for this

situation is not difficult, the geometrical specification is. For this reason, we have chosen to assume that the outside of a boundary is always the ambient. A means to connect compartments physically so that heat can be transported by conduction is under active study.

3.4.4 Ceiling Jet

Relatively early in the development of a fire, fire-driven ceiling jets and gas-to-ceiling convective heat transfer can play a significant role in room-to-room smoke spread and in the response of near-ceiling mounted detection hardware. Cooper [54] details a model and computer algorithm to predict the instantaneous rate of convective heat transfer from fire plume gases to the overhead ceiling surface in a room of fire origin. The room is assumed to be a rectangular parallelepiped and, at times of interest, ceiling temperatures are simulated as being uniform. Also presented is an estimate of the convective heat transfer due to ceiling-jet driven wall flows. The effect on the heat transfer of the location of the fire within the room is taken into account. This algorithm has been incorporated into the CFAST model. In this section, we provide an overview of the model. For complete details, we refer the reader to reference [54].

A schematic of a fire, fire plume, and ceiling jet is shown in Figure 9. The buoyant fire plume rises from the height Z_{fire} toward the ceiling. When the fire is below the layer interface, its mass and enthalpy flow are assumed to be deposited into the upper layer at height Z_{layer} . Having penetrated the interface, a portion of the plume typically continues to rise toward the ceiling. As it impinges on the ceiling surface, the plume gases turn and form a relatively high temperature, high velocity, turbulent ceiling jet which flows radially outward along the ceiling and transfers heat to the relatively cool ceiling surface. The convective heat transfer rate is a strong function of the radial distance from the point of impingement, reducing rapidly with increasing radius. Eventually, the relatively high temperature ceiling jet is blocked by the relatively cool wall surfaces [55]. The ceiling jet then turns downward and outward in a complicated flow along the vertical wall surfaces [56], [57]. The descent of the wall flows and the heat transfer from them are eventually stopped by upward buoyant forces. They are then buoyed back upward and mix with the upper layer.

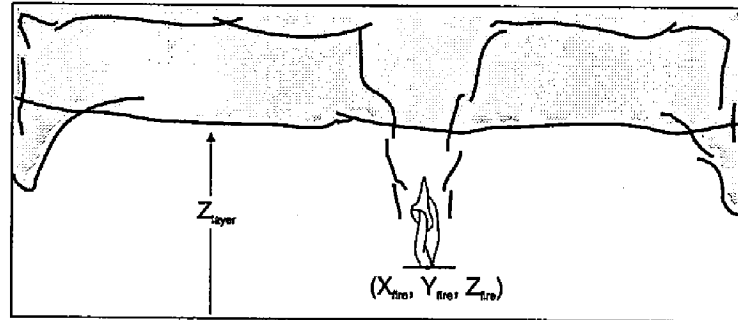


Figure 9. Convective heat transfer to ceiling and wall surfaces via the ceiling jet.

The average convective heat flux from the ceiling jet gases to the ceiling surface, \dot{Q}_{ceil} , can be expressed in integral form as

$$\dot{Q}_{ceil} = \int_0^{X_{wall}} \int_0^{Y_{wall}} \dot{q}''_{ceil}(x,y) dx dy \quad (75)$$

The instantaneous convective heat flux, $\dot{q}''_{ceil}(X,Y)$ can be determined as derived by Cooper [54]:

$$\dot{q}''_{ceil}(x,y) = h_l (T_{ad} - T_{ceil}) \quad (76)$$

where T_{ad} , a characteristic ceiling jet temperature, is the temperature that would be measured adjacent to an adiabatic lower ceiling surface, and h_l is a heat transfer coefficient. h_l and T_{ad} are given by

$$\frac{h_l}{\tilde{h}} = \begin{cases} 8.82 Re_H^{-1/2} Pr^{-2/3} \left(1 - \left(5 - 0.284 Re_H^{2/5} \right) \frac{r}{H} \right) & 0 \leq \frac{r}{H} < 0.2 \\ 0.283 Re_H^{0.3} Pr^{-2/3} \left(\frac{r}{H} \right)^{-1.2} \frac{\frac{r}{H}^{-0.0771}}{\frac{r}{H}^{+0.279}} & 0.2 \leq \frac{r}{H} \end{cases} \quad (77)$$

$$\frac{T_{ad} - T_u}{T_u \dot{Q}_H^{*2/3}} = \begin{cases} 10.22 - 14.9 \frac{r}{H} & 0 \leq \frac{r}{H} < 0.2 \\ 8.39 f\left(\frac{r}{H}\right) & 0.2 \leq \frac{r}{H} \end{cases} \quad (78)$$

where

$$f\left(\frac{r}{H}\right) = \frac{1 - 1.10 \left(\frac{r}{H}\right)^{0.8} + 0.808 \left(\frac{r}{H}\right)^{1.6}}{1 - 1.10 \left(\frac{r}{H}\right)^{0.8} + 2.20 \left(\frac{r}{H}\right)^{1.6} + 0.690 \left(\frac{r}{H}\right)^{2.4}} \quad (79)$$

$$r = \left((X - X_{fire})^2 + (Y - Y_{fire})^2 \right)^{1/2} \quad (80)$$

$$\tilde{h} = \rho_u C_p g^{1/2} H^{1/2} \dot{Q}_H^{*1/3}; \quad Re_H = \frac{g^{1/2} H^{3/2} \dot{Q}_H^{*1/3}}{v_u}; \quad \dot{Q}_H^* = \frac{\dot{Q}'}{\rho_u C_p T_u (gH)^{1/2} H^2} \quad (81)$$

$$\dot{Q}' = \begin{cases} \dot{Q}_{fc} \frac{\sigma \dot{M}^*}{1 + \sigma} & Z_{fire} < Z_{layer} < Z_{ceil} \\ \dot{Q}_{fc} & \begin{matrix} Z_{fire} \geq Z_{layer} \\ Z_{layer} = Z_{ceil} \end{matrix} \end{cases} \quad \dot{M}^* = \begin{cases} 0 & -1 < \sigma \leq 0 \\ \frac{1.04599\sigma + 0.360391\sigma^2}{1 + 1.37748\sigma + 0.360391\sigma^2} & \sigma > 0 \end{cases} \quad (82)$$

$$\sigma = \frac{1 - \frac{T_u}{T_l} + C_T \dot{Q}_{EQ}^{*2/3}}{\frac{T_u}{T_l}}; \quad C_T = 9.115 \quad (83)$$

$$\dot{Q}_{EQ}^* = \left(\frac{0.21 \dot{Q}_{fc}}{C_p T_l \dot{m}_p} \right)^{3/2} \quad (84)$$

In the above, H is the distance from the (presumed) point source fire and the ceiling, X_{fire} and Y_{fire} are the position of the fire in the room, Pr is the Prandtl number (taken to be 0.7) and ν_u is the kinematic viscosity of the upper layer gas which is assumed to have the properties of air and can be estimated from $\nu_u = 0.04128(10^7)T_u^{5/2}/(T_u+110.4)$. \dot{Q}_H^* and \dot{Q}_{EQ}^* are dimensionless numbers and are measures of the strength of the plume at the ceiling and the layer interface, respectively.

When the ceiling jet is blocked by the wall surfaces, the rate of heat transfer to the surface increases. Reference [54] provides details of the calculation of wall surface area and convective heat flux for the wall surfaces.

3.5 Species Concentration and Deposition

3.5.1 Species Transport

The species transport in CFAST is really a matter of bookkeeping to track individual species mass as it is generated by a fire, transported through vents, or mixed between layers in a compartment. When the layers are initialized at the start of the simulation, they are set to ambient conditions. These are the initial temperature specified by the user, and 23 percent by mass (21 percent by volume) oxygen, 77 percent by mass (79 percent by volume) nitrogen, a mass concentration of water specified by the user as a relative humidity, and a zero concentration of all other species. As fuel is burned, the various species are produced in direct relation to the mass of fuel burned (this relation is the species yield specified by the user for the fuel burning). Since oxygen is consumed rather than produced by the burning, the "yield" of oxygen is negative, and is set internally to correspond to the amount of oxygen used to burn the fuel (within the constraint of available oxygen limits discussed in sec. 3.1.2).

Each unit mass of a species produced is carried in the flow to the various rooms and accumulates in the layers. The model keeps track of the mass of each species in each layer, and knows the volume of each layer as a function of time. The mass divided by the volume is the mass concentration, which along with the molecular weight gives the concentration in volume percent or ppm as appropriate.

3.5.2 HCl Deposition

Hydrogen chloride produced in a fire can produce a strong irritant reaction that can impair escape from the fire. It has been shown [58] that significant amounts of the substance can be removed by adsorption by surfaces which contact smoke. In our model, HCl production is treated in a manner similar to other species. However, an additional term is required to allow for deposition on, and subsequent absorption into, material surfaces.

The physical configuration that we are modeling is a gas layer adjacent to a surface (Figure 10). The gas layer is at some temperature T_g with a concomitant density of hydrogen chloride, ρ_{HCl} . The mass transport coefficient is calculated based on the Reynolds analogy with mass and heat transfer: that is, hydrogen chloride is mass being moved convectively in the boundary

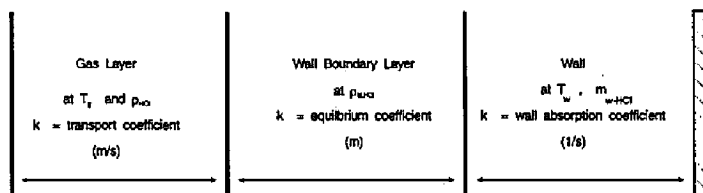


Figure 10. Schematic of hydrogen chloride deposition region.

layer, and some of it simply sticks to the wall surface rather than completing the journey during the convective roll-up associated with eddy diffusion in the boundary layer. The boundary layer at the wall is then in equilibrium with the wall. The latter is a statistical process and is determined by evaporation from the wall and stickiness of the wall for HCl molecules. This latter is greatly influenced by the concentration of water in the gas, in the boundary layer and on the wall itself.

The rate of addition of mass of hydrogen chloride to the gas layer is given by

$$\frac{d}{dt}m_{HCl} = \text{source} - k_c \times (\rho_{HCl} - \rho_{bHCl}) \times A_w \quad (85)$$

where source is the production rate from the burning object plus flow from other compartments.

For the wall concentration, the rate of addition is

$$\frac{d}{dt}d_{HCl,w} = k_c \times (\rho_{HCl} - \rho_{bHCl}) - k_s \times m_{HCl,w} \quad (86)$$

where the concentration in the boundary layer, ρ_{bHCl} , is related to the wall surface concentration by the equilibrium constant k_e ,

$$\rho_{bHCl} = d_{HCl,w} / k_e \quad (87)$$

We never actually solve for the concentration in the boundary layer, but it is available, as is a boundary layer temperature if it were of interest. The transfer coefficients are

$$k_c = \frac{\dot{q}}{\Delta T \rho_g c_p} \quad (88)$$

$$k_e = \frac{b_1 e^{1500/T_w}}{1 + b_2 e^{1500/T_w} \rho_{hcl}} \left(1 + \frac{b_5 (\rho_{H_2O})^{b_6}}{(\rho_{H_2O,sat} - \rho_{H_2O,g})^{b_7}} \right) \quad (89)$$

$$k_s = b_3 e^{-\left(\frac{b_4}{R T_w}\right)} \quad (90)$$

The only values currently available [59] for these quantities are shown in Table 5. The "b" coefficients are parameters which are found by fitting experimental data to eqs (85) through (90). These coefficients reproduce the adsorption and absorption of HCl reasonably well. Note though that error bars for these coefficients have not been reported in the literature.

The experimental basis for poly(methyl methacrylate) and gypsum cover a sufficiently wide range of conditions that they should be usable in a variety of practical situations. The parameters for the other surfaces do not have much experimental backing, and so their use should be limited to comparison purposes.

Table 5. Transfer coefficients for HCl deposition

Surface	b_1 (m)	b_2 (m ³ /kg)	b_3 (s ⁻¹)	b_4 (J/g-mol)	b_5 a	b_6 c	b_7 c
Painted Gypsum	0.0063	191.8	0.0587	7476.	193	1.021	0.431
PMMA	9.6×10^{-5}	0.0137	0.0205	7476.	29	1.0	0.431
Ceiling Tile	4.0×10^{-3}	0.0548	0.123	7476.	30 ^b	1.0	0.431
Cement Block	1.8×10^{-2}	5.48	0.497	7476.	30 ^b	1.0	0.431
Marinite®	1.9×10^{-2}	0.137	0.030	7476.	30 ^b	1.0	0.431

a units of b_5 are (m³/kg)^(b₇-b₆)

b very approximate value, insufficient data for high confidence value

c non-dimensional

4 Verification of the Model

4.1 Available Experimental Data

Several systematic test series have been undertaken specifically to provide data for comparison with model predictions. In other cases, tests in which fire properties have been systematically varied (for various reasons) have been modeled using current computer fire simulations. In the first group are the study of Alpert et al. [60] for a single room connected to a short, open corridor, and those of Cooper et al. [61] and Peacock et al. [24] for gas burner fires in a room-corridor-room configuration. Although the second group is large, the works of Quintiere and McCaffrey [62], and Heskestad and Hill [63] are particularly detailed.

Cooper et al. [61] reported an experimental study of the dynamics of smoke filling in realistic, full-scale, multi-room fire scenarios. A major goal of the study was to generate an experimental database for use in the verification of mathematical fire simulation models. The test space involved 2 or 3 rooms, connected by open doorways. During the study, the areas were partitioned to yield four different configurations. One of the rooms was a burn room containing a methane burner which produced either a constant heat release rate of 25, 100, or 225 kW or a time-varying heat release rate which increased linearly with time from zero at ignition to 300 kW in 600 s. An artificial smoke source near the ceiling of the burn room provided a means for visualizing the descent of the hot layer and the dynamics of the smoke filling process in the various spaces. The development of the hot stratified layers in the various spaces was monitored by vertical arrays of thermocouples and photometers. A layer interface was identified and its position as a function of time was determined. An analysis and discussion of the results including layer interface position, temperature, and doorway pressure differentials is presented. These data were later used by Rockett et al. [64], [65] for comparison to a modern predictive fire model [66].

Quintiere and McCaffrey [62] described a series of experiments designed to provide a measure of the behavior of cellular plastics in burning conditions related to real life. They experimentally determined the effects of fire size, fuel type, and natural ventilation conditions on the resulting room fire variables, such

as temperature, radiant heat flux to room surfaces, burning rate, and air flow rate. This was accomplished by burning up to four cribs made of sugar pine or of a rigid polyurethane foam to provide a range of fire sizes intended to simulate fires representative of small furnishings to chairs of moderate size. Although few replicates were included in the test series, fuel type and quantity, and the room door opening width were varied. The data from these experiments were analyzed with quantities averaged over the peak burning period to yield the conditions for flashover in terms of fuel type, fuel amount, and doorway width. The data collected were to serve as a basis for assessing the accuracy of a mathematical model of fire growth from burning cribs.

Heskestad and Hill [63] performed a series of 60 fire tests in a room/corridor configuration to establish accuracy assessment data for theoretical fire models of multi-room fire situations with particular emphasis on health care facilities. With steady state and growing fires from 56 kW to 2 MW, measurements of gas temperatures, ceiling temperatures, smoke optical densities, concentrations of CO, CO₂, and O₂, gas velocities, and pressure differentials were made. Various combinations of fire size, door opening size, window opening size, and ventilation were studied. To increase the number of combinations, only a few replicates of several of the individual test configurations were performed.

Except for the data of Cooper et al. [61] and Quintiere and McCaffrey [62] which are not available in machine readable form, the above data, along with other experimental results, have been reviewed by Peacock, Davis and Babrauskas [67]. They provide a single consistent form for the experimental data from several series of experiments. Five sets of experimental data which can be used to test the limits of a typical two-zone fire model are detailed. Availability of ancillary data (such as smaller-scale test results) is included. These descriptions, along with the data should allow comparisons between the experiment and model predictions. The base of experimental data ranges in complexity from one-room tests with individual furniture items to a series of tests conducted in a multiple-story hotel equipped with a zoned smoke control system. These data will be used as the set of experimental results for comparisons in this paper.

4.2 Previous Comparisons with Experimental Data

Several researchers have studied the level of agreement between computer fire models and real-scale fires. These comparisons fall into two broad categories: fire reconstruction and comparison with laboratory experiments. Both categories provide a level of verification for the models used. Fire reconstruction, although often more qualitative, provides a higher degree of confidence for the user when the models successfully simulate real-life conditions. Comparisons with laboratory experiments, however, can yield detailed comparisons that can point out weaknesses in the individual phenomena included in the models.

Fire reconstructions: Nelson [68] used simple computer fire models along with existing experimental data to develop an analysis of a large high-rise building fire. This analysis showed the value of available analytical calculations in reconstructing the events involved in a multiple-story fire. Bukowski [69] has applied the FAST model (an earlier version of the CFAST model) in a litigation against the United States Government. At the request of the Justice Department, the model was used to recreate a multiple-fatality fire in a residence. The analysis reproduced many details of the fire including conditions consistent with damage patterns to the building, the successful escape of three older children, and three fatalities including the locations of the bodies and the autopsy results. Emmons applied computer fire modeling to the MGM Grand Hotel fire of 1980. This work, conducted during the litigation of this fire was only recently published [70]. Using the HARVARD 5 model, Prof. Emmons analyzed the relative contributions of booth seating, ceiling tiles, decorative beams, and the HVAC system on the outcome of the fire.

Comparisons with laboratory experiments: Rockett, Morita, and Cooper [65] used the HARVARD VI multi-room fire model to simulate the results of real-scale, multi-room fire experiments. These experiments can be characterized by fire sizes of several hundred kW and total compartment volume of about 1000 m³. While the model was generally found to provide favorable simulations, several areas where improvements were needed were identified. They pointed out limitations in modeling of oxygen-limited burning, mixing of gases at vents, convective heat transfer, and plume entrainment.

Jones and Peacock [16] presented a limited set of comparisons between the FAST model and a multi-room fire test. The experiment involved a constant fire of about 100 kW in a three-compartment configuration of about 100 m³. They noted "slight over-prediction" of the upper layer temperature and satisfactory prediction of the layer interface position. Again, convective heating and plume entrainment were seen to limit the accuracy of the predictions. A comparison of predicted and measured pressures in the rooms showed good agreement. Since pressure is the driving force for flow between compartments, this agreement was seen as important.

Levine and Nelson [71] used a combination of full-scale fire testing and modeling to simulate a fire in a residence. The 1987 fire in a first-floor kitchen resulted in the deaths of three persons in an upstairs bedroom, one with a reported blood carboxyhemoglobin content of 91 percent. Considerable physical evidence remained. The fire was successfully simulated at full scale in a fully-instrumented seven-room two-story test structure. The data collected during the test have been used to test the predictive abilities of two multiroom computer fire models: FAST and HARVARD VI. A coherent ceiling layer flow occurred during the full-scale test and quickly carried high concentrations of carbon monoxide to remote compartments. Such flow is not directly accounted for in either computer code. However, both codes predicted the carbon monoxide buildup in the room most remote from the fire. Prediction of the pre-flashover temperature rise was also good. Prediction of temperatures after flashover that occurred in the room of fire origin was less good. Other predictions of conditions throughout the seven test rooms varied from good approximations to significant deviations from test data. Some of these deviations are believed to be due to phenomena not considered in any computer models.

Deal [72] reviewed four computer fire models (CCFM [17], FIRST [13], FPETOOL [73] and FAST) to ascertain the relative performance of the models in simulating fire experiments in a small room (about 12 m³ in volume) in which the vent and fuel effects were varied. Peak fire size in the experiments ranged up to 800 kW. All the models simulated the experimental conditions including temperature, species generation, and vent flows, quite satisfactorily. With a variety of conditions, including narrow and normal vent widths, plastic and wood fuels, and flashover and sub-flashover fire temperatures, competence of the models at these room geometries was demonstrated.

Duong [74] studied the predictions of several computer fire models (CCFM, FAST, FIRST, and BRI [14]), comparing the models with one another and with large fires (4 to 36 MW) in an aircraft hanger (60,000 m³). For the 4 MW fire size, he concluded that all the models are reasonably accurate. At 36 MW, however, none of the models did well. Limitations of the heat conduction and plume entrainment algorithms were seen to account for some of the inaccuracies.

4.3 Model Parameters Selected for Comparison

Comparisons of model predictions with experimental measurements serves two purposes: 1) to determine, within limits, the accuracy of the predictions for those quantities of interest to the users of the models (usually those extensive variables related to hazard), and 2) to highlight the strengths and weaknesses of

the underlying algorithms in the models to guide future improvements in the models. The predicted variables selected for comparison must deal with both of these purposes.

Most of the studies discussed above present a consistent set of variables of interest to the model user: gas temperature, gas species concentrations, and layer interface position. To assess the accuracy of the physical basis of the models, additional variables must be included. Pressure drives the movement of gases through openings. The pyrolysis rate, and heat release rate of the fire in turn, produces the gases of interest to be moved.

In this section, we will consider all these variables for comparison:

- upper and lower layer gas temperature,
- layer interface position,
- gas species concentration.
- fire pyrolysis and heat release rate,
- room pressure, and
- vent flow,

Although there are certainly other comparisons of interest, these will provide an indication of the match of the model to the experimental data.

4.4 Experimental Data Selected for Comparison

A total of five different real-scale fire tests were selected for the current comparisons to represent a range of challenges for the CFAST model:

- 1) A single-room test using upholstered furniture as the burning item was selected for its well-characterized and realistic fire source in a simple single-room geometry [75]. Figure 11 shows the room and instrumentation used during the tests. Heat release rate, mass loss rate, and species yields are available for the test. This should allow straightforward application of the model. Peak fire size was about 2.9 MW with a total room volume of 21 m³.

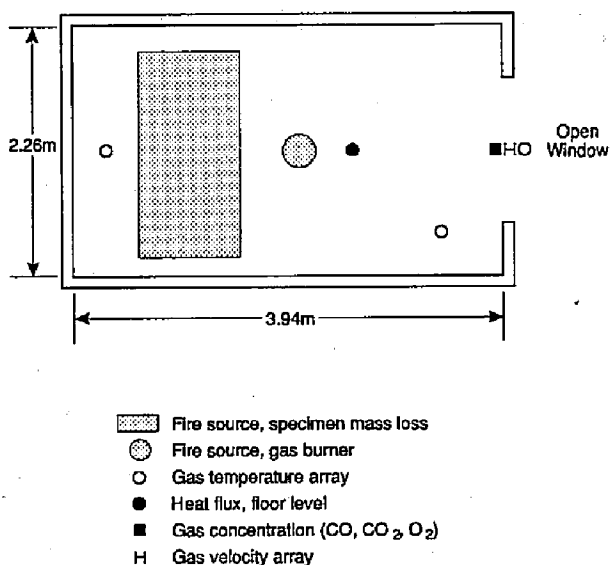


Figure 11. Single-room furniture fire test.

- 2) Like the first test, this test is a single-room fire test using furniture as the fire source [76]. It expands upon that data set by adding the phenomenon of wall burning. Figure 12 shows the test room and exhaust hood arrangement. Peak fire size was about 7 MW. Room size is similar to the first test.

- 3) This data set is actually an average of a series of 11 replicate tests in a three-room configuration with simple steady-state gas burner fires [24]. Figure 13 shows the room configuration and instrumentation for the test. It provides a basic set of quantities that are predicted by current fire models for small to medium size fires. Since all fires were gas burner fires, simulation should be straightforward. It is of particular interest since it was undertaken as a part of a program to develop a methodology for the evaluation and accuracy assessment of fire models. Fire size was about 100 kW with a total volume of 100 m^3 .

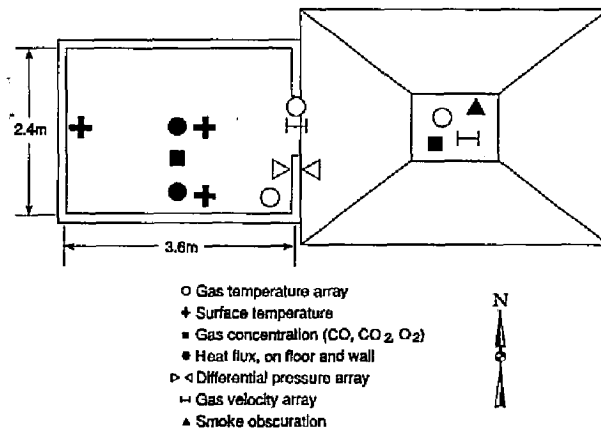


Figure 12. Single-room furniture fire test with wall burning.

- 4) This data set is part a series of tests conducted in a multiple room configuration with more complex gas burner fires than the previous data set [63], [77]. This study was included because it expands upon that data set by providing larger and time-varying gas burner fires in a room-corridor configuration. Figure 14 shows the room configuration and instrumentation for the test. Fire size was about up to 1 MW with a total volume of 200 m^3 .

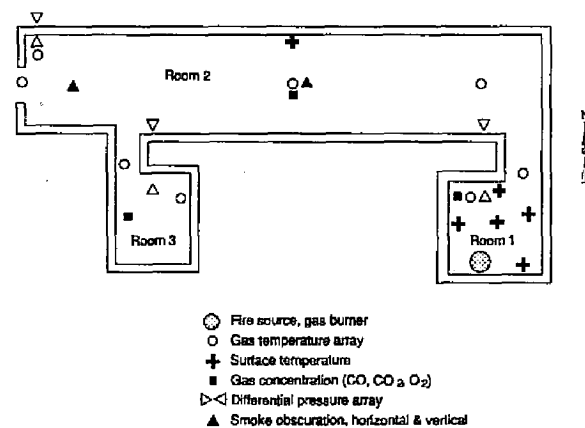


Figure 13. Three-room gas burner tests with a corridor.

- 5) By far the most complex test, this data set is part of a series of full-scale experiments conducted to evaluate zoned smoke control systems, with and without stairwell pressurization [78]. It was conducted in a seven story hotel with multiple rooms on each floor and a stairwell connecting to all floors. Figure 15 shows the room configuration and instrumentation for one of the eight floors of the building. This data set was chosen because it would be considered beyond the scope of most current fire models. Measured temperatures and pressure differences between the rooms and floors of the building are extensive and consistent. Peak fire size was 3 MW with a total building volume of $140,000 \text{ m}^3$.

4.5 Discussion

All of the simulations were performed with the CFAST model on an MS-DOS² compatible computer. For each of the data sets, the model data were developed from the building and fire descriptions provided in the original reports. Obtaining building geometry, construction materials, and room interconnections was straightforward. Usually, description of the fire source was more difficult. Where freeburn data were available, such data were used to describe the heat release rate, pyrolysis rate, and species yields. In other cases, estimates from tests of similar materials or textbook values were used to determine missing quantities.

How to best quantify the comparisons between model predictions and experiments is not obvious. The necessary and perceived level of agreement for any variable is dependent upon both the typical use of the variable in a given simulation (for instance, the user may be interested in the time it takes to reach a certain temperature in the room), the nature of the experiment (peak temperatures would be of little interest in an experiment which quickly reached steady state), and the context of the comparison in relation to other comparisons being made (a true validation of a model would involve proper statistical treatment of many compared variables).

Insufficient experimental data and understanding of how to compare the numerous variables in a complex fire model prevent a true validation of the model. Thus, the comparisons of the differences between model predictions and experimental data in this paper are intentionally simple and vary from test to test and from variable to variable due to the changing nature of the tests and typical use of different variables.

4.5.1 Layer Temperature and Interface Position

Arguably the most frequent question asked about a fire is "How hot did it become?" Temperature in the rooms of a structure is an obvious indicator to answer this question. Peak temperature, time to peak temperature, or time to reach a chosen temperature tenability limit are typical values of interest. Quality of the prediction (or measurement) of layer interface position is more difficult to quantify. Although observed valid in a range of experiments, the two-layer assumption is in many ways just a convenience for modeling. From a standpoint of hazard, time of descent to a chosen level may be a reasonable criterion (assuming some in the room will then either be forced to crawl beneath the interface to breathe the "clean" atmosphere near the floor or be forced to breathe the upper layer gases). Minimum values may also be used to indicate general agreement. For the single-room tests with furniture or wall-burning, these are appropriate indicators to judge the comparisons between model and experiment. For the more-closely

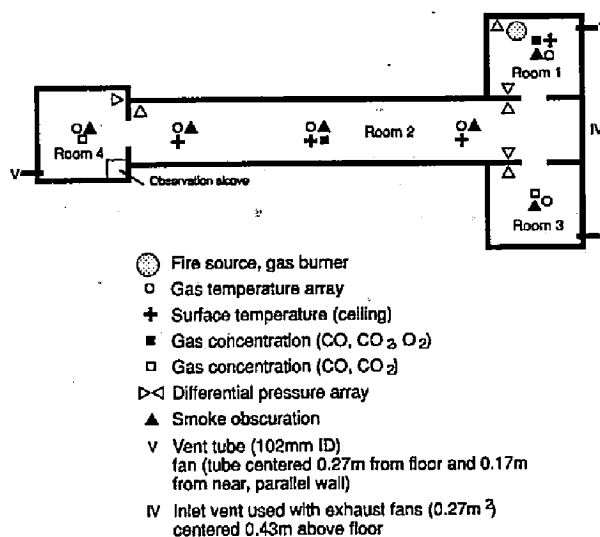


Figure 14. Four-room gas burner tests with a corridor.

² The use of company names or trade names within this report is made only for the purpose of identifying those computer hardware or software products with which the compatibility of the CFAST programs has been tested. Such use does not constitute any endorsement of those products by the National Institute of Standards and Technology.

steady-state three- and four-room tests with corridor or the multiple-story building tests, a steady-state average better characterizes the nature of the experiment.

Figures 18-20 and Tables 5-7 show the upper layer temperature, lower layer temperature, and interface position for the tests studied. Like all zone-based fire models, CFAST calculates conditions within each room as an upper and a lower volume (layer), each with uniform conditions throughout the volume at any instant of time. Thus, for the model, the temperature environment within a room can be described by an upper and lower layer temperature and by the position of the interface between these two layers. By contrast, experimental measurements often take the form of a vertical array of measurement points describing a profile of temperature. Techniques for collapsing these profiles to data that can be compared to zone fire models are available [67] and are used here to facilitate the comparison. (See Figure 19 for an example of the calculated and experimentally measured temperature profiles.)

For the single-room tests, predicted temperatures and layer interface position show obvious similarities to the measured values. Peak values occur at similar times with comparable rise and fall for most comparisons. Interface height for the single-room with wall-burning is a notable exception. Unlike the model prediction, the experimental measurement does not show the rise and fall in concert with the temperature measurement. Peak values are typically higher for upper layer temperature and lower for lower layer temperature and layer interface position. For all the tests, including the single-room tests, times to peak values and times to 100 °C predicted by the model average within 25 s of experimentally measured values.

Systematic deviations exist for the remaining three data sets. Differences between model predictions and experimental measurements change monotonically over time (rising for the three-room test and falling for the four-rooms tests. Modelling of heat conduction (losing too much or too little heat to the surfaces) or lack of modelling of leakage (rooms are presumed perfectly sealed unless vents are included to simulate leakage) may account for the trends. The comparison of interface position for the four-room test with corridor seems an anomaly. Although a nearly closed space, the roughly level interface position from the experiment seems more typical of a test more open to the ambient. The model calculations would appear to better represent the mixing which would occur in a closed volume. Again, leakage may be a factor. With some leakage in the space, lower temperatures for both the lower and upper layer and higher (and more uniform) interface position would be calculated.

In general, upper layer temperature and interface position predicted by the model are somewhat higher than experimental measurements, with the differences ranging from -46 to 230 °C for the temperature and -0.19 to 1.5 m for the interface position. Conversely, the lower layer temperature is somewhat lower for

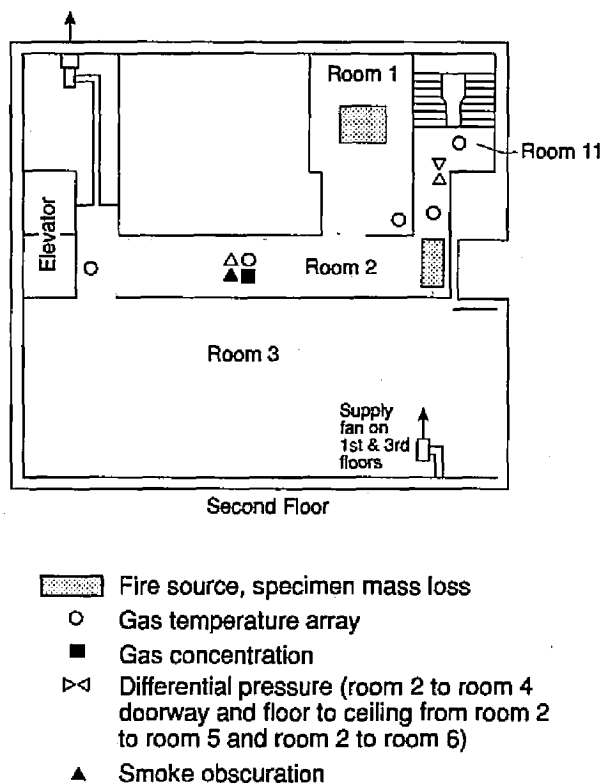


Figure 15. Second floor for multiple-story building tests.

Table 6. Comparison of experimental measurements and model predictions of upper layer temperature (°C) for several tests

Numbers in parentheses are model predictions	Peak Value (°C)	Time to Peak (s)	Time to 100°C (s)	Steady-State Value (°C)	Similar Shape?
Single-room furniture tests ^a (Tests 1 and 6)	790 (970) 920 (970)	500 (510) 450 (510)	290 (310) 290 (310)	-- ^b	✓
	590 (790) 900 (790)	510 (510) 510 (510)	330 (340) 330 (340)	--	✓
Single-room tests with wall burning (Tests 1 and 2)	750 (710)	710 (700)	100 (120)	--	✓
	810 (1550)	520 (470)	100 (70)	--	✓
Three-room tests with corridor ^c (SET 4, 11 replicates)	--	--	100 (110) 830 (n.r.) n.r.	230 (250) 75 (90) 45 (45)	
Four-room tests with corridor ^c (Tests 19 and 21)	--	--	195 (190) n.r. (270) n.r. n.r.	240 (470) 70 (110) 55 (35) 40 (35)	✓
	--	--	200 (190) n.r. (230) n.r. n.r.	260 (440) 80 (140) 65 (60) 50 (60)	
Multiple-story building (Test 7)	--	--	390 (375) 210 (150) n.r.	270 (340) 110 (65) 15 (15)	✓

^a Two measurement positions within the room were available from the experimental data.

^b Not appropriate for the experiment.

^c Multiple entries indicate multiple comparable rooms in the test structure.

the model than for the experiments (-60 to 5 °C). Presuming conservation of energy (an underlying assumption in *all* fire models), these three observations are consistent. A higher interface position gives rise to a smaller upper volume (and larger lower volume) within a room. With the same enthalpy in a smaller upper volume, higher temperatures result. This lends credence to the assumption of enthalpy conservation. Limitations inherent in the model also account partially for these trends. In the current version of CFAST, the lower layer is presumed to be clear. For the lower layer, energy is gained *only* by mixing or convection from surfaces. Adding radiative exchange to the lower layer would reduce the upper layer temperature and increase the lower layer temperature. Layer interface position is primarily affected by entrainment by the fire or at vents. Plume entrainment in CFAST is based on the work of McCaffrey [34] on circular plumes in relatively small spaces. For large fires in small spaces where the fire impinges on the ceiling (such as the single room tests with wall burning) or very small fires in large spaces (such as atria), these correlations may not be as valid.

4.5.2 Gas Species

The fire chemistry scheme in CFAST is essentially a species balance from user-specified species yields and the oxygen available for combustion. Once generated, it is a matter of bookkeeping to track the mass of species throughout the various control volumes in a simulated building. It does, however, provide another check of the flow algorithms within the model. Since the major species (CO and CO₂) are generated only by the fire, the relative accuracy of the predicted values throughout multiple rooms of a structure should be comparable. Figure 20 and Table 9 show measured and predicted concentrations of O₂, CO₂, and CO in two of the tests studied.

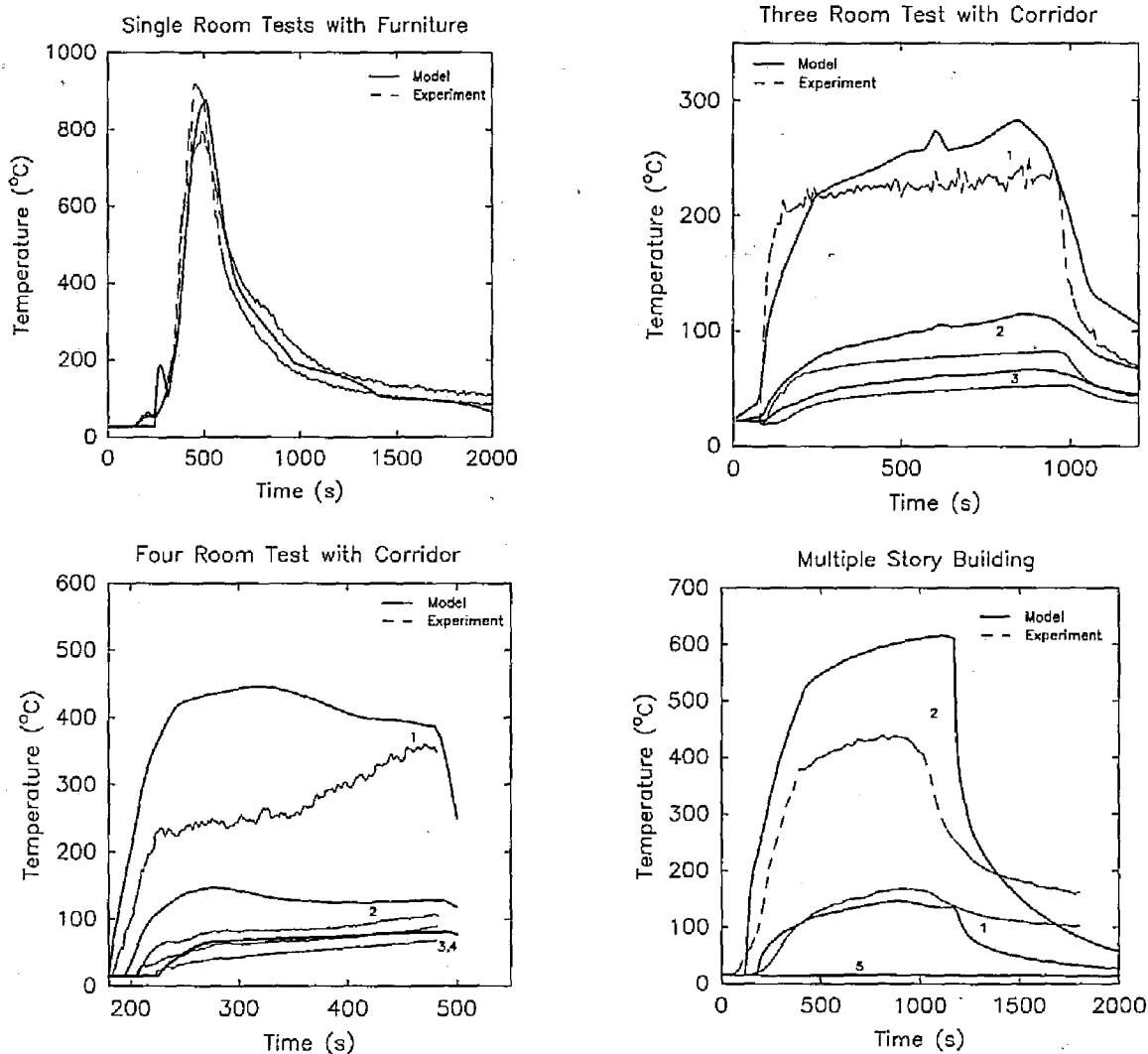


Figure 16. Comparison of measured and predicted upper layer temperatures for several tests.
(Numbers indicate comparable rooms in the test structure.)

For the single-room tests with furniture, the predicted concentrations are lower than those measured experimentally (averaging 5 percent low). This is probably due to the treatment of oxygen limited burning. In CFAST, the burning rate simply decreases as the oxygen level decreases. A user specified lower limit determines the point below which burning will not take place. This parameter could be finessed to provide better agreement with the experiment. For the present comparisons, it was always left at the default value.

For the four room test with corridor, the asymptotic values of the gas concentrations agree quite well. At first glance, the model predictions reach this equilibrium more quickly. An appreciation of the differences between the modeled parameters and the experimental measurements put this in perspective. From Figure 18, it takes about 100 s for the upper layer to descend to the level of the gas sampling port in the

Table 7. Comparison of experimental measurements and model predictions of lower layer temperature ($^{\circ}\text{C}$) for several tests

Numbers in parentheses are model predictions	Peak Value ($^{\circ}\text{C}$)	Time to Peak (s)	Time to 100°C (s)	Steady-State Value ($^{\circ}\text{C}$)	Similar Shape?
Single-room furniture tests ^a	570 (650) 590 (650)	500 (510) 420 (510)	370 (380) 390 (380)	-- ^b	✓
	230 (340) 590 (340)	510 (510) 500 (510)	410 (440) 390 (440)	--	✓
Single-room tests with wall burning	710 (250)	710 (700)	240 (220)	--	✓
	700 (620)	520 (450)	290 (290)	--	✓
Three-room tests with corridor ^c	--	--	n.r. n.r. n.r.	70 (40) 30 (30) 23 (30)	
	--	--	n.r. n.r. n.r.	75 (45) 21 (19) 21 (15)	✓
	--	--	n.r. n.r. n.r.	70 (32) 20 (17) 20 (15)	
Multiple-story building	--	--	400 (n.r.) n.r. n.r.	40 (37) 85 (70) 14 (16)	✓

See notes for Table 1.

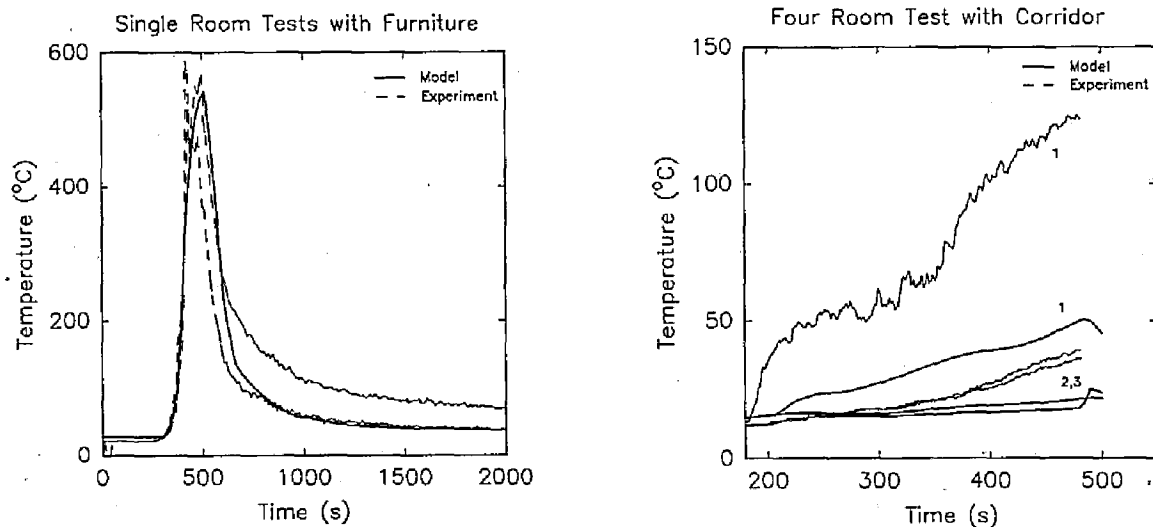


Figure 17. Comparison of measured and predicted lower layer temperatures for several tests. (Numbers indicate comparable rooms in the test structure.)

test. In addition, it is assumed that this point measurement is the bulk concentration of the entire upper layer. In reality, some vertical distribution not unlike the temperature profile (Figure 19) exists for the gas concentration as well. Since this measurement point is near the lower edge of the upper layer for a

Table 8. Comparison of experimental measurements and model predictions of layer interface position (m) for several tests

Numbers in parentheses are model predictions	Peak Value (m)	Time to Peak (s)	Time to 1 m (s)	Steady-State Value (m)	Similar Shape?
Single-room furniture tests ^a	0.8 (0.7) 0.8 (0.7)	420 (480) 450 (480)	400 (400) (380) 400	--	✓
	0.8 (0.6) 0.9 (0.6)	480 (510) 460 (510)	420 (430) 430 (430)	--	✓
Single-room tests with wall burning	0.2 (0.7)	710 (230)	120 (210)	--	✓
	0.1 (0.6)	500 (410)	80 (280)	--	✓
Three-room tests with corridor ^c	--	--	360 (n.r.) 1210 (n.r.) 90 (270)	1.0 (1.5) 1.2 (1.3) 0.9 (0.7)	✓
Four-room tests with corridor ^c	--	--	n.a.	0.7 (1.7) 1.0 (1.6) 1.0 (1.7) 0.7 (1.7)	
	--	--	n.a.	0.8 (1.1) 0.9 (1.1) 0.8 (1.0) 0.6 (1.0)	
Multiple-story building	--	--	n.a.	0.3 (1.8) 0.8 (2.1) 1.8 (1.8)	

See notes for Table 1.

significant time, it should underestimate the bulk concentration until the layer is large in volume and well mixed.

For the multiple-story building test, predicted values for CO₂, CO, and O₂ are far lower than measured experimentally. Both the lower burning rate limit as well as leakage in the 100 year-old structure probably contribute to the differences between the experiments and model. In addition, values for species yields were simply literature values since no test data were available.

4.5.3 Heat Release and Fire Pyrolysis Rate

Heat release rate and its intimately related fire pyrolysis rate are key indicators of fire hazard [79]. Peak values and time to reach peak values are typical scalar estimates used to represent the time-variant heat release rate and fire pyrolysis rate. For the single-room tests with furniture or wall-burning, these are appropriate indicators to judge the comparisons between model and experiment. For the three- and four-room tests with corridor or the multiple-story building tests, a steady state average is more appropriate.

Table 10 and Figure 21 compare measured and predicted heat release rates for the tests. In the CFAST model, the fire is specified as a series of straight line segments describing the pyrolysis rate, heat release rate, and species yields. Thus, the model predictions could be expected to agree quite well with experimental measurements. For tests where experimental data were available, the agreement is, not surprisingly, excellent – usually within 5 percent of the peak experimental values. Since this effectively

Table 9. Comparison of experimental measurements and model predictions of oxygen concentration for several tests

Oxygen Concentration

Numbers in parentheses are model predictions	Peak Value (%)	Time to Peak (s)	Steady-State Value (%)	Similar Shape?
Single-room furniture fire tests	0.01 (6.1)	510 (490)	-- ^a	✓
	6.9 (10.2)	490 (510)	--	✓
Four-room tests with corridor ^b	--	--	17.9 (12.5) 18.0 (16.4)	✓
	--	--	16.1 (14.0) 18.1 (16.5)	✓
Multiple-story building test ^b	--	--	15.5 (2.9) 20.9 (20.4)	

Carbon Dioxide Concentration

Single-room furniture fire tests	17.0 (6.0)	480 (510)	-- ^a	✓
	10.6 (4.2)	490 (510)	--	✓
Four-room tests with corridor ^b	--	--	2.3 (4.3)	✓
	--	--	2.4 (4.3)	✓
Multiple-story building test ^b	--	--	2.0 (0.9)	

Carbon Monoxide Concentration

Single-room furniture fire tests	2.2 (0.2)	490 (510)	-- ^a	✓
	0.6 (0.1)	440 (510)	--	✓
Multiple-story building test ^b	--	--	0.8 (0.8)	

^a not appropriate for the test.

^b multiple entries indicate comparable rooms in the test structure.

just shows how well a series of line segments reproduces experimental measurement, this level of agreement is expected. Times to peak values are always close. For two tests (the single-room with furniture and wall burning and the multiple-story building), the heat release rate in the room is limited by the available oxygen. Additional burning outside the room (seen in the single-room with furniture) accounts for the remainder of the heat released.

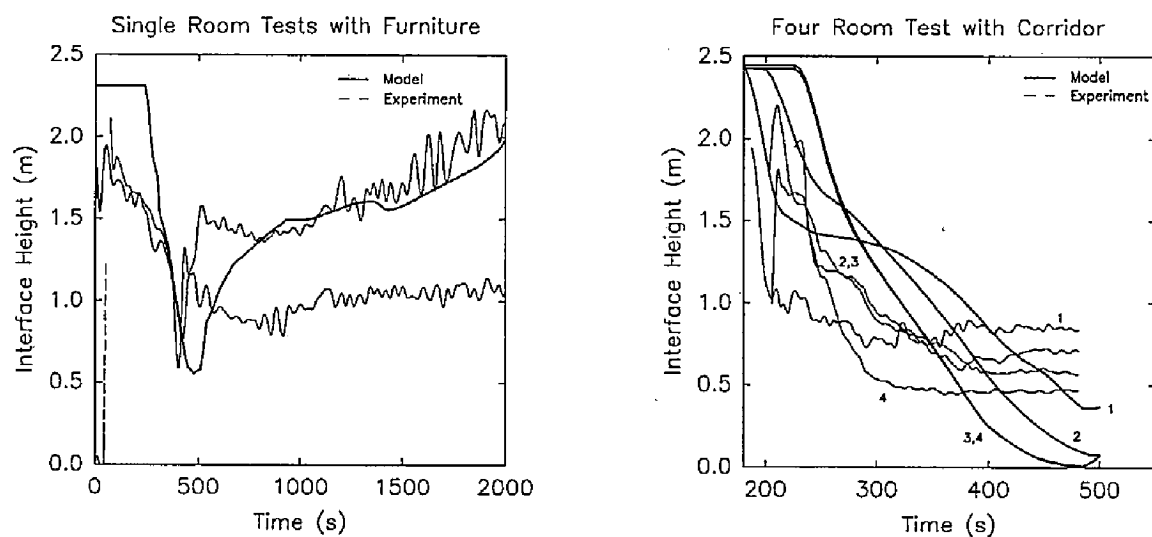


Figure 18. Comparison of measured and predicted layer interface position for several tests. (Numbers indicate comparable rooms in the test structure.)

Table 10. Comparison of experimental measurements and model predictions of heat release rate for several tests

Numbers in parentheses are model predictions	Peak Value (kW)	Time to Peak (s)	Steady-State Value (kW)	Similar Shape?
Single-room furniture fire tests	2450 (2200)	480 (480)	-- ^a	✓
	2600 (2350)	500 (510)	--	✓
Single-room tests with wall-burning	2050 (2000)	230 (200)	--	✓
	4000 (3150)	420 (370)	--	✓
Three-room test with corridor	--	--	86 (87)	✓
Four-room tests with corridor	--	--	n.r. ^b	✓
	--	--	n.r.	✓
Multiple-story building test	--	--	n.r.	✓

^a not appropriate for the test.

^b not available from experimental data.

For the three-room test with corridor, multiple replicate tests put the agreement between the model and experiments in perspective. For all tests in the original study [24], the coefficients of variation (the standard deviation expressed as a percentage of the mean) ranged from 4 to 52 percent. In another study,

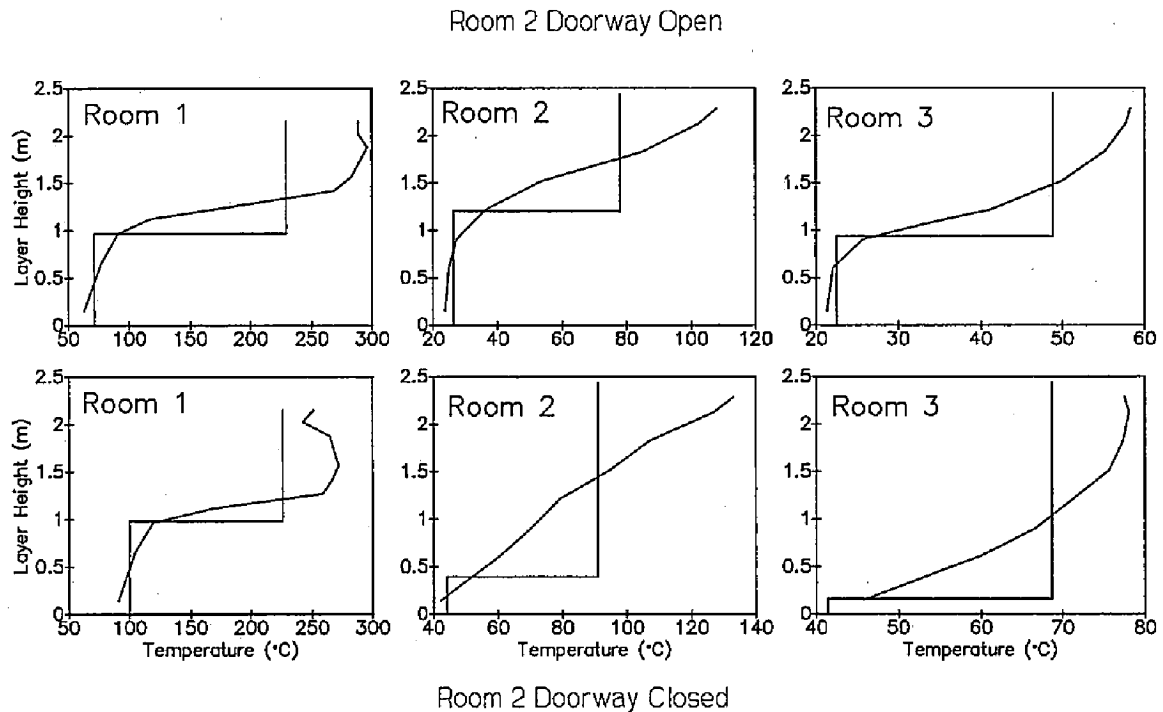


Figure 19. Average two-layer temperature and interface position calculated from experimentally-measured temperature profiles in a three-room experiment.

precision to within 15 percent for fires of 2.5 MW was noted [75]. Thus, the simplification of specifying the fire growth as a series of straight lines is easily justified with the expected accuracy of experimental measurements.

For the multiple-story building test, *no* pyrolysis rate or heat release rate data were available. Estimates of the “steady-state” burning rate, time to reach “steady-state,” and duration of “steady-state” burning were made from available correlations for wood cribs [80], [81]. Although the comparisons for this test should be considered approximate, it was included since, if successful, the scope of the model is extended considerably to a large multiple-story building with mechanical ventilation.

4.5.4 Pressure

The differential pressure across an opening drives the flow through the opening. For each room, the CFAST model calculates a differential pressure at floor level, referenced to ambient. Noting that the ambient pressure is approximately 100 kPa, typical pressure drops across openings induced by fires are but a small fraction of the ambient pressure – typically from less than 1 Pa to perhaps a few hundred Pascals in well-sealed enclosures. The ability to model these extremely small differential pressures provides another check on the flow algorithms in the model. These are, however, expected to be difficult to model and measure accurately. Thus, agreement within a few pascals is often considered acceptable.

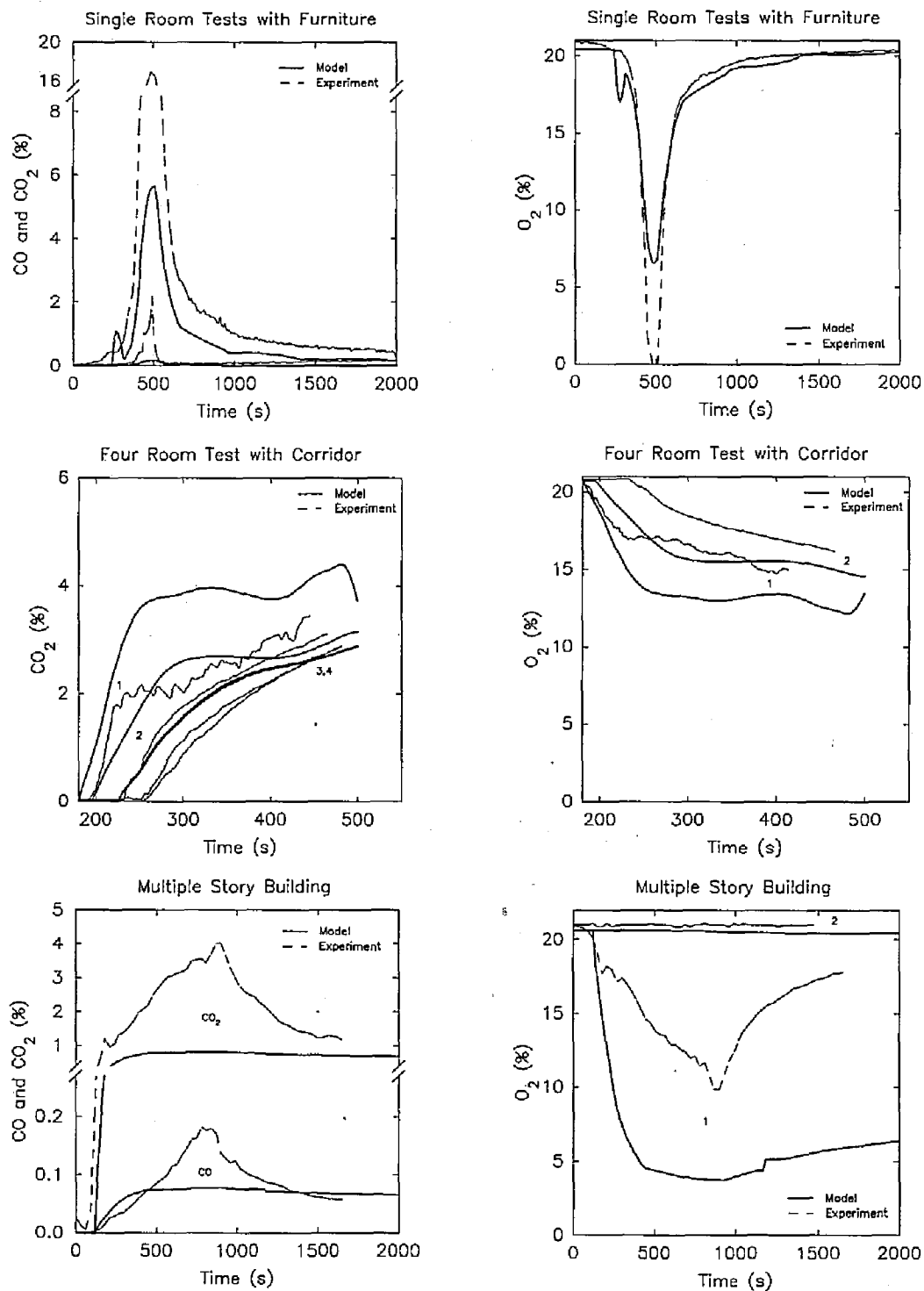


Figure 20. Comparison of measured and predicted gas species concentration for several tests. (Numbers indicate comparable rooms in the test structure.)

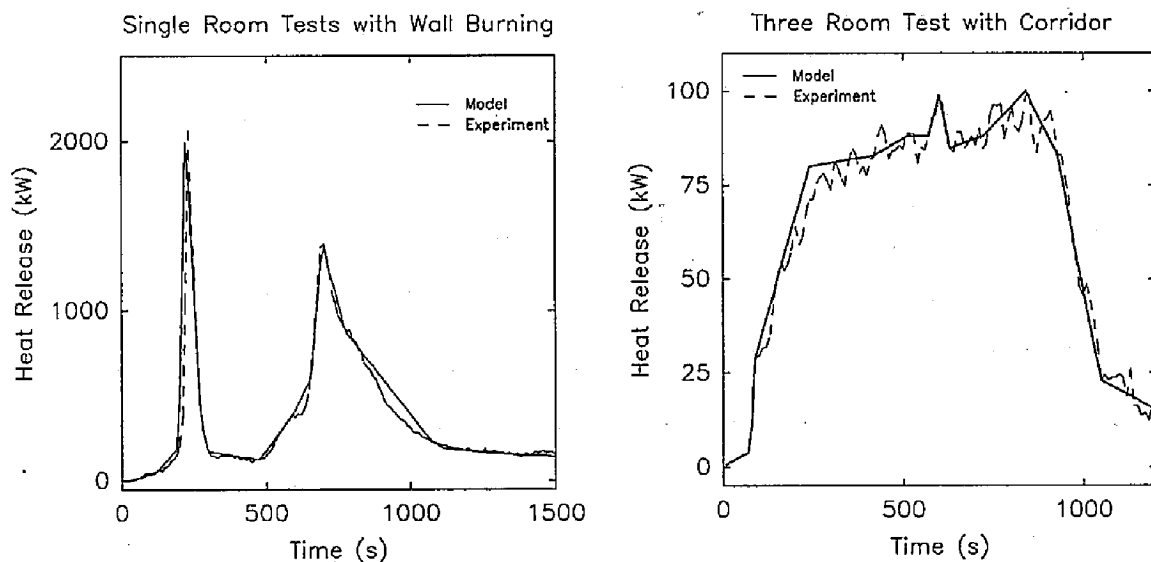


Figure 21. Comparison of measured and predicted heat release rates for two selected tests.

In four of the five experimental test series, measurements (corrected to floor level) were available which could be compared to these predicted values (measurements were not available for the single room tests with furniture).

Figure 22 and Table 11 show the comparisons. For most cases, the agreement is reasonable, with the difference between measured and predicted values typically less than 2 Pa and for some experiments, less than 0.5 Pa. Trends displayed in the experimental data are replicated by the model predictions. Some interesting exceptions are apparent however. In major part, these are due to quantities unknown in the experiments (leakage). Not all of the onus for agreement should be placed on the model, however. Only one of the test series included any estimate of leakage through cracks in the buildings. Logically, unless directed otherwise, the model assumes *no* leakage from any room. This leakage can have a dramatic effect on the results predicted by the model. Figure 23 illustrates the effect of leakage for a single room with a single doorway and an upholstered chair used as the fire source. Leakage areas from 0 to 100 percent of the vent area were simulated with a second vent of appropriate size and placed at floor level (much of the leakage in rooms take place at floor level). Both temperatures and pressures are seen to change by more than a factor of two (other variables can be expected to change with similar variation). Temperatures changes by about 20 percent with only a 10 percent leakage area. The effect on pressure is not quite as straightforward, but for larger leakages changes in concert with the temperature. For the four-room tests with corridor, leakage from the "well sealed rooms" was estimated via measurement at not more than 25 percent of the total vent area.

4.5.5 Flow Through Openings

In the control volume approach, the differential form of the momentum equation for the zones is not solved directly. Rather, the momentum transfer at the zone boundaries is included by using Bernoulli's approximation for the velocity equation. This solution is augmented for restricted openings by using flow coefficients [39], [82] to allow for constriction in vents. The flow coefficients allow for an effective

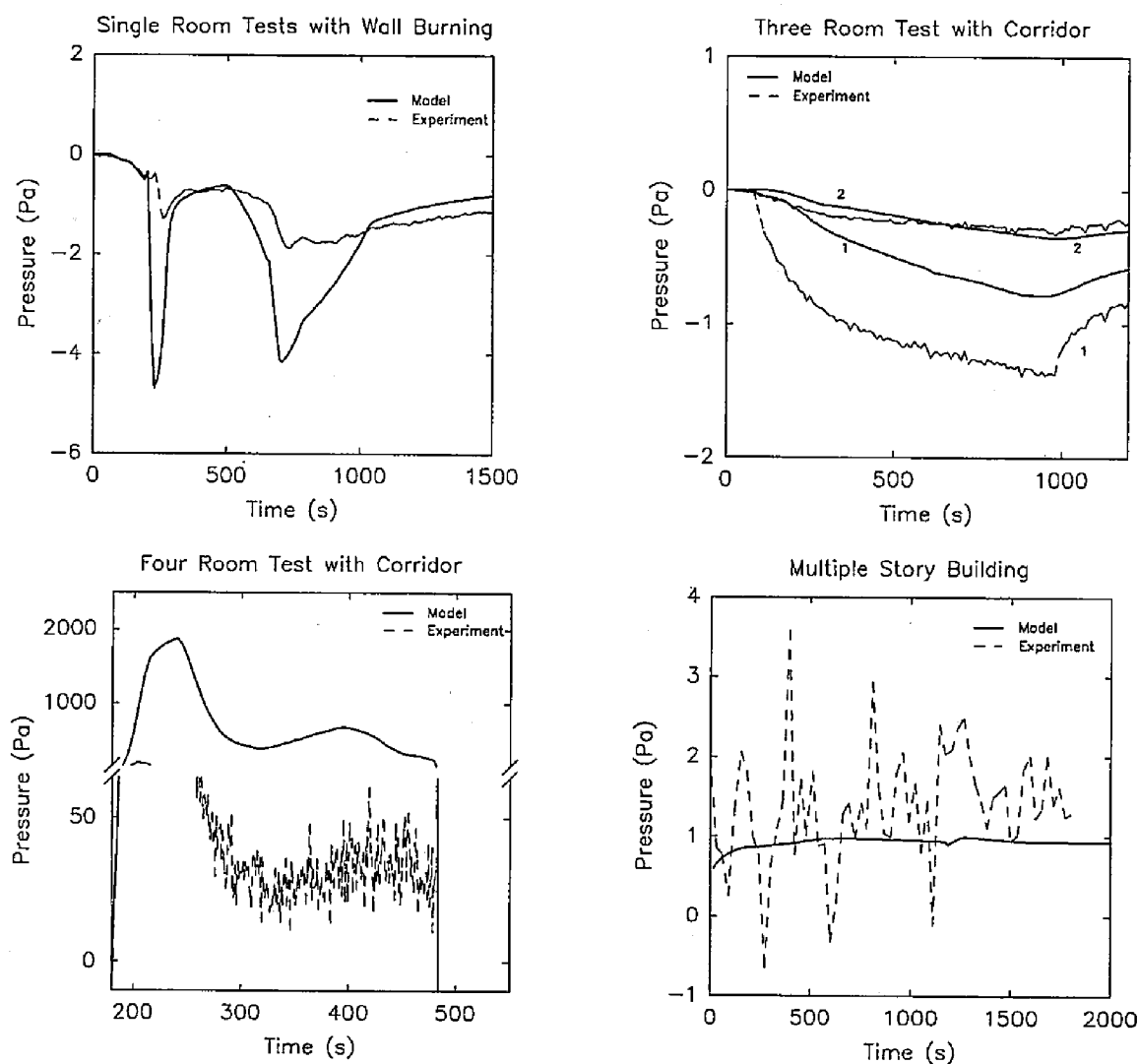


Figure 22. Comparison of measured and predicted pressures for several tests.
(Numbers indicate comparable rooms in the test structure.)

constriction of fluid flow which occurs for vents with sharp edges. In CFAST, these coefficients are for rectangular openings in walls whose surfaces are much larger than the opening.

Figure 24 and ? compare measured and predicted mass flows through doorways in two of the tests studied. For the three-room test with corridor, flow through two doorways of the same test are shown (one between the fire room and the corridor and one between the corridor and the outdoors). Not surprisingly, the flow is typically somewhat underpredicted by the model (from -0.14 to -0.58 kg/s). The vent flow in CFAST includes mixing phenomena at the vents. As hot gases from one compartment leave that compartment and flow into an adjacent compartment, a door jet can exist which is analogous to a normal fire plume, but with an extended flat plume similar to a waterfall. This places its use outside the normal range of the plume model [34] and perhaps beyond its range of validity. However, no reliable correlation yet exists

Table 11. Comparison of experimental measurements and model predictions of room pressure for several tests

Numbers in parentheses are model predictions	Peak Value	Time to Peak	Steady-State Value	Similar Shape?
Single-room tests with wall-burn-ing	-1.9 (-4.6)	730 (750)	--	✓
	-1.9 (-5.6)	520 (490)	--	✓
Three-room test with corridor	--	--	-1.1 (-0.6) -0.2 (-0.5)	✓
Four-room tests with corridor	--	--	-1.0 (-2.1)	✓
	--	--	36 (22)	
Multiple-story building test	--	--	2.4 (1.3)	✓

^a not appropriate for the test.

for the extended flat plume which occurs in vent flow. Examining the trends of prediction of upper layer temperature in tests with multiple rooms (Tables 1 and 2), the typical over-prediction in the room of fire origin is far greater than for other rooms in the structures. The under-prediction of the mass flows probably accounts for this as a cascading effect as you move away from the room of fire origin.

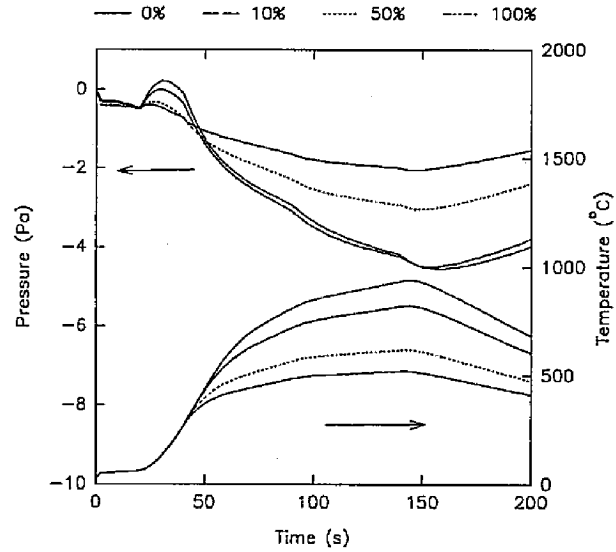


Figure 23. Effect of leakage on calculated temperatures and pressures in an arbitrary single-room fire.

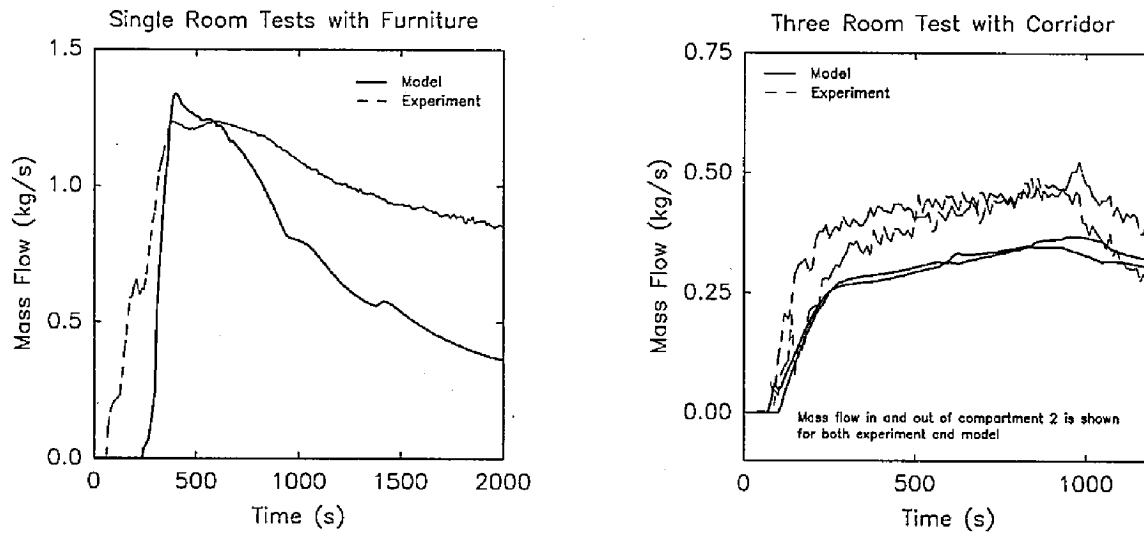


Figure 24. Comparison of measured and predicted mass flow through vents for several tests. (Numbers indicate comparable rooms in the test structure.)

5 Using CEdit

CEdit is an interactive, user-friendly program used to generate most data files for input to the CFAST model. As such, it is difficult to describe all the functions of the program in a reference guide. Rather, it is best learned through use.

The user interface is organized into a series of screens, each of which addresses a general area of the process of modeling a fire. General and key word help is always available except within the key word help section itself. The top of the screen shows which section is active. These names are shown below and are roughly descriptive of the area which is covered. The bottom of each screen shows which special keys are active, or indicates what action is expected. If data can be entered, then the range and units are shown if appropriate. For example, compartment width is in units of length, whereas a title has no dimensions.

Note that the Initialization screen (screen 0) and the Version and Settings screen (screen 11) do not correspond to sections of the data file. Rather, they are used to retrieve a CEdit data file and to customize the CEdit display environment, respectively.

Overview	Title Time specifications
Ambient Conditions	Ambient conditions
Geometry	Floor plan data
Vents(doors,...)	Horizontal flow connections
Vents(ceiling,...)	Vertical flow connections
Fans, Ducts,...	Mechanical ventilation
Thermal Properties	Thermophysical properties of enclosing surfaces
Fire Specification	Description of fire sources Species production
Objects	Object specifications
Files,...	File specifications

In general, CEdit requests either data from the keyboard, or selection information from the function keys (or mouse if present). Any active function keys are shown at the bottom of the screen. If the meaning is not clear, the **show keys** function key, f9, will give further explanation. Otherwise, there are directions as to what further actions are possible. Select an entry to be changed by moving the highlight bar using the arrow keys (\leftarrow \uparrow \downarrow \rightarrow). If alphanumeric input (data) is being requested, the entry must always be completed by pressing the Enter key. For function keys, only a single keystroke is required. Some of the function keys are active throughout CEdit; others are specific to certain screens. Those specific to individual screens are described in more detail on the following pages. Those active throughout the program are discussed below.

key	key label	function
f1	help	You may press the HELP key, f1, at any time to receive context sensitive help describing the current screen or current quantity being entered. Pressing f1 a second time brings up a list of key words for which more detailed help is available.
f2	go to screen	Allows you to move directly from one screen to another within CEdit. From any screen, pressing f2 brings up a menu listing all the screens in CEdit. Using the mouse or the arrow keys, select the screen of interest and press enter or the left mouse button.
f8	change units	You may temporarily change the working engineering units displayed by CEdit and used for data entry at any time by pressing f8 and selecting the quantity to be changed with the up and down arrow keys. Pressing the right or left arrow keys changes the working units of the currently selected quantity. To change the units permanently, you must modify the installation parameters.
f9	show keys	Provides a brief description of the function keys currently active and can be used to provide a quick reference of the current function of each of the keys.
f10	quit	Used to end CEdit.

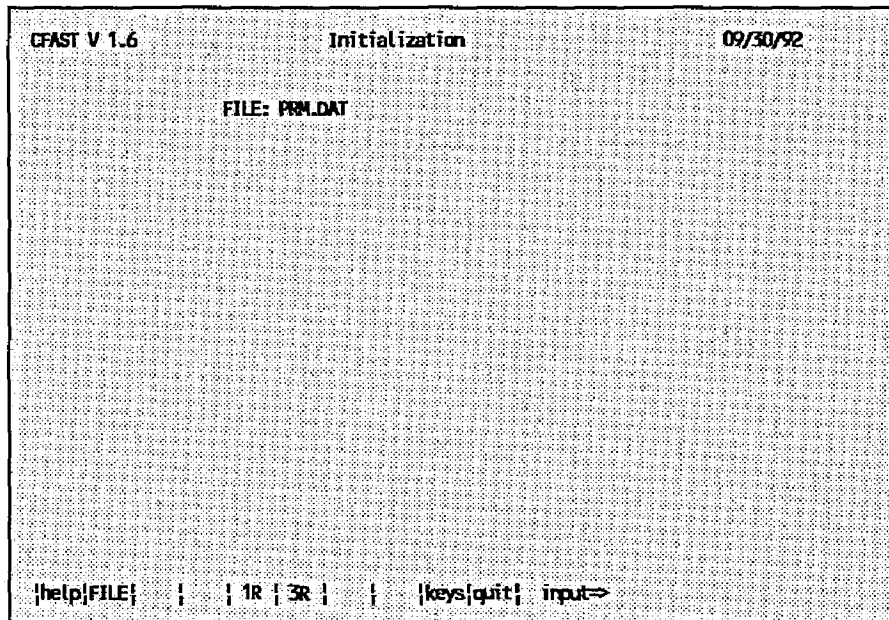
Four additional keys have special meaning in CEdit when pressed on any of the main screens (screens 1-11 above).

key	key label	function
Home	first screen	Move immediately to the Overview screen from any CEdit main screen.
End	last screen	Move directly to the Files screen from any CEdit main screen and save the current changes.
PgDn	Page Down	Move one screen forward. Forward direction is determined by the order of the screens on the go to screen (f2) menu.
PgUp	Page Up	Move one screen backward. Backward direction is determined by the order of the screen on the go to screen (f2) menu.

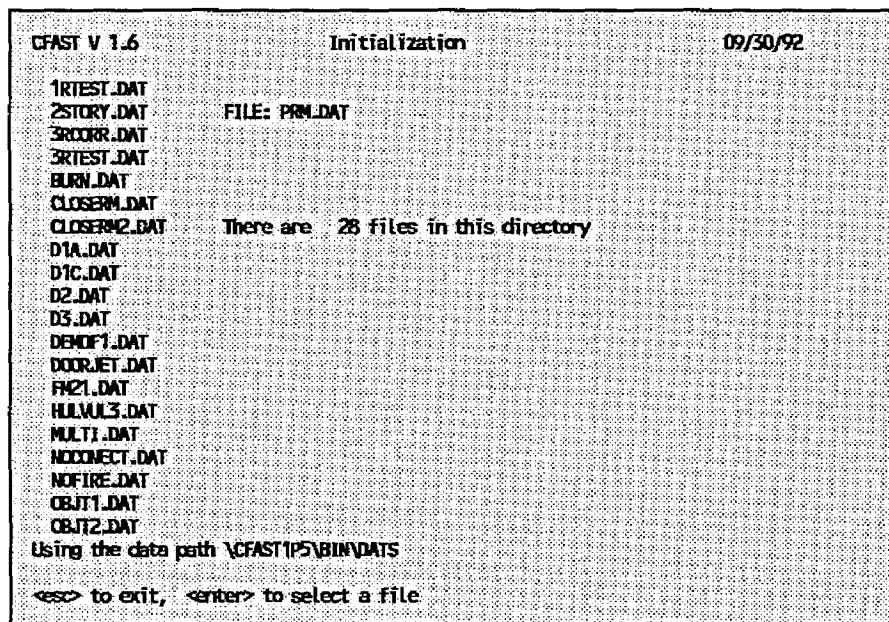
Again, these special keys must be used from one of the main screens to retain their functionality. Alternate meanings exist within many of the subpages or windows displayed by each screen. When an alternate meaning does apply, this is indicated in the sections below.

5.1 Initialization Screen

On the Initialization screen, the CFAST input file to be edited with CEdit is selected in one of three ways.



If the file desired was the last file used by CEdit or the file name was entered on the command line, press Enter to select that file automatically. Alternatively, the name of any existing DOS file may be selected directly by typing in the name of the file. To use the existing example file, type PRM.DAT, and press Enter.



An alternative to entering the file name is to press the select file key, f2, to see a list of files in the current working directory. By default, all files with an extension of .DAT are included in the list. If desired, one may type a file matching pattern (such as *.* to see all files in the subdirectory) before pressing f2. The same rules for wildcards apply here as they do to all DOS file commands.

In addition to showing the name of the current screen, "Initialization" in this case, the name of the module, the version number and the current date are shown. The latter two can change, as CEdit is enhanced, and when run on dates different than shown in the figure.

If a completely new data file is to be created, one of two generic data sets built into CEdit may be selected. Key f5 may be pressed to use a single compartment case and key f6 may be pressed to use a three compartment case.

5.2 Overview Screen

CFAST V 1.6		Overview		09/30/92	
File: PRM.DAT		Title: Example Case for CFAST 1.6 User's Guide			
Geometry	Time	Ambient Conditions		(external)	
Compartments	2 Simulation 200	Temperature	300.00	300.00	
Doors,...	2 Print 10	Pressure	1.0E+05	1.0E+05	
Ceiling vents	1 History 10	Station elev.	0.0	0.0	
MV connects	2 Display 0	Wind speed		0.0	
	Restart 0	Ref. height		10.00	
		Power Law		0.1600	
Fire Specification					
Type Specified fire(constrained)					
Species tracked O2 CO2 CO HCN HCL TUNG H2O CO					
Ceiling jet CEILING					
Range: Alphanumeric (50)		Units: Name or Title			
{help} go		{unit}{keys}{quit} input=>ST 1.6 User's Guide			

The Overview screen presents a summary of the CFAST data file. The title, simulation time, print interval, history interval, display interval, and restart time may be changed on the screen. All other information displayed is changed on other screens in CEdit and is included here (in the "protected text" color) to provide a summary of the data set. Key words in the data file effected by these changes include VERSN, TIMES, and RESTR.

5.3 Ambient Conditions Screen

CFAST V 1.6		Ambient conditions		09/30/92	
	(internal)	(external)			
Temperature	300.00	300.00			
Pressure	1.0E+05	1.0E+05			
Station elev.	0.0	0.0			
Wind speed		0.0			
Ref. height		10.00			
Power law		0.1600			
Compartments	2	Maximum pressure differential	26.53		
Doors,...	2	Maximum elevation change	4.60		
Ceiling vents	1	Total internal volume	73.60		
MV connects	2				

Range: 200.00 to 350.00 Units: Temperature in KELVIN
 {help} go { } { } { } { } {unit} {keys} {quit} {input}=>

On the Ambient Conditions screen, the internal and external ambient temperature, pressure, and station elevation along with information on external wind may be changed. The wind speed, scale height, and power law are used to calculate the wind coefficient for each vent connected to the outside. The wind velocity is specified at some reference height. The power law then provides a lapse rate for the wind speed. An assumption is that the wind speed is zero at the surface. The formula used to calculate the wind speed at the height of any vent is $(\text{wind speed}) \cdot ((\text{vent height})/(\text{scale height}))^{(\text{power law})}$. The wind is applied to each external opening as a change in pressure outside of the vent. It is further modified by the wind coefficient used for the openings. The vent connections, entered on the two vent screens, are summarized here along with the geometry of the structure and the mechanical ventilation connections. This summary information together with additional information concerning pressure, elevation and volume is displayed as an aid to data entry. Changes on this screen effect the TAMB, EAMB, and WIND key words when the data file is saved.

5.4 Geometry Screen

CFAST V 1.6		Geometry		09/30/92	
Dimensions					
Compartment Number:	1	2			
Width:	4.00	4.00			
Depth:	4.00	4.00			
Height:	2.30	2.30			
Floor elevation:	0.0	2.30			
Range: 0.0 to 150.00 Units: Distance in METER [help] go [] [ADD] [DEL] [] [unit] [keys] [quit] input>					

On the Geometry screen, information on the sizes of all of the compartments is entered. The key words associated with this screen are WIDTH, DEPTH, HEIGH, and HI/F. The DELETE key (f5) may be used to delete a compartment.

CFAST V 1.6		Geometry		09/30/92	
Dimensions					
Compartment Number:	1	2			
Width:	4.00	4.00			
Floor	Compartment #	3			
	Width				
	Depth (breadth)				
	Interior height				
	Height of floor above reference level reference is specified in "Ambient"				
Range: 0.0 to 150.00 Units: Distance in METER <esc> to exit, <f2> accept data input>					

Compartments may be added to the simulation with the ADD key (f4) on the Geometry screen. Dimensions of the compartment, along with the height of the compartment floor above the reference height (specified on the Ambient Screen) are entered in the overlaid window.

5.5 Vents(doors,...) Screen

CFAST V 1.6 Vents(doors,...) 09/30/92

Dimensions

Compartment Number: 1 2

Width: 4.00 4.00

Depth: 4.00 4.00

Height: 2.30 2.30

Floor elevation: 0.0 2.30

Vents(doors,...)

with respect to first room					wrt second room			- absolute -		
#	width	sill	soffit	wind	#	sill	soffit	a sill	a soffit	Vent(1->4)
1	1.07	0.0	2.0	0.0	3	0.0	2.0	0.0	2.0	1
2	1.07	1.0	2.0	0.0	3	3.3	4.3	3.3	4.3	1

On the Vents(doors,...) screen, all horizontal flow connections between compartments and openings to the outside are specified. A vent may be added using the ADD key (f4) or deleted using the DELETE key (f5). The OPEN/CLOSE key (f6) allows specification of the vent position over the course of the fire for the currently selected vent.

CFAST V 1.6 Vents(doors,...) 09/30/92

Dimensions

Compartment Number: 1 2

Width: 4.00 4.00

Floor: First Compartment

Second Compartment

with Vent number

#	width	sill	soffit	wind
1	1.0			
2	1.0			

Soffit (with respect to first comp)

Sill (with respect to first comp)

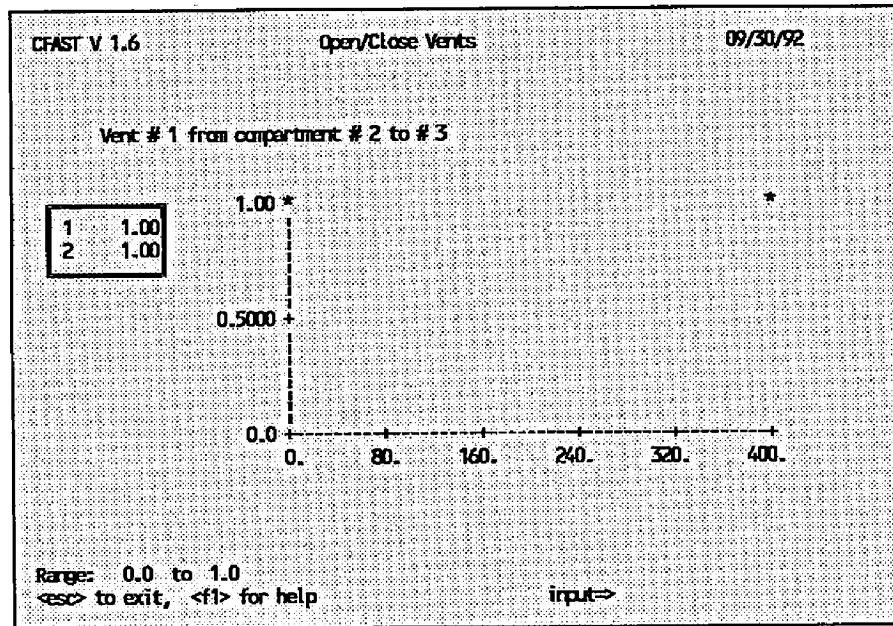
Wind 0.0

Range: 1 to 3 Units: Compartment number

- absolute -

#	a sill	a soffit	Vent(1->4)
1	2.0		1
2	4.3		1

Like adding a compartment on the geometry screen, the ADD key (f4) may be used on the Vents(doors,...) screen. A vent is specified by the two connecting compartments, the vent number, and the size and location of the vent. A connection to the outside is defined by using a compartment number for the "Second Compartment" one greater than the total number of compartments entered on the Geometry screen. Each entry on this screen creates the appropriate HVENT key word in the data file.



The OPEN/CLOSE positions for any vent can be specified by moving the highlight bar to that vent on the main vents screen and pressing the f6 key. The current timeline values (horizontal axis on the graph above) for the selected vent are displayed. Move the highlight bar to the entry to be changed and enter a value from 0 (closed) to 1 (completely open). The default value is 1. This entry is applied in CFAST by multiplying the width of the vent by this value. The number of possible entries on this screen is determined by the number of specified points on the timeline which is specified the Fire Specification screen. For a more complete explanation of the timeline, please read the section in Fire Specification about modification of the duration of the fire. These OPEN/CLOSE events are always related to the course of the fire. One CVENT key word is created in the data file for each complete entry.

5.6 Vents(ceiling,...) Screen

CFAST V 1.6		Vents(ceiling,...)		09/30/92	
Dimensions					
Compartment Number:	1	2			
Width:	4.00	4.00			
Depth:	4.00	4.00			
Height:	2.30	2.30			
Floor elevation:	0.0	2.30			
Vents(ceiling,...)					
- compartment -				- relative -	- absolute -
top	bottom	shape	area	height	height
2	1	C	1.00	2.30	2.30
Units: C or S					
[help] go [ADD] [DEL] [unit] [keys] [quit] input=>					

On the Vents(ceiling,...) screen, all vertical flow connections between compartments and openings to the outside are specified. A vent may be added using the ADD key (f4) or deleted using the DELETE key (f5). Vertical flow entry does not provide an equivalent to CVENT to allow specification of the vent position over the course of the fire.

CFAST V 1.6		Vents(ceiling,...)		09/30/92	
Dimensions					
Compartment Number:	1	2			
Width:	4.00	4.00			
Depth:	4.00	4.00			
Height:	2.30	2.30			
Floor elevation:	0.0	2.30			
- compartment -	Top Compartment				- lute - ght _30
top	Bottom Compartment				
2	Shape				
	Area				
Range: 1 to 3 Units: Compartment number					
<esc> to exit, <f2> accept data input=>					

Vertical flow vents may be added by using the ADD key (f4) on the Vents(ceiling,...) screen to create VVENT key words in the data file. The vent is specified by the upper and lower connecting compartments, the shape of the vent (Circle or Square), and the area of the vent. A connection to the

outside is permitted for either the "Top Compartment" or the "Bottom Compartment". Such a connection is defined by entering a compartment number one greater than the total number of compartments on the Geometry screen. The upper compartment can not have a floor height lower than the ceiling of the lower compartment and must be within 0.1 meters of the ceiling height for the lower compartment.

5.7 Fans, Ducts,... Screen

CFAST V 1.6		Fans, Ducts,...		09/30/92	
Dimensions					
Compartment Number:	1	2			
Width:	4.00	4.00			
Depth:	4.00	4.00			
Height:	2.30	2.30			
Floor elevation:	0.0	2.30			
Exterior Connections					
Compartment	# node	Orientation	Height	Area	
1	1	V	2.10	0.12	
2	3	V	2.10	0.12	
Units: H or V					
{help} go { } {ADD} {DEL} {DUCT} {FAN} {unit} {keys} {quit} {input}=>					

Mechanical ventilation systems are entered using this screen. This includes details of the connections from compartments to the ventilation system, and of the ductwork and fans within the system. These are specified on the three separate pages of the Fans, Ducts screen. On this first page, the connections between compartments and the ventilation system are detailed. These correspond to the MVOPN key word in the CFAST data file. Like the Geometry and Vents screens, these connections may be added with the ADD key (f4) or deleted with the DELETE key (f5). The DUCT key (f6) allows specification of the ductwork on the Duct page. The FANS key (f7) allows specification of the operating characteristics of the fans in the system.

CFAST V 1.6 Fans, Ducts,... 09/30/92

Dimensions

Compartment Number: 1 2
 Width: 4.00 4.00

Floor Compartment Number
 Node Number
 Compartment Orientation (H or V)
 1 Height of midpoint
 2 Area

Area
 0.12
 0.12

Range: 1 to 6 Units: Compartment number
 <esc> to exit, <f2> accept data input=>

Connections from compartments to the ventilation system are added using the ADD key (f4) from the main mechanical ventilation screen. A connection is fully specified by the compartment number, mechanical ventilation node number, orientation (Horizontal or Vertical), height, and area.

CFAST V 1.6 Fans, Ducts,... 09/30/92

Duct Work

node		len	diam	Duct Work			node	
1st	2nd			abs	expanded	joint1	joint2	hght1
1	2	2.30	0.10	0.0020	1.00	1.00	2.10	4.40

Range: 0.0 to 300.00 Units: Distance in METER
 <esc> | | /ADD |DEL | | |unit|keys| | input=>

The ductwork in the ventilation system is specified on the Duct page by pressing f6 from the main screen. Internal connections may be added with the ADD key (f4) or deleted with the DELETE key (f5). Pressing Page Up will return to the main screen.

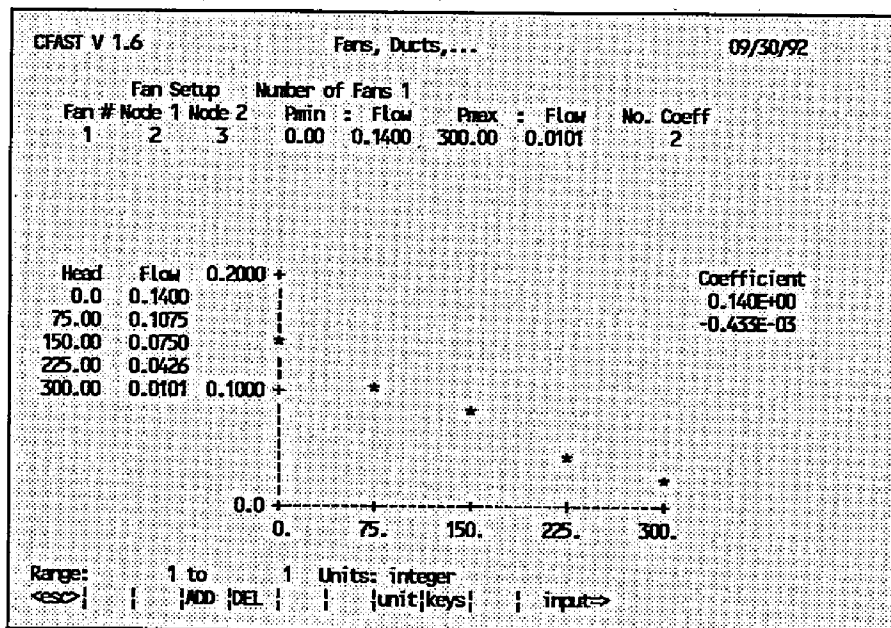
CFAST V 1.6 Fans, Ducts,... 09/30/92

node		Duct Work				node	
1st	2nd	len	diam	abs rough	expanded joint1 joint2	hght1	hght2
1	2	2.30	0.10	0.0020	1.00 1.00	2.10	4.40

Node 1 number
 Node 2 number
 Length
 Diameter
 Absolute Roughness
 Flow Coefficient Node 1 0.0
 Expanded Area of Joint Node 1 1.00
 Abs. Elevation Node 1
 Flow Coefficient Node 2 0.0
 Expanded Area of Joint Node 2 1.00
 Abs. Elevation Node 2

Range: 1 to 176 Units: integer
 <esc> to exit, <f2> accept data input=>

The ADD key on the Duct page creates a window to specify a connection between internal nodes of the mechanical ventilation system. All of the information for the MVDCT and INELV key words in the CFAST data file are entered for a single connection.



Operating characteristics of the fans in the ventilation system are specified on the Fan setup page. Fans may be added with the ADD key (f4) or deleted with the DELETE key (f5). Once a fan has been added to the system, the fan curve may be modified by either entering a set of pressure and flow data or a set of coefficients for the fan curve. In either case, CEdit will calculate the other quantity before leaving the Fan setup page. Pressing Page Up will return to the main screen.

CFAST V 1.6 Fans, Ducts,.... 09/30/92

Fan Setup		Number of Fans 1		Pmin : Flow		Pmax : Flow		No. Coeff
Fan #	Node 1 Node 2	3						
1	2 3	0.00	0.1400	300.00	0.0101			2

Node 1 Number

Node 2 Number

Head

0.0

75.00

150.00

225.00

300.00

Minimum Pressure

Flow at Min Pressure

Maximum Pressure

Flow at Max Pressure

Fan Coefficients will be calculated

Coefficient

0.140E+00

-0.433E-03

300.

Range: 1 to 100 Units: integer

<esc> to exit, <f2> accept data input=>

New fans are added to the system using the ADD key (f4) from the Fans page. A fan is specified by entering internal node numbers, minimum and maximum pressures, and flow at each pressure. A MVFAN key word is created for each entry on this page when the data file is saved.

5.8 Thermal Properties Screen

CFAST V 1.6 Thermal properties 09/30/92

Dimensions

Compartment Number:	1	2
Width:	4.00	4.00
Depth:	4.00	4.00
Height:	2.30	2.30
Floor elevation:	0.0	2.30

Thermal properties from THERMAL.DF

Ceiling properties: GYPSUM GYPSUM

Floor properties: CONCRETE CONCRETE

Wall properties: PINEMOOD PINEMOOD

Range: Alphanumeric (8) Units: Name or Title

[help] go [FILE]ADD [OFF] [DATA] [keys]quit input=>

The Thermal Properties screen details the materials used for the ceiling, walls, and floor of each compartment. The name of a material contained in the CFAST Thermal Database may be entered by first positioning the highlighted selection bar over the entry of interest and typing the material name exactly

as it exists in the database. To make the process easier, a material name may be selected on the Thermal Database page below for the currently highlighted surface. Once a material has been selected on the Database page, it can be designated for additional surfaces by selecting the desired surface and pressing the ADD PICKED key (f4). To specify an adiabatic surface, press the OFF key (f5) to turn OFF the heat transfer calculation for that surface. If the word NONE is displayed for a material, it means that the name entered does not appear in the Thermal Database. Key words associated with this screen include CEILI, WALLS, and FLOOR.

CFAST V 1.6		Thermal Database				09/30/92	
	Conduct	Specifi	Density	Thickne	Emissiv	* CODES *	
DFIRO3M	0.0002	0.9000	790.00	0.0160	0.9000		
PINewood	0.0001	2.50	540.00	0.0160	0.8000	60	U
CONCRETE	0.0018	1.00	2200.0	0.1500	0.9400	188	U
REDONK	0.0002	1.30	640.00	0.0160	0.9000		
FIBERB	0.0	1.25	240.00	0.0160	0.9000		
WOOD	0.0	1.00	250.00	0.0160	0.9800		
DFIROH	0.0001	1.40	510.00	0.0130	0.9900		
DFIRO1M	0.0002	1.50	560.00	0.0160	0.9000		
LIMEGLAS	0.0014	0.7600	2500.0	0.0160	0.9500		
GLASFIBR	0.0	0.7200	32.00	0.0880	0.9000		
KACWOOD	0.0002	1.05	128.00	0.1160	0.9700		
GYP3/4	0.0002	0.9000	790.00	0.0160	0.9000	38	U
GYP1/2	0.0002	0.9000	790.00	0.0130	0.9000		
GYP3/8	0.0002	0.9000	790.00	0.0190	0.9000		
GYP5/8	0.0001	0.9000	770.00	0.0160	0.9000		
BRICK	0.0002	0.9000	790.00	0.0760	0.9000		
GLASS	0.0014	0.7600	2500.0	0.0060	0.1000		
FC1_LO03	0.0002	1.50	790.00	0.0160	0.9000	1	

[help] | | | [PICK] | [unit|keys] | <esc> to exit

The DATA key (f6) displays the CFAST Thermal Database from the Thermal Properties screen. The contents of the database may be examined, and a material can be chosen (and later added in the Thermal Properties screen) by positioning the highlighted selection bar over the material and pressing the PICK MATERIAL key (f6). Press the Page Up and Page Down keys to quickly browse through the database. Move to the first database entry by pressing the Home key or the last entry by pressing the End key. The thermophysical database can not be changed by CEdit.

```

CFAST V 1.6                      Thermal properties                      09/30/92

      Dimensions
Compartment Number:      1      2
      Width:      4.00  4.00
      Depth:      4.00  4.00
      Height:      2.30  2.30
      Floor elevation: 0.0  2.30

      Thermal properties from THERMAL.DF
Ceiling properties:  GYPSUM  GYPSUM
Floor properties:   CONCRETE CONCRETE
Wall properties:    PINEWOOD PINEWOOD

Range: Alphanumeric ( 8)  Units: Name or Title
<esc> to exit, <f1> for help      input->thermal2.df

```

An alternate CFAST Thermal Database can be specified by pressing the FILE key (f3) from the Thermal Properties screen. Enter the alternate database file name and press Enter, or press Esc to leave the name unchanged. Materials selected previously which are not found in the new database are set to NONE and redisplayed. The new database file name becomes the Thermal Database for this input file only. If this file name differs from the database specified in the configuration file (see CF_Set), the THRMF key word is added to the input file when it is saved. It is important to note that once an alternate database has been specified, this database must be available when the model is run with this data input file.

5.9 Fire Specification Screen

```

CFAST V 1.6                      Fire Specification                      09/30/92

Heat of C  Lim O2  Rel Hum.  GW  Pos  Room  Type  CJET
1.8E+04    10.00    0.0    16.00  1    2    OFF

1 1.8E+04
2 1.8E+04

      2.0E+04 +
      *
      1.0E+04 +
      |
      0.0 +-----+
      0.    80.   160.  240.  320.  400.

Pyrolysis Heat_release Height Area H/C O2 CO/CO2 C/CO2 HCN HCL Ct
Range: 0.0010 to 6.0E+04 Units: Heat of Combustion in KILOJOULE/KILOGRAM

```

All data pertaining to the combustion properties of the main fire are entered on this screen. The heat of combustion, mass loss rate, and species yields are entered, along with selection of the fire compartment and fire type as described in the data file format section. The number of possible entries for each time

dependent variable is determined by the number of specified points on the fire timeline below. Note that fire chemistry is only allowed for constrained (type 2) fires. The ceiling jet option can be set by moving to the ceiling jet entry and using the arrow keys to highlight the desired option. The default value for ceiling jet is OFF. Data file key words for this screen include LFBO, LFBT, CHEMI, FPOS, FMASS, FHIGH, FAREA, FQDOT, and CJET. Individual objects may be entered on the Objects screen below.

Note that a time history for the heat of combustion is only available if a time history has been entered for both the mass loss rate and the rate of heat release. Any value entered directly for the heat of combustion is a constant value throughout the simulation. If you have time dependent values available for the mass loss rate and rate of heat release, enter these values and CEdit will calculate the corresponding time history for the heat of combustion.


If the fire compartment for an existing data file is changed, the fire position is recalculated so that the relative position in the original compartment is maintained in the new compartment. If the fire compartment was not set previously, the fire is positioned in the center of the specified compartment. A zero (0) entry for the compartment indicates no main fire leaving only object fires specified on the Objects screen below.

A species may be added to the calculation using the ADD key (f4) or deleted from the calculation using the DELETE key (f5) after moving the highlight bar to the desired species. Each species added to the calculation is represented in the data file by a unique key word.

CFAST V 1.6
Modify Time Interval
09/30/92

The time line shows the relative size of the time intervals

1	0.0
2	400.00



Press <f4> to insert a time point
Press <f5> to delete the time point

Range: 1.00 to 8.6E+04 Units: Time in SECOND
<esc> to exit, <f1> for help, <f8> to change units input=>

The FTIME time points in the data file may be modified by pressing the MODIFY TIME key (f6) from the Fire Specification screen. The timeline is modified by adding new points with the ADD (f4) key, deleting existing points using the DELETE (f5) key, or pointing to an entry and entering a new value. When the ADD key is pressed, a new point is created with a value that splits the time interval between the currently highlighted point and the previous one into two equal intervals, i.e., the midpoint of the interval.

5.10 Objects Screen

CFAST V 1.6		Objects		09/30/92		
Dimensions						
Compartment Number:	1	2				
Width:	4.00	4.00				
Depth:	4.00	4.00				
Height:	2.30	2.30				
Floor elevation:	0.0	2.30				
Objects selected from OBJECTS.DF						
Name	Compartment	Start time	First element	Position		
				X	Y	Z
SOFA	1	10	1	4.00	2.00	0.00
WARDROBE	1	30	3	0.00	2.00	0.00
Range: Alphabetic (8) Units: Name or Title						
{help} go {FILE}ADD {DEL} {DATA} {unit}keys{quit} input=>						

Objects to be burned in the fire scenario can be specified on the Objects screen. Any object name found in the CFAST Objects Database may be entered. Objects may be added with the ADD key (f4) or deleted with the DELETE key (f5). The DATA key (f6) displays the current objects database and provides an easy method for object selection. An alternate database can be specified by pressing the FILE key (f3).

CFAST V 1.6		Objects		09/30/92		
Dimensions						
Compartment Number:	1	2				
Width:	4.00	4.00				
Floor	Name					
	Compartment #	TS.DF				
	Start Time					
Name	First Element	Position				
SOFA		X	Y	Z		
WARDROBE		4.00	2.00	0.00		
		0.00	2.00	0.00		
	X					
	Y					
	Z					
Range: Alphabetic (8) Units: Name or Title						
<esc> to exit, <f2> accept data, <f6> pick input=>						

The ADD key (f4) on the Objects screen uses an overlaid window to specify a new object. Entry includes the object name, compartment, and the object position. The object position uses a similar x, y, z coordinate system to the fire position on the Fire Specification screen. The first element entry indicates

where on the object ignition begins, however, it is not used by the model at this time. Entry is required for future compatibility with the CFAST model. A value of 1 should be entered unless a different value is known. In addition, a time should be entered indicating the earliest time during the simulation that the CFAST model should check the fire scenario to determine if conditions have been met for the object to begin burning. If the flux to the object and the surface temperature are high enough beyond this time in the simulation, the object starts to burn. Each complete entry on this screen creates an OBJECT entry in the data file.

CRAFT V 1.6	Objects Database	09/30/92
-------------	------------------	----------

	Type	Ignition Temp	Length	Width	Thickness	# Elements
TABLE	2	273.00	1.00	1.00	0.20	9
DESK	2	273.00	1.00	1.00	0.20	9
SOFA	2	300.00	1.00	1.00	0.20	9
WARDROBE	2	300.00	1.00	1.00	0.20	9

PANEL

[help] | | | [PICK] |unit|keys| | <esc> to exit

The contents of the CFAST Objects Database may be examined, and an object can be selected by positioning the highlighted selection bar over the object and pressing the PICK OBJECT key (f6). This is available in both the Add Objects window and the main Objects screen. Press the Page Up and Page Down keys to quickly browse through the database. Move to the first database entry by pressing the Home key or the last entry by pressing the End key. The objects database can not be changed by CEdit.

An alternate CFAST Objects Database can be specified in a manner similar to the Thermal Properties Database by pressing the FILE key (f3) from the Objects screen. Enter the new database file name and press Enter, or press Esc to leave the name unchanged. If any of the objects specified previously are not found in the new database, a warning message is displayed. Respond "Y" to the warning message only if it is acceptable to have undefined objects deleted. If the new database file name is accepted, it becomes the Objects Database for this input file only. The OBJFL key word is added to the data file when it is saved if this file name differs from the one specified in the configuration file (see CF_Set). It is important to note that once an alternate database has been specified, this database must be available when the model is run with this data input file.

5.11 Files,... Screen

CFAST V 1.6	Files,...	09/30/92
quick estimates	<f5> asks for a time interval	
run time graphics	<f6> use existing display file (if it exists)	
save data file(s)	<f7>	
write to log file	<f8> no	
help go quit		

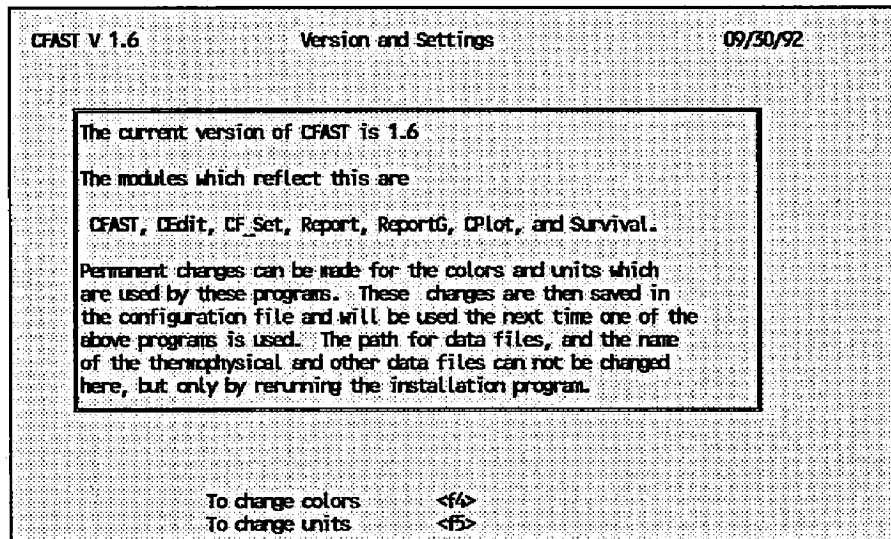
The Files screen is used to specify the file name for the input file and to access some additional options. If problems are encountered within CEdit, you can document the problem by generating a log file with the f8 function key and repeating the sequence of commands which generated the problem. Append a simple graphics descriptor to the CFAST data file by pressing f6 on the Files screen. The resulting display will show selected variables in a simple X-Y plot on the screen as the CFAST model calculates the results. Pressing f6 again indicates that any graphics descriptors currently in the data file are to be rewritten to the data file when it is saved. The graphics descriptors in the current data file can not be modified using CEdit but must be modified using an ASCII text editor.

CFAST V 1.6	Files	09/30/92
* Main data file to run	PRM.DAT	
History file	PRM.HI	
Restart file	no file specified	
Thermal properties file	THERMAL.DF	
Objects data file	OBJECTS.DF	
a * indicates that the file has been modified and not saved		
<div style="border: 1px solid black; padding: 5px;">Use the cursor keys to point to the file to be saved. Then press <enter>. To change the file name, enter a new name and press <enter>.</div>		

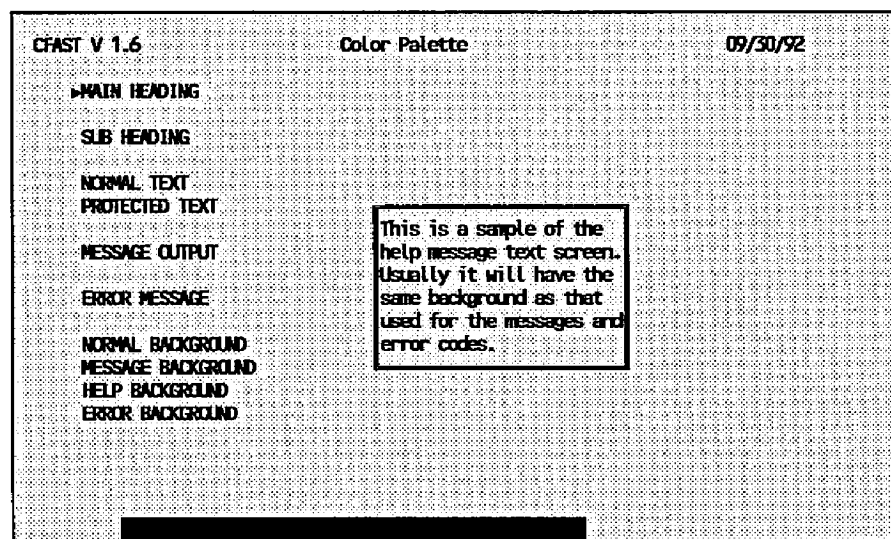
Once data for a test case has been entered or modified using CEdit, you should save the data to disk to run with the CFAST model. To save the data to a disk file, press f7. Type the file name and press

Enter. The output from the CFAST model may be written to a disk file for further processing by programs such as CPlot or to restart CFAST. The DUMPR and RESTR data file key words are created for the corresponding entries on this screen. File names for the Thermal and Objects Databases are displayed as summary items and can not be changed on this screen. To change these database file names, you must use the FILE option on the appropriate Thermal Properties or Objects screen.

5.12 Version and Settings Screen



The display colors and units within CEdit can be altered using the version and settings screen. Unlike the f8 key on the individual screens, the unit selection here makes the changes permanent, as would be accomplished with the CF_Set utility.



Any or all of the colors used by CEdit for screen displays may be changed. Use the arrow keys up and down to select the type of display text to be changed and the right and left arrow keys to select the color

for the foreground or background. The defaults have been selected to produce acceptable displays on both monochrome and color displays.

CFAST V 1.6		Set Units				09/30/92
Base Units	Current Units	Possible Units				
Temperature	KELVIN	KELVIN	CELSIUS	RANKINE	FAHRENHEIT	
Pressure	PASCAL					
Length	METER					
Energy	KILOJoule					
Mass	KILOGRAM					
Time	SECOND					
Time	SECOND					

To change units, highlight the basic unit to be changed, then point to the unit desired. Pointing is done either with the cursor keys or the mouse.

As supplied, most of the engineering units used for interactive input and display by CEdit are standard SI units. Energy defaults to kJ since rates of energy release are typically specified in kJ/s (kiloWatts). Use the up and down arrow keys to select the unit to change and the left and right arrow keys to change the units. This screen is also available from each of the main screens in CEdit by pressing the UNIT key (f8).

5.13 Quitting CEdit

One or more of the data files have been altered and not saved. Do you want to quit anyway?

Yes or No input→

When data entry for the input file is finished, press the QUIT (f10) key from any main screen. If changes have been made without saving, a warning window is displayed. Enter Y and press Enter to quit without saving current changes. Respond N to return to CEdit, then press the END key to access the Files screen.

6 Using CFAST

The following chapter describes the running of CFAST including explanations of the various outputs. The CFAST program is the actual fire model in the HAZARD package. This chapter consists of five sections. The first section describes the basics of running the program. Section two gives a brief description of the default output. Section three explains in some detail the various options to allow the user to customize the text output for his or her own use. A brief example of the default graphical output is in section four. The fifth section lists an example print out from CFAST. The example text and graphic output comes from using the datafile PRM.DAT as described in the chapter on CEdit.

There are several ways to run CFAST. Normally, it is selected from the HAZARD shell. However, CFAST does run from the DOS command line. If CEdit has already been used to set up a file, enter the command:

```
cfast
```

In this case, CFAST uses the last file edited by CEdit. This is not recommended when running PRM.DAT. PRM.DAT has both a graphics display as well as the ASCII text history. Both types of output default to the screen so the text and graphics overwrite each other leading to messy and confusing output. To get around this problem use the command line:

```
cfast prm.dat prm.out
```

This allows the graphics display to draw to the screen and the ASCII text to write to the output file PRM.OUT. Order is important, the datafile must come first. It is also important to know that anything in the second file will be overwritten.

Two keys allow some interaction with the model while it runs. The first is the escape key. When pressed, the escape key terminates the run. The second key is <f5> function key. Pressing the <f5> function key causes the current simulation time and last time step to print to the text output. When the text output goes to the screen the user can see the progress of the model. When the model runs with an output file as in the example, the information prints in the file.

For example, pressing <f5> during the run might produce:

```
Time =      9.58550207410571      DT =      0.353489940990121
```

The output means the model has completed about 9.59 s. of simulated time and the last completed time step is about 0.353 s. long. The first second of simulation time takes a while to run because of the start up of the solver, so the <f5> function key doesn't provide a lot of information. After the first second, time steps larger than 0.2 seconds mean the model is having little problem solving the differential equations and is moving very quickly. Times between 0.1 and 0.2 seconds say the model is moving through the simulation at a moderate speed. Step sizes between 0.1 and 0.01 seconds indicate possible trouble. Steps sizes less than 0.01 seconds indicate the model is having real trouble solving the differential equations.

Due to the effect of the computer's internal precision on the solution of the equations, the results from other computers may differ slightly from those found below. The output is labeled and most of it is self explanatory. However, a general description of the output follows including an explanation of the abbreviations.

6.1 Default Text Output

The default text output for CFAST 2.0 differs significantly from earlier versions. It is compact and easier to read than earlier versions although it contains less information. It provides a simple overview for the user to make sure the case runs as expected. Using the /r reporting options allow the user to get more information on the various states the model calculates. The /r option also disables the compact text output.

The output for each compartment is listed across the screen and the compartments are listed down the screen starting with compartment one and ending with the outside. The examples show the initial and final conditions for PRM.DAT.

Time = . 0.0 seconds.

Compartment	Upper Temp. (K)	Lower Temp. (K)	Inter. Height (m)	Pyrol Rate (kg/s)	Fire Size (W)
1	300.0	300.0	2.3	1.400E-03	2.530E+04
2	300.0	300.0	2.3	0.000	0.000
Outside					0.000

Time = 200.0 seconds.

Compartment	Upper Temp. (K)	Lower Temp. (K)	Inter. Height (m)	Pyrol Rate (kg/s)	Fire Size (W)
1	1252.	475.1	0.63	0.278	4.831+06
2	828.7	325.4	1.0	0.000	0.000
Outside					1.609E+03

The first column contains the compartment number. On each row with its compartment number from left to right is the upper layer temperature, lower layer temperature, the height of the interface between the two layers, the total pyrolysis rate, and finally the total fire size. The only value given for the outside is the total heat release rate of vent fires venting to the outside.

6.2 Reporting Options, /R:WINFST

When the user wants more information than the default output provides, use the /R reporting option. This option allows customizing the output to provide the information the user wants while not including extra information. Invoke this option from the command line using:

cfast <data file> /r:<option list>

or

cfast /r:<option list> <data file>

The options are listed consecutively without commas or spaces between. The option is not case sensitive for either the `r` or the option list. Order in the option list is also not significant. When invoked the reporting option overrides the default output and reports only the information that the user requests. The following sections describe each of the options. Each section refers to a specific part of the print out at the end of the chapter and appears in the order the output appears.

To get the output in section 5 use the following command:

```
cfast prm.dat prm.out /r:winfst
```

In general the above command provides more information than a user wants. It generate so much information it can easily overwhelm the user. So if, for example, the user is interested in the predicted interaction between a wall material and the hot gas layer, he or she can use the following command:

```
cfast prm.dat prm.out /r:wn
```

or

```
cfast /r:nw prm.dat prm.out
```

The short option list gives information on gas temperatures and wall temperature profiles with very little excess information. A description of each option follows in separate sub sections.

6.2.1 Output for Option /R:I

To get a summary of the input file use `/R:I`. This option prints the initial conditions to the output before the actual run starts. The initial conditions brake down into seven sections. Each is described below with the section name.

Title: The title line consists of the version of CFAST and the title included in the file. The first line of the output is the title line. It is the only section of the initialization output without a section header.

Overview: The overview gives a general description of the case. The output is fairly self explanatory as the example shows. However, a couple of items need mentioning. The Checksum at present doesn't do anything. It is for future verification that a file has not been changed. In the second line the header "Doors, ..." is the number of horizontal natural flow connections in the vent connections section farther down. "Ceil. Vents, ..." gives the number of vertical natural flow connections. The last header on the line "MV Connections" has the number of vents for the mechanical flow connections in the vent connections section.

Ambient Conditions: This section like the overview section needs little elaboration. It gives the starting atmospheric conditions for the simulation both for outside and inside the structure.

Compartments: The compartments section gives a summary of the geometry for the simulation. A simple table summarizes the geometry with compartments running down the page in numerical order. The various dimensions for each compartment are on the row with its compartment number. Two columns need explanation. The second to last column "Ceiling Height" gives the height of the ceiling relative to

the station height in the Ambient Conditions section. Similarly the "Floor Height" refers to the height of the floor above the station height.

Vent Connections: Vent connections further divides into three distinct parts. Each part has its own sub heading. A description of each follows.

Horizontal Natural Ventilation is the first table in the vent connections sections. Each row in the table characterizes one vent. The first two columns contain the two compartments connected by the vent. Each vent is ordered first by the lower number of the two compartments and then numeric order on the second compartment. The third column gives the vent number. Column four is the width of the vent. The next two columns report the sill and soffit height for the vent relative to the floor of the first compartment. The seventh and eighth columns have a second listing of the sill and soffit height, this time relative to the station height. Area of the vent is in the last column.

Vertical Natural Ventilation prints out in a similarly simple table. Again each vent is one row of the table. The first column is the upper compartment. The upper compartment is the compartment where the vent opens into the floor. The second column is the lower compartment where the vent is in the ceiling. The third column describes the shape of the vent, which can be either round or square. The fourth column gives the area of the vent. The last two columns are the height of the vent, relative to the floor of the lower room and relative to the station height respectively.

Mechanical Flow Connections uses two tables. The first table lists all the connections to compartments and ducts. Each row is either a connection or duct. The first column tells to which system the duct or connection belongs. A system is a set of continuously linked connections, ducts and fans. The example contains only one system. If a second system had been part of the file, a line would have been skipped before starting into the second system. The second and fourth columns give both ends of either the connection or duct. The words "comp" or "node" proceeds the numbers in these two columns. "Comp" means a compartment number. Rows with a compartment number in either the "from" or "to" columns are connections to compartments, which are basically vents. The rest of the rows define ducts. The third and fifth columns give the elevations of the proceeding columns. The sixth column is the length which only applies to ducts. Connections do not have a length so the column is left blank. Next comes the cross sectional area. The last column tells the absolute roughness. This value is the resistance the duct provides to the flow of air. Like the length, this value only has meaning for a duct so it is blank for a connection. Air flows both ways though connections and ducts. The headers "from" and "to" say nothing about the direction of air flow. The headers only provide a convenient way of listing both ends of a duct or connection.

The second table lists the fans. The first five columns in the fan table appear almost the same as the connections and ducts table. The table lists, in order, the number of the system the fan is a part, the "from" node and its height, the "to" node and its height. A fan actually draws air from the first or "from" node and pushes it to the second or "to" node. In the second table, the headers give the direction of the flow of air. The sixth column is the fan number as defined in CEdit. The next two columns are the minimum and maximum pressures at which the fan curve is defined. The rest of the row is made up of the two to five fan curve coefficients defined by CEdit.

Thermal Properties: The thermal properties section brakes into two parts. The first part is a table that lists the material for each surface of each compartment. The compartments appear as rows down the page in numerical order. From left to right next to the compartment number comes the material for the ceiling, wall and floor. The second part lists the entries in the thermal data base. The first line gives the database file used. Next comes a listing of each material used. For each listing of a material, the name is followed by the conductivity, specific heat, density, thickness and emissivity. Additionally, the HCl constants used

to calculate the HCl deposition for the surface are displayed. The final column indicates any applicable codes. See Appendix **whatever** for a detailed explanation of these codes.

Fires: The fire section lists all the information about the main fire and any object fires that might exist. All the information for each fire is listed separately. If there is a main fire, it comes first. Each fire listing has the same form. First is the name of the fire followed by a list of general information. Listed left to right is the compartment the fire is in, the type of fire, the x, y, z position, the relative humidity, the lower oxygen limit, and finally the pyrolysis temperature. A table of time history curves for the fire follows. The table contains all the time history curves for the fire. Each row on the table is a specific time given in the left most column. The rest of the columns give the values at that particular time. The column headers are keywords used in the datafile. The keyword meanings are: fmass is pyrolysis rate; hcomb is heat of combustion; fqdot is heat release rate; flhigh is height of fire; C/CO2 is carbon to carbon dioxide ratio; CO/CO2 is the carbon monoxide to carbon dioxide ratio; H/C is the hydrogen to carbon ratio; O/C is the oxygen to carbon ratio; HCN is the hydrogen cyanide production rate; and HCl is the hydrogen chloride production rate.

6.2.2 Output for Option /R:N

An expanded version of the compact default output called the normal print out can be obtained using the /R:N option. When requested, the normal print out is the first information printed at each interval. The first part of the print out looks similar to the default print out. It is laid out along the same lines, with the calculated values for each compartment listed left to right and compartments listed down. The left most column has the compartment. The next three columns also give the same values as the default output. They are upper layer temperature, lower layer temperature and interface height. The output changes at this point. The fifth column gives the upper layer volume. In the sixth, in parenthesis, is the percent of the total compartment volume the upper layer takes up. The pressure difference from ambient follows in the seventh column. The rest of the columns are the temperature of the surfaces that are turned on in degrees Kelvin.

The second table of the normal print out has information about the fires. In essence it is two tables joined. The first table lists information by fire. It starts with the main fire, if there is one, and then the object fires down the page. The fires are listed in the second column followed by the plume flow rate, the pyrolysis rate and the fire size. The next three columns are then skipped. The next column with information is the amount of heat given off by each fire convectively, followed by the amount of heat given off radiately. The second part starts after all the fires have been individually listed. It gives the totals for all fires in each compartment. The first column has the compartment number. The compartments start at one and are listed down the page in order. The third to fifth columns are the same as the first part except the values are totals for the compartment and not just for one fire. The sixth column has the total heat release rate that occurs in the upper layer. The next column has the same total in the lower layer. The eighth column has the total size of vent fires in the compartment. The last column of the table gives the flux on a point object laying at the center of the floor.

6.2.3 Output for Option /R:S

The /R:S option gets two tables displaying information about the amounts of species in each layer. The species information follows the normal print out. The first table gives species concentrations for the upper layers of all the compartment and the second reports the same for the lower layers of all the compartments. Again the compartments are listed down the page and the information across the page. The species are each given in one of several different terms. Below each header is the units for the given value. Most of the headers are simply the chemical formula for the species being tracked. However, a couple are not obvious. "TUHC" is the total unburned hydrocarbons or the pyrolyzed fuel that hasn't burned yet. "OD" is the obscuration density which is a measure of the amount of smoke. The last four columns, "HCl c", "HCl f", "HCl uw" and "HCl lw", are the amount of HCl deposition on the ceiling, floor, upper wall and lower wall respectively.

6.2.4 Output for Option /R:F

Vent flow, given in mass flow rates, is obtained by using this option. The section for vent flow is titled "Vent Flow (kg/s)." Because flow is always given in positive values, each vent is listed twice. Once for flow going from compartment A to compartment B and a second time for flow from B to A. As the example shows the first column lists the compartment the flow comes from. The second is the compartment the flow is going to. The third column has the number of the vent between the two compartments. The fourth column lists the type of vent. An H in this column stands for horizontal flow such as a doorway or window. A V here would mean vertical flow such as a ceiling vent. Support in the print out for vertical flow is not yet available.

The next four columns describe the types of flow going from one compartment to another. Each cell that is blank in these columns and the two following means the value is zero. The headers for these four columns are a simple code describing the flow. In this code U stands for upper layer and L stands for the lower layer. Here is how to read each of the headers. The first is U->U which should read, flow from the upper layer of the first compartment to the upper layer of the second. The second is U->L->U which reads, flow from the upper layer of the first through the lower layer of the second to the upper layer of the second compartment. The third is L->L which means the flow from the lower layer of the first to the lower layer of the second. And finally L->U->L reads, flow from the lower layer of the first through the upper layer of the second to the lower layer of the second. The last two columns continue the code with the addition of E which means the mass entrained. So we have E->U which means mass entrained into the upper layer of the second compartment, and E->L for mass entrained into the second compartment's lower layer.

6.2.5 Output for Option /R:W

The /R:W reports wall temperature profiles for each of the surfaces in each of the compartments in a section titled "Interior Wall Temperature Profiles." As with the rest of the output the compartments and surfaces run down and the output runs left to right. In the first column is the compartment number. The second column gives the surface using the labels ceiling, up wall, low wall, or floor. Up wall refers to the part of the wall up above the interface and in contact with the hot upper layer. Low wall means the part of the wall below the interface. The next ten columns are the temperature of the first ten nodes of the wall starting with the surface temperature. The rest of the nodes are listed in rows of ten nodes directly below the first ten until all nodes have been listed.

6.2.6 Output for Option /R:T

To get the "Tenability Measures" table to print out use the /R:T option. It is the last table for each output when requested. **Here goes the reference for Tenability** describes tenability. The table is very simple. Each compartment is listed down the page. Across the page run the seven tenability calculations made by CFAST for a person in the compartment from the beginning of the simulation. They are in order from left to right fed1, fed2, fed3, temp1, temp2, ct and flux.

6.2.7 Sample Output

The sample output described above is shown on the following pages in the order generated by the program. Refer to the sections above for a description of the output.

OVERVIEW

Data file is prm.dat (Checksum 00000000)

Compartments Doors, ... Ceil. Vents, ... MV Connects

2 2 1 2

Simulation Time (s)	Print Interval (s)	History Interval (s)	Restart Interval (s)
---------------------------	--------------------------	----------------------------	----------------------------

200	5	5	0
-----	---	---	---

Ceiling jet is off for all surfaces.
History file is PRM.HI

AMBIENT CONDITIONS

Interior Temperature (K)	Interior Pressure (Pa)	Exterior Temperature (K)	Exterior Pressure (Pa)	Station Elevation (m)	Wind Speed (m/s)	Wind Ref. Height (m)	Wind Power
300.	101300.	300.	101300.	0.00	0.0	10.0	0.16

COMPARTMENTS

Compartment	Width (m)	Depth (m)	Height (m)	Area (m ²)	Volume (m ³)	Ceiling Height (m)	Floor Height (m)
1	4.00	4.00	2.30	16.00	36.80	2.30	0.00
2	4.00	4.00	2.30	16.00	36.80	4.60	2.30

VENT CONNECTIONS

Horizontal Natural Flow Connections (Doors, Windows, ...)

From Compartment	To Compartment	Vent Number (m)	Width (m)	Sill Height (m)	Soffit Height (m)	Abs. Sill (m)	Abs. Soffit 2 ((m^2)	Area
1	Outside	1	1.07	0.00	2.00	0.00	2.00	2.14
2	Outside	1	1.07	1.00	2.00	3.30	4.30	1.07

Vertical Natural Flow Connections (Ceiling, ...)

Top Compartment	Bottom Compartment	Shape	Area (m^2)	Relative Height (m)	Absolute Height (m)
2	1	Square	1.00	2.30	2.30

Mechanical Flow Connections (Fans, Ducts, ...)

Connections and Ducts

System	From	From Elev. (m)	To	To Elev. (m)	Length (m)	Area (m^2)	Rough (mm)
1	Comp 1	2.10	Node 1	2.10		0.12	
	Node 1	2.10	Node 2	4.40	2.30	0.08	0.00
	Node 3	4.40	Comp 2	2.10		0.12	

Fans

System	From	From Elev. (m)	To	To Elev. (m)	Fan Number	Minimum (Pa)	Maximum (Pa)	Fan Curve
1	Node 2	4.40	Node 3	4.40	1	0.00	300.00	0.14 -4.33E-04

THERMAL PROPERTIES

Compartment	Ceiling	Wall	Floor
1	GYPSUM	SOFTWOOD	CONCRETE
2	GYPSUM	SOFTWOOD	CONCRETE

Thermal data base used: THERMAL.DF

Name	Conductivity	Specific heat	Density	Thickness	Emissivity	HCL B's (1->4)				
Codes										
GYPSUM	0.160	900.	790.	1.600E-02	0.900	6.30E-03	1.92E+02	5.87E-02	7.48E+03	
CONCRETE	1.75	1.000E+03	2.200E+03	0.150	0.940	0.00E+00	0.00E+00	0.00E+00	0.00E+00	
SOFTWOOD	0.120	1.380E+03	510.	1.900E-02	0.900	0.00E+00	0.00E+00	0.00E+00	0.00E+00	

U
U
U

FIRES

Name: Main Fire

Compartment	Fire Type	Position (x,y,z)			Relative Humidity	Lower O2 Limit	Pyrolysis Temperature
1	Constrained	2.00	2.00	0.00	0.0	10.00	300.

Time (s)	Fmass (kg/s)	Hcomb (J/kg)	Fqdot (W)	Fhigh (m)	C/CO2 (kg/kg)	CO/CO2 (kg/kg)	H/C (kg/kg)	O/C (kg/kg)	HCN (kg/kg)	HCL (kg/kg)
0.	1.40E-03	1.81E+07	2.53E+04	0.00	0.00	1.00E-02	0.33	0.00	0.00	0.00
400.	1.40E-03	1.81E+07	2.53E+04	1.00E-02	0.00	1.00E-02	0.33	0.00	0.00	0.00

Name: SOFA Referenced as object # 1

Compartment	Fire Type	Position (x,y,z)			Relative Humidity	Lower O2 Limit	Pyrolysis Temperature
1	Constrained	4.00	2.00	0.00	0.0	10.00	300.

Time (s)	Fmass (kg/s)	Hcomb (J/kg)	Fqdot (W)	Fhigh (m)	C/CO2 (kg/kg)	CO/CO2 (kg/kg)	H/C (kg/kg)	O/C (kg/kg)	HCN (kg/kg)	HCL (kg/kg)
0.	0.00	1.89E+07	0.00	0.00	0.00	0.00	0.16	0.00	0.00	0.00
100.	8.00E-03	1.87E+07	1.50E+05	0.00	1.20E-02	0.00	0.16	0.00	0.00	0.00
150.	3.20E-02	1.87E+07	6.00E+05	0.00	1.40E-02	1.72E-02	0.16	0.00	0.00	0.00
215.	0.17	1.89E+07	3.12E+06	0.00	2.30E-02	1.76E-02	0.16	0.00	0.00	0.00
290.	0.15	1.89E+07	2.80E+06	0.00	2.40E-02	1.97E-02	0.16	0.00	0.00	0.00
400.	2.10E-02	1.90E+07	4.00E+05	0.00	6.00E-03	1.93E-02	0.16	0.00	0.00	0.00
500.	1.20E-02	1.87E+07	2.25E+05	0.00	0.00	1.15E-02	0.16	0.00	0.00	0.00
700.	1.10E-02	1.82E+07	2.00E+05	0.00	0.00	0.00	0.16	0.00	0.00	0.00
1200.	3.00E-03	1.67E+07	5.00E+04	0.00	0.00	0.00	0.16	0.00	0.00	0.00
2400.	0.00	1.89E+07	0.00	0.00	0.00	0.00	0.16	0.00	0.00	0.00

Name: WARDROBE Referenced as object # 2

Compartment	Fire Type	Position (x,y,z)			Relative Humidity	Lower O2 Limit	Pyrolysis Temperature
1	Constrained	0.00	2.00	0.00	0.0	10.00	300.

Time (s)	Fmass (kg/s)	Hcomb (J/kg)	Fqdot (W)	Fhigh (m)	C/CO2 (kg/kg)	CO/CO2 (kg/kg)	H/C (kg/kg)	O/C (kg/kg)	HCN (kg/kg)	HCL (kg/kg)
0.	0.00	1.59E+07	0.00	0.00	0.00	0.00	0.33	0.00	0.00	0.00
30.	0.00	1.59E+07	0.00	0.00	0.00	0.00	0.33	0.00	0.00	0.00
100.	3.14E-02	1.59E+07	5.00E+05	0.00	1.60E-02	0.23	0.33	0.00	0.00	0.00
130.	8.17E-02	1.59E+07	1.30E+06	0.00	1.90E-02	0.13	0.33	0.00	0.00	0.00
170.	0.33	1.59E+07	5.30E+06	0.00	4.00E-03	9.00E-03	0.33	0.00	0.00	0.00
220.	1.57E-02	1.59E+07	2.50E+05	0.00	0.00	1.60E-02	0.33	0.00	0.00	0.00
230.	3.77E-02	1.59E+07	6.00E+05	0.00	0.00	3.10E-02	0.33	0.00	0.00	0.00
370.	1.57E-02	1.59E+07	2.50E+05	0.00	0.00	6.30E-02	0.33	0.00	0.00	0.00
1200.	3.10E-03	1.61E+07	5.00E+04	0.00	0.00	0.00	0.33	0.00	0.00	0.00

Time = 200.0 seconds.

Compartment	Upper Temp. (K)	Lower Temp. (K)	Inter. Height (m)	Upper Vol. (m^3)		Pressure (Pa)	Ceiling Temp. (K)	Up wall Temp. (K)	Low wall Temp. (K)	Floor Temp. (K)
1	1252.	475.1	0.63	27.	(73%)	-6.68	1115.	1140.	885.1	556.7
2	828.7	325.4	1.0	21.	(56%)	1.30	590.1	578.1	422.6	322.2

Compartment	Fire	Plume Flow (kg/s)	Pyrol Rate (kg/s)	Fire Size (W)	Fire in Upper (W)	Fire in Lower (W)	Vent Fire (W)	Convec. (W)	Radiat. (W)	On Target (W/m^2)
	Main	3.324E-02	1.400E-03	2.530E+04				2.530E+04	0.000	
	SOFA	1.54	0.134	2.535E+06				2.535E+06	0.000	
	WARDROBE	1.41	0.143	2.271E+06				2.271E+06	0.000	
1		2.99	0.278	4.831E+06	0.000	4.831E+06	0.000			1.383E+05
2		0.000	0.000	0.000	0.000	0.000	0.000			2.614E+04
Outside							1.609E+03			

Upper Layer Species

Compartment	N2 (%)	O2 (%)	CO2 (%)	CO (ppm)	HCN (ppm)	HCL (ppm)	TUHC (ppm)	H2O (%)	OD (1/m)	HCl c (mg/m^2)	HCl f (mg/m^2)	HCl uw (mg/m^2)	HCl lw (mg/m^2)
1	62.4	4.27	3.16	879.	0.000	0.000	6.299E-04	29.8	1.26	0.000	0.000	0.000	0.000
2	60.9	3.39	2.76	773.	0.000	0.000	8.056E-03	32.6	1.53	0.000	0.000	0.000	0.000

Lower Layer Species

Compartment	N2 (%)	O2 (%)	CO2 (%)	CO (ppm)	HCN (ppm)	HCL (ppm)	TUHC (ppm)	H2O (%)	OD (1/m)	HCl c (mg/m^2)	HCl f (mg/m^2)	HCl uw (mg/m^2)	HCl lw (mg/m^2)
1	76.0	17.6	0.548	153.	0.000	0.000	2.752E-04	5.75	0.465	0.000	0.000	0.000	0.000
2	79.3	20.7	2.928E-04	1.683E-02	0.000	0.000	0.000	5.398E-03	6.080E-06	0.000	0.000	0.000	0.000

Vent Flow (kg/s)

From	To	Number	Type	U->U	U->L->U	L->U->L	L->L	E->U	E->L
1	3	1	H		0.955				
2	3	1	H		1.60		2.945E-02		
3	1	1	H			0.710	1.66		0.455
3	2	1	H						

Interior Wall Temperature Profiles

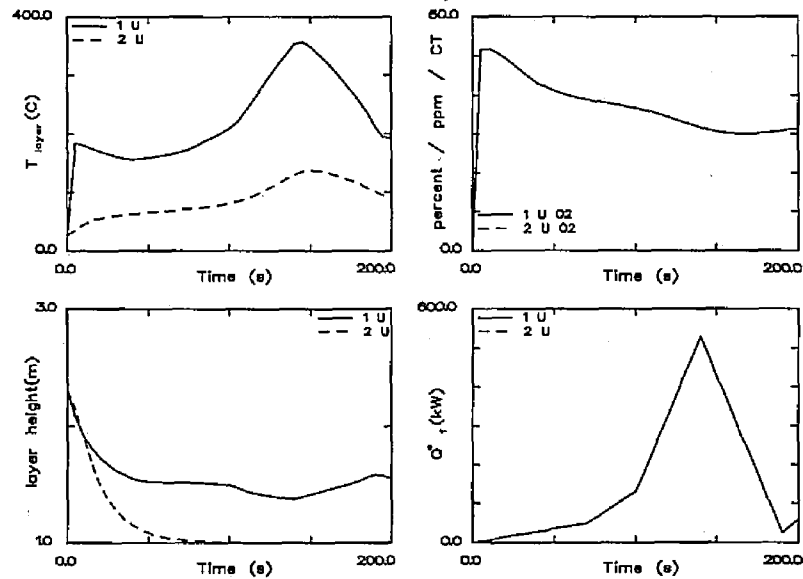
Compartment	Wall	Temp. (K)	Temp. (K)	Temp. (K)	Temp. (K)	Temp. (K)	Temp. (K)	Temp. (K)	Temp. (K)	Temp. (K)	Temp. (K)
1	Ceiling	1115.	1114.	1114.	1113.	1112.	1111.	1109.	1107.	1105.	1103.
1	Up wall	1100.	1097.	1093.	1090.	1086.	1082.	448.8	337.4	319.5	318.2
1	Low wall	1140.	1139.	1139.	1138.	1137.	1135.	1133.	1130.	1127.	1124.
1	Floor	1120.	1116.	1112.	1107.	1101.	1096.	392.1	314.6	305.5	305.1
1		885.1	884.9	884.2	882.9	881.2	879.0	876.2	873.0	869.3	865.2
1		860.5	855.4	849.8	843.8	837.3	830.3	345.6	305.7	301.8	301.6
1		556.7	555.6	552.4	547.1	539.6	530.1	518.6	505.0	489.6	472.3
2	Ceiling	453.2	432.4	410.1	386.3	361.1	334.5	300.2	300.0	300.0	300.0
2	Up wall	590.1	590.0	589.7	589.2	588.6	587.7	586.7	585.4	584.0	582.4
2	Low wall	580.7	578.7	576.6	574.3	571.8	569.1	347.9	312.1	306.4	306.1
2	Floor	578.1	577.9	577.5	576.9	576.0	574.8	573.4	571.8	569.9	567.7
2		565.3	562.7	559.8	556.7	553.3	549.8	326.3	304.1	301.5	301.4
2		422.6	422.5	422.3	422.0	421.4	420.8	420.0	419.0	417.9	416.7
2		415.3	413.8	412.2	410.4	408.5	406.4	309.7	301.3	300.5	300.4
2		322.2	322.1	321.8	321.4	320.7	319.9	318.9	317.8	316.5	315.0
2		313.5	311.7	309.9	307.9	305.9	303.7	300.0	300.0	300.0	300.0

Tenability Measures

Compartment	FED1	FED2	FED3	TEMP1	TEMP2	Ct	Flux
1	0.228	4.23	9.906E-03	984.	1.700E+09	0.000	7.925E+03
2	0.000	1.263E-03	7.030E-03	50.9	6.888E-03	0.000	1.505E+03

6.3 Default Graphical Output

While PRM.DAT runs, the default graphics display to the screen. The default graphics consist of four graphs. The upper left hand graph displays the upper layer temperature for each compartment. The upper right graph shows the %O₂ in the upper layer. The lower left hand graph gives the height above the floor of the interface between the upper and lower layer. The last graph in the lower right is of the heat release rate of the fire. The graphs update according to the display interval in the input file, in this case every 5 seconds. When the CFAST run is over, the graph clears from the screen and returns to text mode. An example of the final display for PRM.DAT is:



7 Using CPlot

The CFAST model provides 3-D pictorial results and graphs while the model is executing. The model predicts the environment produced by a fire in one of several compartments, and follows smoke and toxic gases from one compartment to another, separately predicting values for each of the variables in both the upper and lower layers. The results of these calculations are written to a special data file (the "history" file) at designated time steps. CPlot is intended to provide a visual interface to generate graphs and tables from the time histories saved by the model. CPlot has the capability to form a list of variables, read in their values at each time interval, list the values in tabular form, plot the values, and save the variables in a formatted file for use with other software. In addition, it has the capability to read history files created by other programs to plot along with CFAST data. It can read these files for several runs of each program and combine them into one or more plots and lists. To start CPlot enter the command:

```
cplot
```

See Appendix ? for alternative CPlot command lines.

Once the CPlot command line has been entered, identifying information and a "command prompt" are displayed. Commands to direct the generation of the tables and graphs may now be entered. Commands available at the "command prompt" are:

```
ADD, DELETE
AGAIN
CLEAR
DEFAULT
DIRECTORY
END
HELP
FILE, ASCII, RAPID, TENAB
LIST
PLOT, REPLOT
READ
REVIEW
SAVE
SHIFT
VARIABLE
```

These commands can be broken into five major groups that describe the process used to generate tabular or graphical output with CPlot. Each command has a sub-menu from which specific choices are made or actions taken. The following is a description of each of the commands. At least three characters must be used to identify a command.

7.1 Entering Data Into CPlot

The general procedure for using CPlot is to select the data from one or more files, then plot or print the data. The first step involves selecting the file. CPlot can currently read four types of data files:

- data created by the CFAST model (CFAST history files),

- data created by the TENAB model (TENAB history files)[83],
- data created in specially formatted ASCII text files from other programs including RAPID, a program developed by the Building and Fire Research Laboratory for analysis of large-scale fire tests[84], and
- ASCII text files, with data which is blank delimited.

The command for reading each of these file types is **FILE**, **TENAB**, **RAPID**, or **ASCII**, respectively. Variables for the TENAB, RAPID, and ASCII file types are specified at the same time as the command. For the CFAST history file, variables are selected with the **ADD** command. In addition to the file type and variable selection commands, several utility commands are available to provide support for data entry.

FILE Allows the user to specify the CFAST history file name. To select particular variables from a selected history file, use the **ADD** command.

TENAB Reads a file in the TENAB format. The TENAB program produces estimates for a number of tenability criteria for persons exposed to a fire environment predicted by the CFAST model. The user must enter the "person number" and the desired criteria to be read from the file. The possibilities are:

Tenab Variable List

1. Fractional Effective Dose Due to Gases - Bukowski
2. Fractional Effective Dose Due to Gases - Purser
3. Fractional Effective Dose Due to CO2 - Purser
4. Temperature - Deg C
5. Fractional Effective Dose Due to Convective Heat
6. CT (G-MIN/M3)
7. Flux (KW-MIN/M2)
8. Derksen Curve

RAPID Reads a file in the RAPID format after querying for the channels to read. In order for this to work, there must be a channel which corresponds to the default channel as selected by the **DEFAULT** command. Normally this is the time channel, but it can be any other desired channel.

ASCII Reads a file in columnar ASCII format after querying for the columns to read. In order for this to work, there must be a column which corresponds to the default column as selected by the **DEFAULT** command. Normally this is the time, but it can be any other desired column.

If a CFAST history file has been specified using the **FILE** command, variables must then be selected with the **ADD** command. The variables currently available are:

boundary surface temperature (ceiling, floor)	WALL	C
entrained mass flow in the plume	ENIRAIN	kg/s
hcl wall surface concentration	HCL	kg/m ²
heat release in lower layer	LELUME	kW
heat release in upper layer	UELUME	kW
heat release in flame out a vent	VEIRE	kW
heat release rate of the fire	HEAT	kW
layer height	INIE	m
layer temperature	TEMP	C
layer mass density	MASS	kg/m ³
mass flow from the plume into the upper layer	PLUME	kg/s
pyrolysis rate of the fuel	PYROL	kg/s
pressure	PRES	Pa
radiation field to a target	TARGET	W/m ²
species density	SPECIES	
total radiative heat flux into the layer	RAD	W
total convective heat flux into the layer	CONVEC	W
vent flow	VENT	kg/s
vent entrainment	JET	kg/s
volume of the upper layer	VOLUME	m ³

ADD

This command is used to build a list of CFAST variables to be read into the active list. This command applies only to files selected with the **FILE** command. **ADD** may be entered by itself or together with a list of variables that are to be added. If it is entered alone, the variables that are to be added to the list are requested. For example:

```
> ADD
- INPUT VARIABLES TO BE ADDED>TEMP,PRES
```

or

```
> ADD TEMP,PRES
```

For each variable selected, a series of questions are displayed in order to identify exactly the type of variable desired. One question displayed for all variables is:

WHICH COMPARTMENT? ->

For layer dependent variables, the user is requested to input the layer (U for upper or L for lower):

WHICH LAYER? ->

The current default value is assumed for each question when the Enter key is pressed without providing a response to the prompt. See the **DEFAULT** command to change these default values.

If the **VENTFLOW** variable is chosen, the compartments of origin and destination are requested along with the vent number. If the **SPECIES** variable is selected, the species name (O₂, CO₂,...) is requested.

The maximum number of variables allowed in the active list at any one time is 40. If the list is full or the variable is currently in the active list, the addition is disallowed, and control returns to the CPlot command prompt.

The **AGAIN**, **CLEAR**, **DELETE**, **READ**, and **REVIEW** commands allow the user to view and manipulate the list of variables read with the data entry commands.

AGAIN Repeats the input of a list of variables for a new CFAST history file. CPlot maintains a list of the most recently acquired CFAST variables. As an example, select a file with the **FILE** command, and select a set of variables. Now use the **FILE** command again to select a new file. Enter the **AGAIN** command to select the original list of variables for this new file. This function simplifies direct comparisons between runs of CFAST. It works only with files selected with the **FILE** command.

CLEAR Empties the current variable list.

DELETE When this command is entered, the current list of CFAST variables is displayed on the screen. The user is asked to select the variables to delete by entering the associated number from the list. The variables must be entered on a single line separated by commas or blanks. If the variable number entered does not correspond to one currently on the list, it is ignored. After the deletions have been completed, a new list is displayed. If the list is currently empty, an appropriate error message is displayed. One caution concerning order. The variables are deleted by the associated number in the list, not by rank ordering within the group. This is important in conjunction with use of the **AGAIN** command.

READ Used to force a read of the data files. This is most useful for script files which can be processed automatically to display data. It is equivalent to pressing an enter at the "read prompt" in the interactive mode.

REVIEW At times, the user may wish to view the current list before entering a command. This may be done with the **REVIEW** command. It prints out the current list along with the compartment number, species, and layer specified for each of the variables.

7.2 Generating Tables and Graphs With CPlot

Once the data has been selected and read, CPlot can plot or print the data values. The commands **LIST** and **PLOT** allow the user to generate a table of values or a graph for selected variables. The **SHIFT** command allows the user to shift the abscissa (horizontal) or ordinate (vertical) axis of a variable.

LIST Lists the values of any of the variables in the current list to the screen. The variables desired and the time range for the list are requested. Once the list is displayed on the screen, it can be printed with the **PRINT SCREEN** key.

PLOT

After entering the **PLOT** command, the current list of variables is displayed. To group variables together for a single graph use parentheses. Separate variables within the parentheses by commas or blank spaces. Variables to be plotted together on a single graph must be of the same type. As an example:

```
Select 1->4 graphs by grouping variables
with parentheses followed by a return >(1 2 3 4)
```

will plot 1 graph with 4 variables to the screen,

while:

```
Select 1->4 graphs by grouping variables
with parentheses followed by a return >1,2,3,4
```

or

```
Select 1->4 graphs by grouping variables
with parentheses followed by a return >1 2 3 4
```

plots 4 graphs of 1 variable each to the screen.

Normally, CPlot will scale the axes automatically. However, if the automatic formatting option has been turned off using the **DEFAULT** command, the user is given the opportunity to change the range of the X and Y axes along with the graph legends before the graph is drawn. The maximum and minimum values for the X and Y axes are displayed followed by a request for any changes. Press enter if no change is desired. The next axis change request is displayed:

```
The Min/Max for Temperature are:
X =      0.00 TO      2000.00
Y =      0.00 TO      1000.00

<ENTER> If no changes are desired.
Xmin =      0.00, Change to =
Xmax =     2000.00, Change to =
Ymin =      0.00, Change to =
Ymax =     1000.00, Change to =
```

Similar prompts are made for the legends for each graph. The user is allowed to change the text for each curve label and the position. If no changes are desired, the Enter key may be pressed to accept the suggested values for the legend text and position:

```
Legend for 1 (Temperature 1 U ) is (R 1 U) . :
<ENTER> For no change:
Legend for 2 (Temperature 2 U ) is (R 2 U) . :
<ENTER> For no change:

Legend for graph 1 is at X=      40.00, Y=      945.49
<ENTER> If no changes are desired.
X =      40.00, Change to =
Y =      945.49, Change to =
```

When all changes have been made, the selected graphs are plotted.

SHIFT

Used to adjust the variable axes. For example, it may be used when plotting variables from different files to normalize the data to a common ignition time or initial temperature. The required input is a selection of the axis to shift, the amount of shift, and a list of channels. Please note that shifting the time axis for a single variable will shift the time axis for all variables associated with that particular file. Such an effect occurs because only one vector of values is kept to represent the timeline for each file.

7.3 Saving Data With CPlot

The **SAVE** command allows the user to create an ASCII text file in one of two formats. These files may be used for future CPlot runs or for exporting CFAST or TENAB data to other programs.

SAVE

Saves the values for the variables in the current list into a file. The format used depends on the option chosen by the **DEFAULT** command. Columnar data can be used for spreadsheet and charting programs. Row data is used to make the data compatible with the data processing program (RAPID) designed for the reduction of experimental data in the Building and Fire Research Laboratory.

The user is prompted for the file name. A verification is made to determine if the file currently exists. If the file does exist, the user is asked if the new data should write over the old file. If the response is NO, no data is stored in the file. If the response is YES or the file does not already exist, the file is created, and the data stored.

Columnar data files are straightforward with each variable listed. The time channel is the first column.

For files in the row format, each variable in the list is saved with the following line at the beginning of each block of data:

```
I6,I6,A6,*-----COMMENT-----
```

The first I6 represents the number of data points for that variable, the next I6 specifies the number given to that variable on the list, and the A6 is the actual variable name. Everything after the "*" is a comment block and contains information relevant to that particular variable, such as species number, compartment number, layer, etc. The actual numerical data is written using the format 7E11.5.

7.4 Changing the Default Parameters in CPlot

The **DEFAULT** command allows the user to change a number of default parameters within CPlot. These defaults include the format of the graphical output along with values assumed by CPlot when the user presses the Enter key without specifying input.

DEFAULT

Enables the user to set default parameters for the following:

Default compartment specifies the compartment number to be used whenever the user presses an Enter in response to a question requesting a compartment number. **Ventflow destination** specifies the compartment number for the "to compartment" for vent flows. **Default species** and **default layer** specify the species and layer, respectively, to be used whenever the user presses an Enter in response to a request for a species or a layer. **Character set** is a number from 1 to 25 which specifies a different typeface to be used. Only character sets 4, 7, 24, and 25 are supplied with CFAST. **Graphics device** specifies where the graphic output is placed. Allowable outputs are type 1 or SCREEN for output to the screen, and type 6 or HPGL for output to a file formatted for Hewlett-Packard format devices. **Automatic plot formatting** allows the user to customize the format of the graphical output. A response of Yes instructs CPlot to format the axes and legends automatically. A response of No allows the user to select the axis limits and legend text manually for each plot. **Channel for abscissa** specifies the channel number to be used for the horizontal axis for data read from RAPID format data files with the **RAPID** command. **Factor for abscissa** specifies the data column number to be used for the horizontal axis for data read in ASCII format. **Type of save file** specifies the format of the file written by the **SAVE** command. Finally, **Draw curves in color (Y/N)** and **Draw curves with dashed lines (Y/N)**, allow the user to customize the lines to be drawn for each variable in a plot.

The defaults are saved in a permanent file on the disk so the next execution of CPlot will use the defaults most recently selected.

7.5 Getting Online Help in CPlot

The **HELP** and **VARIABLE** commands provide some simple online help when using CPlot.

HELP	This command may be entered any time the user is prompted for an option. The purpose is to list to the screen the available commands with a brief explanation of each. After listing the commands, another option is requested.
VARIABLE	Shows the list of variables which are available for the files selected with the FILE command (CFAST history files). This list is identical to the one shown in the introduction to this CPlot section.
DIRECTORY	Shows a list of files in the current (or remote if set) directory. Functions in a manner similar to the "dir" ("ls" in Unix) command. Wildcards are used in the usual fashion.

7.6 Exiting CPlot

The **END** command terminates the execution of CPlot. If desired, any data which has been read into CPlot should be saved prior to entering this command. Any data not saved is lost upon exiting CPlot and must be re-entered if it is to be used again.

8 Using Exitt, Tenab, and Survival

All three of the egress and tenability programs use a common interface to specify input and output file names for the programs. When one of the programs is selected within the HAZARD shell, a dialog box is presented to allow the user to fill in four file names for the program. These files are:

Program	File 1	File 2	File 3	File 4
Exitt	CFAST History File	Buidling Description	Printed Output	Exitt Egress Output
Tenab		Exitt Egress File		Tenability Plotting Output
Survival		Building Description		Tenability Plotting Output

The printed output can be viewed with any text editor, including the one built into the HAZARD shell (accessed from the file menu or by pressing (f7)).

9 Utility Programs

There are several programs which are not really part of the simulation model but are aids in using the software. These utility programs are provided to ease the implementation and use of the model. Except for Report and ReportG, they must be run from the DOS command line. The utilities include:

List_obj	List the OBJECTS database
List_tpp	List the thermophysical properties database
List_clr	Test the graphics compatibility of the graphics drivers and the video display
Obj2df	Convert the prototype objects database to the direct access version used by the model (see Appendix C)
CF_set	Set the search paths, colors and other miscellaneous information for the various programs.
Report	Provide an ASCII output of the run, based on the history file generated by the original CFAST run
ReportG	Animate the graphics display - this routine will reproduce the run time graphics as was shown by CFAST in the original. This is especially useful for those who use the version of the model which does not generate run time graphics, and those who wish to do a side by side comparison of various runs of the model.

The first five routines, List_obj, List_tpp, List_clr, Obj2df and CF_set, are simply entered as commands. The latter two use a file and the option "/r<options>." For Report, the meaning of "<options>" is the same as CFAST

W => wall temperature profiles
I => building configuration
N => normal temperature/interface history
F => flow field
S => species
T => type 1 FED results (fixed nose per compartment)

or combinations, such as /rIN for a normal output sequence. For ReportG, the value of "<options>" is a wait time between frames. With no time specified, the screen is updated as rapidly as ReportG can access the data file. With an option /r10, there is a ten second pause between each frame, and so on.

10 Conclusions and Future Plans

We intend to continue to improve the hazard methodology. There are four avenues for improvements:

- Increase the number and improve the capability of the phenomena which are modeled,
- Improve the usability of the package,
- Provide derivative applications, and
- Expand the scope of the use of the methodology.

We can not proceed with other improvements until we reach a sufficient level of physical understanding. Given that basis, the next step is to expand the scope of the use of the methodology, which is dealing with the human and economic aspects of the fire problem. Examples of improvements in this area would be extending the methodology to large buildings with the rules for congestion and queuing, parameter analysis, risk, and calculating the cost of the devastation caused by a fire, and the cost of fire protection schemes. The next step is to provide the "what if" capability and include a spectrum of calculations reflecting the uncertainty in the data available.

We are committed to providing at least a rudimentary form of the statistical model for a parameter analysis of the range of scenarios which might occur. The general thrust will be to include more phenomena, such as a self-consistent fire, interactive human behavior and structural effects. As we look into the future to see where we might go, it would be appropriate to consider whether we put in gentle suggestions about the inadvisability of some selection. For example, if there exists no case where some particular fire can occur, then if someone tries to model such a fire, a warning message might appear. As an example, consider a 100 megawatt fire from an oil-well blowout in a subway tunnel. It might be a case to look at, but it is unusual. There is an attempt to do this in the data editor but much could still be done.

For fire investigation, a portable computer (hand held) which allowed one to walk through a building (before or after) and catalog the contents of a building would be a useful extension of the methodology. This could be brought back to the office and used directly as input to the model for geometric specification and data initialization. As the Cellular Digital Packet Data becomes more prevalent, onsite inspections will allow such handheld computers to interact directly with desk bound servers for maintaining databases and ascertaining code compliance. As the model becomes more sophisticated, and the complexity increases, researchers, code officials, and everyone else will have to depend on such stratagems. There simply is not enough time to fuss with all of the details. This is the arena which should allow us to pursue the goal of a better qualitative understanding of fires, well as doing more of it faster.

As the concept of fire safe structures takes hold, the question will arise of how much does some improvement cost, how much will it save, and what are the likely actions of those involved in a fire. One area we have not discussed explicitly is the valuation of a building or system subject to a fire, and what the worst or most probable fire and concomitant dollar loss would be. Such a capability would be on top of that for estimating the effect of fire.

HAZARD is now published with some sample cases. It would be beneficial to enhance its use by providing a set of cases from start to finish with a data file and a video of the actual case burned in a test facility. We could have a presentation of fire and its consequences. This might include (computer) video and concomitant data sets for simulation.

One of the important extensions of the hazard methodology necessitates a multiplatform capability, which we have been pursuing. So far we have concentrated on the SGI Iris and PC compatibles. Eventually

this will be extended to the Sun, and other Unix platforms. If OS/2 and/or Windows NT become available, our experience with building a GUI should allow us to port to these operating systems. The Mac is sufficiently different that we do not have the resources to support it.

The concept of general building/people/fire interactions needs to be included. There are three aspects which we need to address. The first is the people/building interaction. The second is an integrated model for highrise and residential. The third is an editor for people movement rules. The fire model is sufficiently fast that the run time graphics is almost irrelevant. It should be possible to develop Survival so that the people interact with the fire by having Survival call the CFAST kernel.

The front end (GUI) for HAZARD v2.0 will be a vast improvement over the text based interface we currently utilize. We intend to extend this to all aspects, including the use of the FPETool idea as a utility within HAZARD. Our concept of a GUI will be embodied first in CEdit and the Hazard shell. In the first instance, we will have a simple single file editing session. The long range plan is to allow editing of multiple sessions and concurrent execution of the model. In some ways this goes beyond our original goal of providing a simple filter to prevent egregious mistakes, but it will allow us to make the databases much more versatile without encumbering the user of the system too much. We will extend the editor to include the graphics output as well as the people placement and specification of those items which affect the behavior of people.

One of the most important extensions of the hazard methodology is the concept of automated parameter variation, which includes incorporating probability of actual events to ascertain the relative effect of particular scenarios. This capability will increase the usefulness of our models manyfold. As part of this work, we will develop a mechanism to ascertain the sensitivity of the outcome to the parameters themselves (fine variation) as well as their variation (gross variation). A critical point will be to decide upon a reasonable extent of variation. For example, if we consider a door that will be open or closed, should we consider it to be absolutely closed, with leakage, a crack $\frac{1}{8}$, $\frac{1}{4}$, $\frac{1}{2}$ and fully open, or some other combination?

10.1 New phenomena

There are many new phenomena which we need to incorporate. Those under active consideration include

- Compartment to compartment heat transfer via conduction,
- Flow within compartments (hybrid),
- Burning at corners (furniture, adjoining walls),
- Structural effects (barriers to smoke and fire spread as well as load bearing capability)
- Improved pyrolysis model (based on more fundamental physical aspects of materials)
- Construction design files (databases used for building and ship design)
- Self consistent fire - both a flame spread model and a pyrolysis model
- Improved understanding of species generation such as CO/CO₂ and its source,
- Vitiation effects on combustion and toxicity
- General radiation model - odd shapes and heat transfer between compartments
- Two directional heat transfer in walls (non-congruent thermocline)
- Better detector and other sensor activation (include new detectors)
- Deposition and agglomeration of smoke and other species
- Suppression - include fire size, drop size and distance effects, geometry of the fire
- Multiple layers, zones (hybrid modification) - a must for detector siting

Modifications to all modules to utilize FDMS[85],[86] databases
Corrosion - add on for HCl - important for semiconductor industry and warehouses.
Smoke movement in tall shafts, stairways and atria
CASE methodology and audit capability

10.2 Limitations

There are phenomena which can be done better.

- *General* - Pyrolysis (and flame spread) models still depend on test methods
No heating/cooling in HVAC ducts
Reverse flow in fans
- *Entrainment* - fire plume and doorway jet entrainment are based on the same experimental correlations. The fire plume (for large spaces) and the doorway jet (in general) are often used outside the normal range of validity of these correlations.
- *User specification* - the level of agreement is critically dependent upon careful choice of the input data for the model. A better understanding of typical fire induced leakage in buildings would facilitate more accurate description of the building environment.
- *Statistical treatment of the data* - presentation of the differences between model predictions and experimental data in [?] are intentionally simple. With a significant base of data to study, appropriate statistical techniques to provide a true measure of the "goodness of fit" should be investigated.
- *Experimental measurements* - measurement of leakage rates, room pressure, or profiles of gas concentration are atypical in experimental data. These measurements are critical to assessing the accuracy of the underlying physics of the models or of the models ability to predict toxic gas hazard.

An important part of our work is developing into providing various types of databases. This is an important underpinning of the cooperative venture. Companies will be able to make decisions on products or building assemblies. At present we are redoing the FDMS concept. There are two reasons: 1) it is very difficult to add new types of tables. This has resulted in many people abandoning its use; and 2) for the fire modeling work we need a consistent and well defined database structure for data which is used for validation, the various data sets we use within the models, and so on. We are developing the new structure and modules with the caveat in mind that previous work should fit into and be usable.

10.3 New Technology

Technologies which we should address and embrace include the diversity of computer platforms which are evolving, networks and multiprocessor systems, and new hardware such as CDROM.

CDROM: The first technology we intend to address is our distribution medium. Multimedia is on the rise and the prediction for CDROM sales is 2-3 million in 1993 alone. As sales grow, the per unit cost comes down, and is now only about three times that of a standard floppy. Using the CDROM as a medium would allow us to include the databases which will be necessary to utilize the new generation of

fire models. In addition, we could include video sequences of some of the sample and test cases. We need to run actual fires of some of the samples files which we distribute with HAZARD and include the video with the distribution.

Networks: At present there are over 100 million microcomputers in use. This number, including high end workstations, is likely to continue to increase. Manufacturers are beginning to develop small-scale parallel systems, and the cost of adding a processor board is only about 20% of the cost of a new system. The implication is that 2 to 10 processor systems are likely to become the norm for computer systems. Also, office systems are being networked. This is especially for those people we are trying to reach, who have both homogeneous and heterogeneous systems. We should be able to take advantage of these hardware configurations. This utilization will become more important as the models become more complex and there is a concomitant increase in the computing time. We will begin developing a method to utilize this parallelism.

10.4 Capabilities and Processing Power

For real time fire fighting, we could have a portable computer (hand held) which allowed one to walk through a building (before or after) and catalog the contents of a building. This could be brought back to the office and used directly as input to the model for geometric specification and data initialization.

All large buildings have breakout panels for various alarms. Indeed, some fire departments can display floor plans of buildings in the command center at a fire. It is a logical next step to plug these displays into the alarm system to see the current status of a building and then make a prediction of the next five minutes.

Another area is that of risk. Risk is the next step up from a hazard calculation, and requires a much more general understanding of the parameters which affect the outcome of a fire and its impact on humans and structures. This application would require an automated application of the model over types of fires, day and night scenarios, position of the fire and so on. The number of such calculations can become enormous. Some means of doing this in finite time will need to be found.

As we extend the capability of the zone models, we are encountering the inherent limitations of these types of models. The general concept of a zone or control volume model uses a volume as one of the variables. Inherently there is no spatial information available. The first deviation from this viewpoint was the necessity of including height vs. width information in order to calculate flow through a normal vent, such as a door. The second came when flow through a ceiling/floor opening and mechanical ventilation were included. We have extended the concept for the position of the fire. We must now take one more step and define the spatial component of a compartment.

10.5 Summary

The quest is to provide a tool which will help improve the understanding of fires. This is not an attempt to make the application of models trivial, but rather to provide a mechanism to allow researchers, fire protection engineers, and others access to the most current understanding of the behavior of fires. To reach this goal, we try to improve the physical basis of the model. At the same time, we hope to allow more extensive calculations such as long corridors, three dimensional effects (the "capabilities and processing power" section), and the use of faster computers, distributed processing, and automatic transfer of data. Although the concept of a more intuitive interface is a goal, there really is no such thing as an intuitive user interface. Our goal is to provide a tool which aids, and does not hinder, understanding of fire effects and phenomena.

11 References

- [1] Bukowski, R.W., Peacock, R.D., Jones, W.W., and Forney, C.L., "Technical Reference Guide for the HAZARD I Fire Hazard Assessment Method," Handbook 146, Volume II, National Institute of Standards and Technology, June 1989.
- [2] Bukowski, R.W., Peacock, R.D., Jones, W.W., and Forney, C.L., "Software User's Guide for the HAZARD I Fire Hazard Assessment Method," Handbook 146, Volume I, National Institute of Standards and Technology, June 1989.
- [3] Peacock, R. D., Jones, W. W., Bukowski, R. W., and Forney, C. L., Technical Reference Guide for the HAZARD I Fire Hazard Assessment Method, Version 1.1, Natl. Inst. Stand. Technol., Handbook 146, Volume II (1991).
- [4] Peacock, R. D., Jones, W. W., Bukowski, R. W., and Forney, C. L., Technical Reference Guide for the HAZARD I Fire Hazard Assessment Method, Version 1.1, Natl. Inst. Stand. Technol., Handbook 146, Volume II (1991).
- [5] Reid, R., Prausnitz, J., and Sherwood, T., The Properties of Gases and Liquids, McGraw-Hill 3rd Edition, p. 193, New York (1973).
- [6] Incropera, F.P. and De Witt, D.P., Fundamentals of Heat and Mass Transfer, 3rd Ed., John Wiley & Sons, New York (1990).
- [7] The SFPE Handbook of Fire Protection Engineering, DiNenno, Beyler, Walton, Custer and Watts, Editors, Society of Fire Protection Engineers, Boston (1990)
- [8] Friedman, R., "Survey of Computer Models for Fire and Smoke," *Factory Mutual Research Corp.*, Norwood, MA, 02062 1990.
- [9] Cooper, L.Y., "A Mathematical Model for Estimating Available Safe Egress Time in Fires," *Fire and Materials*. 1982, 6(4), 135-144.
- [10] Babrauskas, V., "COMPF2-A Program for Calculating Post-Flashover Fire Temperatures," *Natl. Bur. Stand. (U.S.)* 1979, *Tech. Note 991*, 76 p.
- [11] Davis, W. D. and Cooper, L. Y., "Computer Model for Estimating the Response of Sprinkler Links to Compartment Fires With Draft Curtains and Fusible Link-Actuated Ceiling Vents," *Fire Technology* 1991, 27 (2), 113-127.
- [12] Mitler, H.E. and Emmons, H.W., "Documentation for CFCV, the Fifth Harvard Computer Fire Code," *Nat. Bur. Stand. (U.S.)* 1981, *NBSGCR 81-344*, 187 p.
- [13] Mitler, H. E. and Rockett, J., "A User's Guide for FIRST, a Comprehensive Single Room Fire Model," *Natl. Bur. Stand. (U. S.)* 1987, *NBSIR 87-3595*.
- [14] Tanaka, T., "A Model of Multiroom Fire Spread," *Nat. Bur. Stand. (U.S.)* 1983, *NBSIR 83-2718*, 175 p.

- [15] Gahm, J. B., "Computer Fire Code VI, Volume I," *Nat. Bur. Stand. (U.S.)* 1983, *NBS GCR 83-451*, 116 p.
- [16] Jones, W. W., A Multicompartment Model for the Spread of Fire, Smoke and Toxic Gases, *Fire Safety Journal* 9, 55 (1985); Jones, W. W. and Peacock, R. D., Refinement and Experimental Verification of a Model for Fire Growth and Smoke Transport, *Proceedings of the 2nd International Symposium on Fire Safety Science, Tokyo* (1989); Jones, W. W. and Peacock, R. D., "Technical Reference Guide for FAST Version 18" *Natl. Inst. Stand. Technol. Tech. Note* 1262 (1989).
- [17] Forney, G. P. and Cooper, L. Y., The Consolidated Compartment Fire Model (CCFM) Computer Application CCFM-VENTS - Part II: Software Reference Guide, *Nat. Inst. Stand. Technol., NISTIR 90-4343* (1990).
- [18] Jones, W. W. and Forney, G. P. "A Programmer's Reference Manual for CFAST, the Unified Model of Fire Growth and Smoke Transport," *Natl. Inst. Stand. Technol.* 1990, *Tech. Note* 1283, 104 p.
- [19] Mitler, H. E. "Comparison of Several Compartment Fire Models: An Interim Report," *Natl. Bur. Stand. (U.S.)* 1985, *NBSIR 85-3233*, 33 p.
- [20] Jones, W. W. "A Review of Compartment Fire Models," *Natl. Bur. Stand. (U.S.)* 1983, *NBSIR 83-2684*, 41 p.
- [21] Babrauskas, V., Lawson, J. R., Walton, W. D., Twilley, W. H., "Upholstered Furniture Heat Release Rates Measured with a Furniture Calorimeter," *Natl. Bur. Stand. (U.S.)*, *NBSIR 82-2604*, 1982.
- [22] Babrauskas, V. and Krasny, J. F., "Fire Behavior of Upholstered Furniture," *Natl. Bur. Stand. (U.S.)*, *Monogr. 173*, 1985.
- [23] Lee, B.T., "Effect of Ventilation on the Rates of Heat, Smoke, and Carbon Monoxide Production in a Typical Jail Cell Fire," *Natl. Bur. Stand. (U.S.)*, *NBSIR 82-2469*, 1982.
- [24] Peacock, R. D., Davis, S., Lee, B. T., "An Experimental Data Set for the Accuracy Assessment of Room Fire Models," *Natl. Bur. Stand. (U.S.)*, *NBSIR 88-3752*, April 1988, p. 120.
- [25] Babrauskas, V., Levin, B.C., Gann, R.G., "A New Approach to Fire Toxicity Data for Hazard Evaluation," *ASTM Standardization News*, September 1986.
- [26] Notarianni, K. A. and Davis, W. D., Use of Computer Models to Predict the Response of Sprinklers and Detectors in Large Spaces, *Society of Fire Protection Engineers and Worcester Polytechnic Institute. Computer Applications in Fire Protection. Proceedings. June 28-29, 1993, Worcester, MA*, pp. 27-33 (1993).
- [27] Cooper L. Y. and Forney, G. P., The consolidated compartment fire model (CCFM) computer application CCFM-VENTS - part I: Physical reference guide. *Natl. Inst. Stand. Technol., NISTIR 4342* (1990).

- [28] Forney, G. P. and Moss, W. F., Analyzing and Exploiting Numerical Characteristics of Zone Fire Models, Natl. Inst. Stand. Technol., NISTIR 4763 (March 1992).
- [29] Jones, W. W. and Bodart, X., Buoyancy Driven Flow as the Forcing Function of Smoke Transport Models, Natl. Bur. Stand. (U. S.), NBSIR 86-3329 (1986).
- [30] Rehm, R. G. and Forney, G. P., "A Note on the Pressure Equations Used in Zone Fire Modeling," Natl. Inst. Stand. Technol., NISTIR 4906 (1992).
- [31] Babrauskas, V., "Development of the Cone Calorimeter - A Bench Scale Heat Release Rate Apparatus Based on Oxygen Consumption," *Fire and Materials* 8, 1984, p 81.
- [32] "Standard Test Method for Heat and Visible Smoke Release for Materials and Products Using and Oxygen Consumption Calorimeter," ASTM E1354-90, *American Society for Testing and Materials*, Philadelphia, PA 1990.
- [33] Morehart, J. H., Zukowski, E. E., and Kubota, T., "Characteristics of Large Diffusion Flames Burning in a Vitiated Atmosphere," Third International Symposium on Fire Safety Science, Edinburgh 1991.
- [34] McCaffrey, B. J., "Momentum Implications for Buoyant Diffusion Flames," *Combustion and Flame* 52, 1983, p. 149.
- [35] Cetegen, B. M., "Entrainment and Flame Geometry of Fire Plumes," Ph.D. Thesis, California Institute of Technology, Pasadena 1982.
- [36] Tewarson, A., Combustion of Methanol in a Horizontal Pool Configuration, Factory Mutual Research Corp., Norwood, MA, Report No. RC78-TP-55 (1978).
- [37] McCaffrey, B. J., Entrainment and Heat Flux of Bouyant Diffusion Flames, Natl. Bur. Stand. (U. S.), NBSIR 82-2473, 35 p. (1982).
- [38] Koseki, H., Combustion Properties of Large Liquid Pool Fires, *Fire Technology*, 25(3), 241-255 (1989).
- [39] Quintiere, J. G., Steckler, K., and Corley, D., An Assessment of Fire Induced Flows in Compartments, *Fire Science and Technology* 4, 1 (1984).
- [40] Quintiere, J. G., Steckler, K. and McCaffrey, B. J., "A Model to Predict the Conditions in a Room Subject to Crib Fires," First Specialist Meeting (International) of the Combustion Institute, Talence, France 1981.
- [41] Cooper, L. Y., Calculation of the Flow Through a Horizontal Ceiling/Floor Vent, Natl. Inst. Stand. Technol., NISTIR 89-4052 (1989).
- [42] Klote, J. H., A Computer Model of Smoke Movement by Air Conditioning Systems, NBSIR 87-3657 (1987).
- [43] 1989 ASHRAE Handbook Fundamentals, American Society of Heating, Refrigeration and Air Condition Engineers, Inc., Atlanta, GA 1989.

- [44] Forney, G. P., Computing Radiative Heat Transfer Occurring in a Zone Fire Model, Natl. Inst. Stand. Technol., NISTIR 4709 (1991).
- [45] Siegel, R. and Howell, J. R., Thermal Radiation Heat Transfer, Hemisphere Publishing Corporation, New York, second ed. (1981).
- [46] Hottel, H. C., Heat Transmission, McGraw-Hill Book Company, New York, third ed. (1954).
- [47] Hottel, H. and Cohen, E., Radiant Heat Exchange in a Gas Filled Enclosure: Allowance for non-uniformity of Gas Temperature, American Institute of Chemical Engineering Journal 4, 3 (1958).
- [48] Yamada, T. and Cooper, L. Y., Algorithms for Calculating Radiative Heat Exchange Between the Surfaces of an Enclosure, the Smoke Layers and a Fire, Building and Fire Research Laboratory Research Colloquium, July 20, 1990.
- [49] Jones, W. W. and Forney, G. P., Improvement in Predicting Smoke Movement in Compartmented Structures, Fire Safety J., 21, pp 269-297 (1993).
- [50] Schlichting, H., "Boundary Layer Theory," translated by J. Kestin, Pergammon Press, New York, 1955.
- [51] Golub, G. H. and Ortega, J. M., Scientific Computing and Differential Equations, An Introduction to Numerical Methods. Academic Press, New York (1989).
- [52] Strang, G. and Fix, G. J., An Analysis of the Finite Element Method. Prentice-Hall, Englewood Cliffs, New Jersey (1973).
- [53] Moss, W. F. and Forney, G. P., "Implicitly coupling heat conduction into a zone fire model." Natl. Inst. Stand. Technol., NISTIR 4886 (1992).
- [54] Cooper, L. Y., Fire-Plume-Generated Ceiling Jet Characteristics and Convective Heat Transfer to Ceiling and Wall Surfaces in a Two-Layer Zone-Type Fire Environment, Natl. Inst. Stand. Technol., NISTIR 4705, 57 p. (1991).
- [55] Cooper, L. Y., Heat Transfer in Compartment Fires Near Regions of Ceiling-Jet Impingement on a Wall. J. Heat Trans., 111, pp. 455-460 (1990).
- [56] Cooper, L. Y., Ceiling Jet-Driven Wall Flows in Compartment Fires. Combustion Sci. and Technol., 62, pp. 285-296 (1988).
- [57] Jaluria, Y. and Cooper, L. Y., Negatively Buoyant Wall Flows Generated in Enclosure Fires. Progress in Energy and Combustion Science, 15, pp. 159-182 (1989).
- [58] Galloway, F. M., Hirschler, M. M., "A Model for the Spontaneous Removal of Airborne Hydrogen Chloride by Common Surfaces," *Fire Safety Journal* 14, 1989, pp. 251-268.

- [59] Galloway, F. M., Hirschler, M. M., "Transport and Decay of Hydrogen Chloride: Use of a Model to Predict Hydrogen Chloride Concentrations in Fires Involving a Room-Corridor-Room Arrangement," *Fire Safety Journal* 16, 1990, pp. 33-52.
- [60] Alpert, R. L., et al., "Influence of Enclosures on Fire Growth: Volume I: Test Data," *Factory Mutual Research Corp.*, Norwood MA. 1977, *FMRC No. OAOR2.BU-1 through 7*.
- [61] Cooper, L. Y., Harkleroad, M., Quintiere, J. G., and Rinkinen, W. J., "An Experimental Study of Upper Hot Layer Stratification in Full-Scale Multiroom Fire Scenarios," *J. Heat Trans.* 1982, 104, 741-749.
- [62] Quintiere, J. G., and McCaffrey, B. J., "The Burning of Wood and Plastic Cribs in an Enclosure," 2 vols., *Nat. Bur. Stand. (U.S.)* 1980, *NBSIR 80-2054*.
- [63] Heskestad, G., and Hill, J. P., "Experimental Fires in Multiroom / Corridor Enclosures," *Natl. Bur. Stand. (U.S.)* 1986, *NBSGCR 86-502, CIB W14/85/10 (USA)*.
- [64] Rockett, J. A., Morita, M., and Cooper, L. Y., "Comparisons of NBS/Harvard VI Simulations and Full-scale Multi-room Fire Test Data," in *Proceedings of 2nd International Symposium of Fire Safety Science*, Tokyo, Japan. 1988, 481-490.
- [65] Rockett, J. A., Morita, M., and Cooper, L. Y., "Comparisons of NBS/Harvard VI Simulations and Data from all Runs of a Full-scale Multi-room Fire Test Program," *Fire Safety J.* 1989, 15, 115-169.
- [66] Rockett, J. A., and Morita, M., "The NBS Harvard VI Multi-room Fire Simulation," *Fire Sci. Technol.* 1985, 5(2), 159-164.
- [67] Peacock, R. D., Davis, S., and Babrauskas, V., Data for Room Fire Model Comparisons. *J. Res. Natl. Inst. Stand. Technol.* 96, 411 (1991).
- [68] Nelson, H. E., "An Engineering View of the Fire of May 4, 1988 in the First Interstate Bank Building, Los Angeles, California," *Natl. Inst. Stand. Technol.* 1989, *NISTIR 89-4061*, 39 p.
- [69] Bukowski, R. W., "Reconstruction of a Fatal Residential Fire at Ft. Hood, Texas," *First HAZARD I Users' Conference*, Natl. Inst. Stand. Technol., Gaithersburg, MD, June 5-6, 1990.
- [70] Emmons, H.W., "Why Fire Model? The MGM Fire and Toxicity Testing," *Fire Safety J.*, 13 77-85 1988.
- [71] Levine, R. S. and Nelson, H. E., "Full Scale Simulation of a Fatal Fire and Comparison of Results with Two Multiroom Models," *Natl. Inst. Stand. Technol.* 1990, *NISTIR 90-4268*, 105 p.
- [72] Deal, S. "A Review of Four Compartment Fires with Four Compartment Fire Models," *Fire Safety Developments and Testing*, Proceedings of the Annual Meeting of the Fire Retardant Chemicals Association. October 21-24, 1990, *Ponte Verde Beach, Florida*, 33-51.
- [73] Nelson, H. E., "FPETOOL: Fire Protection Engineering Tools for Hazard Estimation," *Natl. Inst. Stand. Technol.* 1990, *NISTIR 4380*, 120 p.

- [74] Duong, D. Q., "The Accuracy of Computer Fire Models: Some Comparisons with Experimental Data from Australia," *Fire Safety J.* 1990, 16(6), 415-431.
- [75] Babrauskas, V., "Upholstered Furniture Room Fires -- Measurements, Comparison with Furniture Calorimeter Data, and Flashover Predictions," *J. Fire Sci.* 1984, 4, 5-19.
- [76] Lee, B. T., Effect of Wall and Room Surfaces on the Rates of Heat, Smoke, and Carbon Monoxide Production in a Park Lodging Bedroom Fire, *Natl. Bur. Stand. (U. S.)*, 1985, NBSIR 85-2998, 78 p.
- [77] Heskestad, G., and Hill, J. P., "Propagation of Fire and Smoke in a Corridor," *Proceedings of the 1987 ASME/JSME Thermal Engineering Joint Conference 1987, Honolulu, HI*, 371-379.
- [78] Klote, J. H., "Fire Experiments of Zoned Smoke Control at the Plaza Hotel in Washington DC," *Natl. Inst. Stand. Technol.* 1990, NISTIR 90-4253, 75 p.
- [79] Babrauskas, V. B. and Peacock, R. D., "Heat Release Rate: The Single Most Important Variable in Fire Hazard." *Fire Safety J.* 18 (1992) 255-272.
- [80] Quintiere, J. G., and McCaffrey, B. J., "The Burning of Wood and Plastic Cribs in an Enclosure," *Natl. Bur. Stand. (U. S.)* 1980, NBSIR 80-2954, 2 vols.
- [81] Delichatsios, M. A., "Fire Growth Rate in Wood Cribs," *Combustion and Flame* 1976, 27, 267-278.
- [82] Emmons, H. W., "Vent Flows," Section 1, Chapter 8 in *The SFPE Handbook of Fire Protection Engineering*, C. L. Beyler, Ed., *National Fire Protection Association*, Quincy, MA 1988.
- [83] Bukowski, R.W., Peacock, R.D., Jones, W.W., and Forney, C.L., Technical Reference Guide for the HAZARD I Fire Hazard Assessment Method, Handbook 146, Volume II, National Institute of Standards and Technology, June 1991
- [84] Peacock, R.D., Breese, J.N., Forney, C.L., A Users Guide for RAPID, Version 2.3, National Institute of Standards and Technology Special Publication 798 (1991)
- [85] Portier, R., A Programmer's Reference Guide to FDMS File Formats, National Institute of Standards and Technology Internal Report 5162 (1993).
- [86] Portier, R., Fire Data Management System, FDMS 2.0, Technical Documentation, National Institute of Standards and Technology Technical Note 1407 (1994).

Appendix A: Fan-Duct Systems

John H. Klotz
Building and Fire Research Laboratory
National Institute of Standards and Technology
Gaithersburg, MD 20899

A.1 Introduction

The purpose of this section is to provide background information for the user to help in the analysis of air moving systems. Fan-duct systems can be simulated by a constant volumetric flow approach or a variable flow approach incorporating the fan curve. In this section, emphasis is on the variable flow approach. The flow in a fan-duct system can vary due to pressure changes including those caused by the fire or the wind. When such flow variations are significant, a variable flow analysis of the fan-duct system may be necessary. However, the constant flow approach is very useful and is suggested as a starting point, because of its simplicity and ease of use. In the constant flow approach, the volumetric flow through the fan is constant regardless of the pressure across the fan. For many applications the constant flow approach is sufficient.

A.2 System Types

Fan-duct systems are commonly used in buildings for heating, ventilation, air conditioning, pressurization, and exhaust. Figure 1(a) shows smoke management by an exhaust fan at the top of an atrium, and figure 1(b) illustrates a kitchen exhaust. Cross ventilation, shown in figure 1(c), is occasionally used without heating or cooling. Generally systems that maintain comfort conditions have either one or two fans. Residences often have a systems with a single fan as shown in figure 2(a). In this system return air from the living quarters is drawn in at one location, flows through filter, fan and coils, and is distributed back to the residence. This system does not have the capability of providing fresh outside air. These systems are intended for applications where there is sufficient natural air leakage through cracks in walls and around windows and doors for odor control. Further information about these systems is presented in the by Klotz and Milke (1992) and the American Society of Heating, Refrigerating and Air Conditioning Engineers (ASHRAE 1992).

A.3 Network Concept of Fan-Duct System Simulation

The fan-duct system is represented as a network of nodes each at a specific temperature and pressure. The nodes may be connected by fans, ducts, fittings and other components. Except for fans, air flows through these components from nodes of higher pressure to nodes of lower pressure. For example, the residential system illustrated in figure 2(a) is represented in figure 2(b) as a network of a fan, eight resistances and ten nodes. These resistances incorporate all the resistance to flow between nodes. For instance, the equivalent resistance, R_1 , between nodes 1 and 2 accounts for resistances of the inlet, duct, filter and connection to the fan.

The mass flow rate, \dot{m}_{ij} , to node i from node j can be expressed as a function of the difference in pressure, $p_j - p_i$, between the two nodes.

$$\dot{m}_{ij} = \dot{m}_{ij}(p_j - p_i) \quad (1)$$

The form of the function depends on the type of connection between the two nodes as will be discussed later in detail. The conservation of mass equation for node i can be written as

$$\sum_j \dot{m}_{ij} = 0 \quad (2)$$

This equation is based on the quasi steady flow approximation, which is appropriate for most simulations of mass flow in fan-duct systems. For applications involving rapid changes in pressure (rapid damper closing, explosions etc.), this quasi steady approach is not appropriate. By substitution of eq. (1) into eq. (2) and expressing in terms of pressure, a system of equations can be obtained for all n nodes.

$$\begin{aligned} f_1(p_1, p_2, \dots, p_n) &= 0 \\ &\vdots \\ f_i(p_1, p_2, \dots, p_i, \dots, p_n) &= 0 \\ &\vdots \\ f_n(p_1, p_2, \dots, p_n) &= 0 \end{aligned} \quad (3)$$

Thus the fan-duct system pressures, p_1 to p_n , are solved simultaneously by solving n number of mass balance equations. The number of pressures included in each equation $f_i = 0$ are only p_i and those of the nodes directly connected to node i .

A.4 Fans

There are two general fan classifications: centrifugal and axial. Figure 3 illustrates the basic parts of a centrifugal fan. Flow within a centrifugal fan is primarily in a radial direction to the impeller. Centrifugal fans can produce large static pressures as high as 4000 Pa (16 in H₂O) with efficiencies typically from 65 to 80%. Figure 4 illustrates the basic parts of an axial fan. Flow within an axial fan is parallel to the shaft. Propeller fans (figure 5) are a type of axial fan that are common in many applications including exhaust. Many propeller fans can produce no more than 300 Pa (1.2 in H₂O) with efficiencies of only 25 to 40%.

A.4.1 Fan Performance

This section provides background information about fan performance. For more information about fans, readers are referred to Jorgensen (1983) and ASHRAE (1992). Typical performance of a fan operating

at constant impeller speed is illustrated in figure 6. For this figure, Δp_f is the static pressure of the fan, and \dot{V}_f is the volumetric flow of the fan. The normal operating range of fans is represented by the line segment AB on figure 6. The point B is selected by the fan manufacturer with a margin of safety to avoid unstable flow.

Fans operating in the positively sloping portion (CD of figure 6) of the fan curve exhibit unstable behavior called surging or pulsing. Unstable flow consists of violent flow reversals accompanied by significant changes in pressure, power and noise. There is little information about how long a fan can operate in the unstable region before it is destroyed.

Backward flow through a fan occurs when the static pressure is greater than that at point D . This is also called second quadrant flow. Quadrant terminology is customarily used in description of fan performance. The horizontal axis and the vertical axis divide a plane into four quadrants which for convenience are labeled Q I, Q II, Q III and Q IV on figure 6. Backward flow can be exhibited by all types of fans. The wind blowing into the outlet of a propeller fan can result in backflow, and pressures produced by fires could also produce backflow. Fourth quadrant flow (figure 6) is probably representative of all fans. As Δp_f becomes negative, the flow increases with decreasing Δp_f until a choking condition develops at point E .

It is common practice in the engineering community and fan industry to represent fan performance with Δp_f on the vertical axis and \dot{V}_f on the horizontal axis. Probably the reason is that \dot{V}_f can be thought of as a single valued function of Δp_f for flow in the first and second quadrants. Fan manufacturers generally supply flow-pressure data for the normal operating range, and they often supply data for the rest of the fan curve in the first quadrant. Specific data is not available for either second or fourth quadrant flow. No approach has been developed for simulation of unstable fan operation, and numerical modeling of unstable flow would be a complicated effort requiring research.

A.4.2 Computer Approximation of Fan Performance

Figure 7 illustrates four approaches that can be used to approximate fan performance without simulation of unstable flow. For all of these approaches, the fan curve is used for the normal operating range of AB . Also for all of the approaches, flows above the normal operating range are approximated by a straight line tangent to the fan curve at point A . This results in fourth quadrant flow that is similar to the expected flow provided that Δp_f is not overly far below the horizontal axis. In figure 7(a), flows below the normal range are approximated by a linear curve tangent to the fan curve at point B . This avoids simulation of unstable flows, but the approximated flow is higher than expected in the first quadrant and lower than expected for much of the fourth quadrant.

The approach of figure 7(b) reduces the approximated flow in the first quadrant. In this approach, the fan curve is also used for the range BF , and flows above the normal operating range are approximated by a straight line tangent to the fan curve at point F . To increase the flow in the second quadrant, figure 7(c) uses a line passing through point D with the slope of the fan curve at point A . Both of the modification of figure 7(b) and figure 7(c) are combined in the approach of figure 7(c).

Fan manufacturer data is routinely either in tabular or graphical form. As indicated by Jorgensen (1983), the use of a polynomial form of fan curve is common within the industry.

$$\dot{V}_f = B_1 + B_2 \Delta p_f + B_3 (\Delta p_f)^2 + \dots + B_n (\Delta p_f)^{n-1} \quad (4)$$

The coefficients can be entered as data or calculated by least squares regression from flow and pressure data. For constant volumetric flow applications, the only non-zero coefficient in eq. (4) is B_1 ($n = 1$). For incompressible fluids, eq. (4) is independent of temperature and pressure. For fan data at 20°C, compressibility effects amount to an error of about 6% at a temperature of 200°C.

A.5 Effective Resistances

The resistance, R , of a flow element can be defined as

$$R = \frac{\sqrt{\Delta p}}{\dot{m}} \quad (5)$$

where Δp is the pressure loss through the element corresponding to a mass flow rate, \dot{m} . The effective resistance between two nodes is always positive, however, sometimes one of the resistances between nodes can be negative as will be explained later. To account for this, $R = K^{1/2}$ can be substituted into eq. (5) to give

$$\Delta p = K \dot{m}^2 \quad (6)$$

The total pressure loss, Δp_t , from one node to the next is the sum of the losses, Δp_i , through each flow element, i , between the nodes.

$$\Delta p_t = \sum_i \Delta p_i \quad (7)$$

The effective value, K_e , relates the total pressure loss to the mass flow rate as $\Delta p_t = K_e \dot{m}^2$, and K_i relates the pressure loss through element i as $\Delta p_i = K_i \dot{m}^2$. These pressure losses can be substituted into eq. (7), and canceling like terms yields

$$K_e = \sum_i K_i \quad (8)$$

Values of K_i can be calculated for each element using equations developed later, and K_e can be calculated by eq. (8).

A.6 Resistance of Ducts

For a straight section of duct with constant cross sectional area, the Bernoulli equation incorporating pressure loss, Δp_{fr} , due to friction is commonly written

$$p_1 - p_2 = \Delta p_{fr} + \rho g(Z_1 - Z_2)$$

where the subscripts 1 and 2 refer to the duct inlet and outlet respectively, p is pressure, Z is elevation, g is the acceleration due to gravity, and ρ is the density of the gas. The pressure loss due to friction is expressed by the Darcy equation in most elementary treatments of flow in pipes and ducts (ASHRAE 1993; Murdock 1978; Daily and Harleman 1966; Schlichting 1960; etc.).

$$\Delta p_{fr} = f \frac{L}{D_e} \frac{\rho U^2}{2} \quad (10)$$

where f is the friction factor, L is the duct length, D_e is the effective diameter of the duct and U is the average velocity in the duct ($\dot{m} = \rho UA$ where A is the cross-sectional area of the duct). For a circular duct, the effective diameter is the duct diameter. For rectangular duct, Huebscher (1948) developed the relationship

$$D_e = 1.30 \frac{(ab)^{0.625}}{(a + b)^{0.250}} \quad (11)$$

where a is the length of one side of the duct, and b is the length of the adjacent side. For flat oval duct, Heyt and Diaz (1975) developed the relationship

$$D_e = \frac{1.55A^{0.625}}{P^{0.200}} \quad (12)$$

where A and P are the cross-sectional area and the perimeter of the flat oval duct. The area of a flat oval duct is

$$A = (\pi b^2/4) + b(a - b) \quad (13)$$

and the perimeter of a flat oval duct is

$$P = \pi b + 2(a - b) \quad (14)$$

where a is the major dimension of the flat oval duct, and b is the minor dimension of the duct. Combining eqs. (5) and (9) results in

$$\dot{m}_{ij} = \frac{1}{R} \sqrt{p_j - p_i + \rho g(Z_j - Z_i)} \quad (15)$$

Combining eqs. (6) and (10) results in

$$K = \frac{fL}{2D_e \rho A^2} \quad (16)$$

where A is the cross sectional area of the duct. Colebrook (1938-1939) developed the following equation for the friction factor.

$$\frac{1}{\sqrt{f}} = -2 \log_{10} \left(\frac{\epsilon}{3.7 D_e} + \frac{2.51}{R_e \sqrt{f}} \right) \quad (17)$$

where R_e is the Reynolds number (UD_e/ν where ν is the kinematic viscosity) and ϵ is the roughness of the inside surface of the duct. Data on roughness of duct materials are listed in table 1. A graphical presentation of the Colebrook equation developed by Moody (1944) was used for decades to calculate friction factors. However today it is practical to solve the Colebrook equation with computers.

A.7 Local Loss Resistances

The pressure loss, Δp , through many other elements can be expressed as

$$\Delta p = C_o \frac{\rho U_o^2}{2} \quad (18)$$

where U_o is the average velocity at cross section o within the element, and C_o is a local loss coefficient. This equation is commonly used for inlets, outlets, duct contractions and expansions, heating and cooling coils, dampers, bends and many filters. For a large number of these elements, values of C_o have been empirically determined and are tabulated frequently as functions of geometry in handbooks [10 - 12]. Manufacturers literature also contains some values of C_o . The value of K for these resistances is

$$K = \frac{C_o}{2 \rho A_o^2}$$

where A_o is the area at cross section o .

A.8 Resistance of Junctions

Junctions may be either converging or diverging as illustrated in figure 8. For network representation, a node is located at cross section c of a junction. The pressure losses in the main section depends on the flow in it and on the flow in branch, and the loss in the branch depends on both the flow in it and in the main. The pressure loss in the branch is expressed as

$$p_b - p_c = C_{c,b} \frac{\rho_c U_c^2}{2} \quad (20)$$

and the pressure loss in the main is

$$p_s - p_c = C_{c,s} \frac{\rho_c U_c^2}{2} \quad (21)$$

where $C_{c,b}$ and $C_{c,s}$ are local loss coefficients, p , ρ , and U are pressure, density and average velocity at cross sections b , c and s as illustrated in figure 8. Local loss coefficients for many junctions have been experimentally evaluated, and they are tabulated as functions of geometry and various flow ratios in handbooks along with values of C_o . Converging junctions may have negative local loss coefficients. For example when the flow in the main is much greater than that in the branch, the gas in the branch is pulled by the greater flow similar to the operation of a carburetor.

A.9 Example

Fans were used for smoke control system experiments at the Plaza Hotel building in Washington DC (Klote 1990). For this example, the fire floor was exhausted and the stairwell was pressurized, and detailed information concerning this example is provided in section 4.4 of the main report. The exhaust fan from the corridor of the second floor has a capacity of about $0.94 \text{ m}^3/\text{s}$ (2000 cfm), and the stairwell pressurization fan is about $3.3 \text{ m}^3/\text{s}$ (7000 cfm). Figure 9 shows these fan-duct systems, and the symbols used are those of CEDIT. The fire floor exhaust fan is located between nodes 2 and 3, and the stairwell fan is located between nodes 6 and 7. Further there is a sign convention concerning the direction of normal flow through the fan. At the fan inlet, the node number is followed by a minus sign. At the outlet, the node number is preceded with a plus sign. For these examples the fans are specified at the constant volumetric flow rates listed above. For example, specifying a constant $0.94 \text{ m}^3/\text{s}$ (2000 cfm) fan indicates that this fan will move $0.94 \text{ m}^3/\text{s}$ (2000 cfm) of air regardless of the pressure across the fan. The constant flow rate fan is a useful approximation for many applications.

A.10 References

- ASHRAE 1992. Handbook HVAC Systems and Equipment, American Society of Heating, Refrigerating and Air-Conditioning Engineers, Atlanta, GA.
- ASHRAE 1993. Handbook of Fundamentals, Chapter 32 Duct Design, American Society of Heating, Refrigerating and Air-Conditioning Engineers, Atlanta, GA.
- Colebrook, C.F. 1938-1939. Turbulent Flow in Pipes, With Particular Reference to the Transition Region Between the Smooth and Rough Pipe Laws, Journal of Institution of Civil Engineers (London, England), Vol 11, pp 133-156.
- Heyt, J.W. and Diaz, J. M. 1975. Pressure Drop in Flat-Oval Spiral Air Duct, ASHRAE Transactions, Vol. 81, Part 2, p 221-230.
- Huebscher, R.G. 1948. Friction Equivalents for Round, Square and Rectangular Ducts, ASHVE Transactions (renamed ASHRAE Transactions), Vol. 54, pp 101-144.
- Jorgensen, R. 1983. Fan Engineering, Buffalo Forge Co., Buffalo, NY.
- Klote, J.H. Fire Experiments of Zoned Smoke Control at the Plaza Hotel in Washington DC, ASHRAE Transactions, Vol. 96, Part 2, 1990, pp 399-416.
- Klote, J.K. and Milke, J.A. 1992. Design of Smoke Management Systems, American Society of Heating, Refrigerating and Air-conditioning Engineers, Atlanta, GA.
- Moody, L.F. 1944. Friction Factors for Pipe Flow, Transactions of ASME, Vol 66, p 671-684.
- Murdock, J.W. 1978. Mechanics of Fluids, Marks' Standard Handbook for Mechanical Engineers, 8th ed., Baumeister, et al. editors, McGraw, New York, NY.
- Schlichting, H. 1960. Boundary Layer Theory, 4th ed., Kestin, J. Translator, McGraw, New York, NY.

A.11 Nomenclature

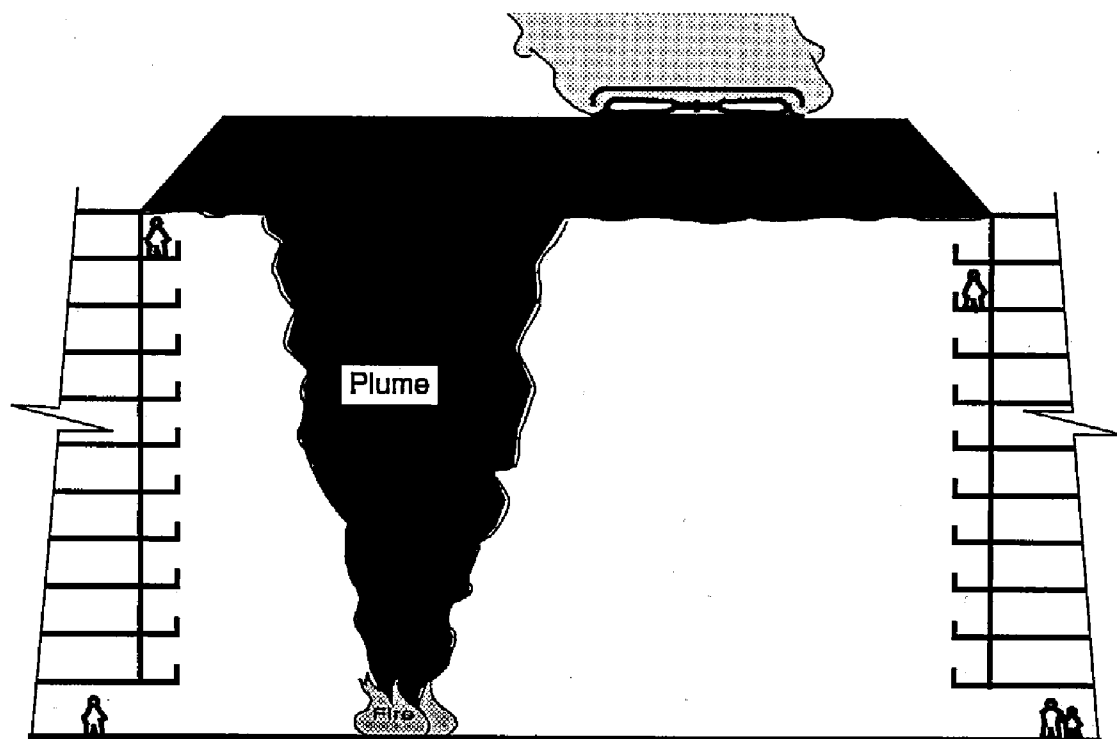
A	area
C	local loss coefficient
D_e	effective diameter
f	friction factor
g	gravitational acceleration
K	square of duct resistance
\dot{m}	mass flow rate
p	pressure
\dot{V}	volumetric flow rate
R	duct resistance
T	temperature
U	average velocity

Z elevation
 Δp pressure loss
 ϵ roughness of interior duct walls
 ρ density
 Subscripts

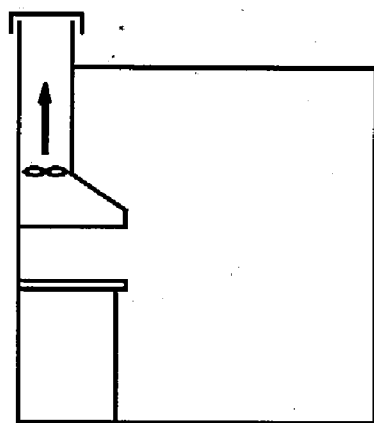
b section b
 c section c
 e effective
 f fan
 fr friction
 o section o
 s section s

Table 1. Absolute Roughness Values

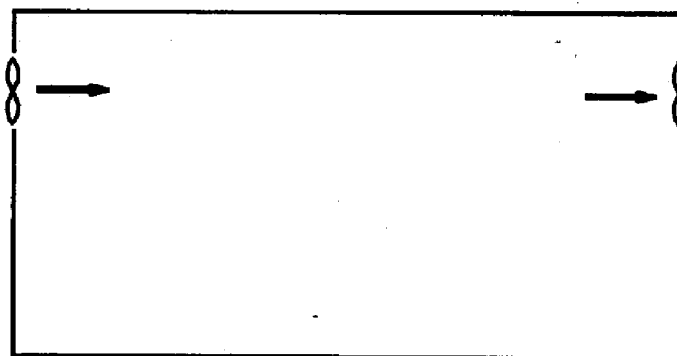
Duct Material	Roughness Category	Absolute Roughness, ϵ	
		mm	ft
Uncoated Carbon Steel, Clean. PVC Plastic Pipe. Aluminum.	Smooth	0.03	0.0001
Galvanized Steel, Longitudinal Seams, 1200 mm Joints. Galvanized Steel, Continuously Rolled, Spiral Seams, 3000 mm Joints. Galvanized Steel, Spiral Seam with 1, 2 and 3 Ribs, 3600 mm Joints.	Medium Smooth	0.09	0.0003
Galvanized Steel, Longitudinal Seams, 760 mm Joints.	Average	0.15	0.0005
Fibrous Glass Duct, Rigid. Fibrous Glass Duct Liner, Air Side With Facing Material.	Medium Rough	0.9	0.003
Fibrous Glass Duct Liner, Air Side Spray Coated. Flexible Duct, Metallic. Flexible Duct, All Types of Fabric and Wire. Concrete.	Rough	3.0	0.01



(a) Atrium Smoke Management

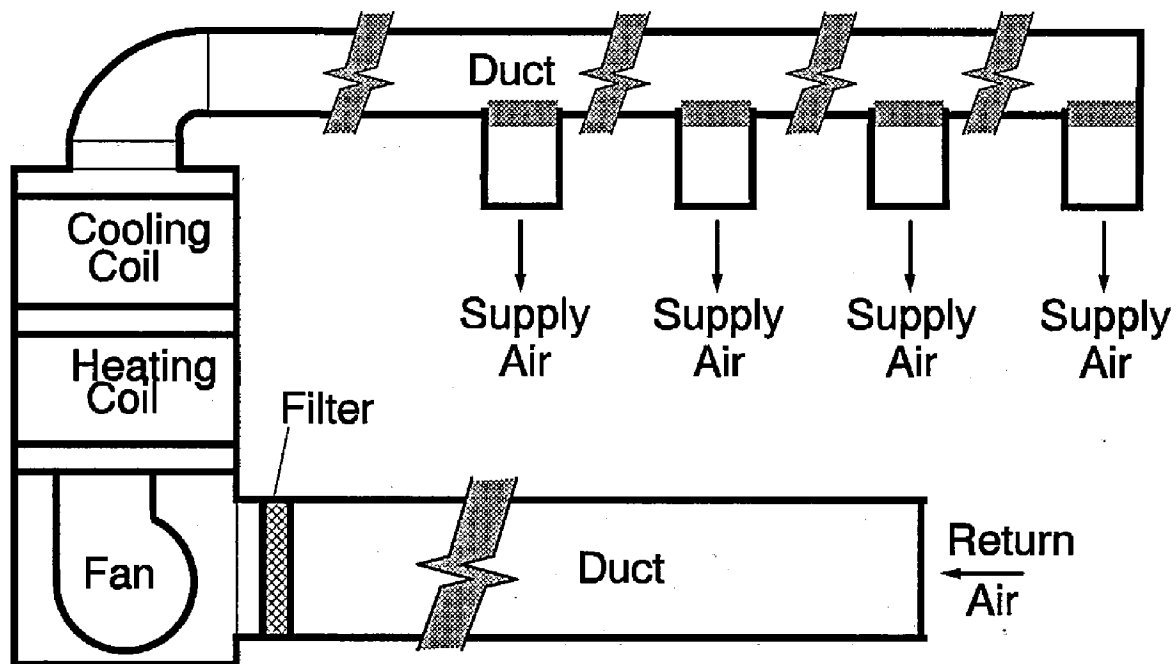


(b) Kitchen Exhaust

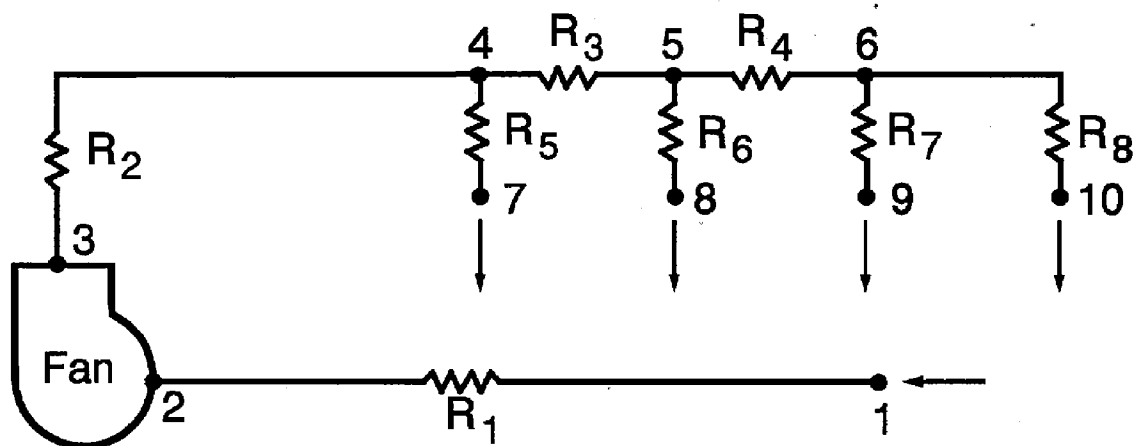


(c) Space With Cross Ventilation

Figure 1. Some simple fan-duct systems



(a) Residential Air Conditioning System



(b) Network Representation of the System Above

Figure 2. Diagram and network representation of a residential system

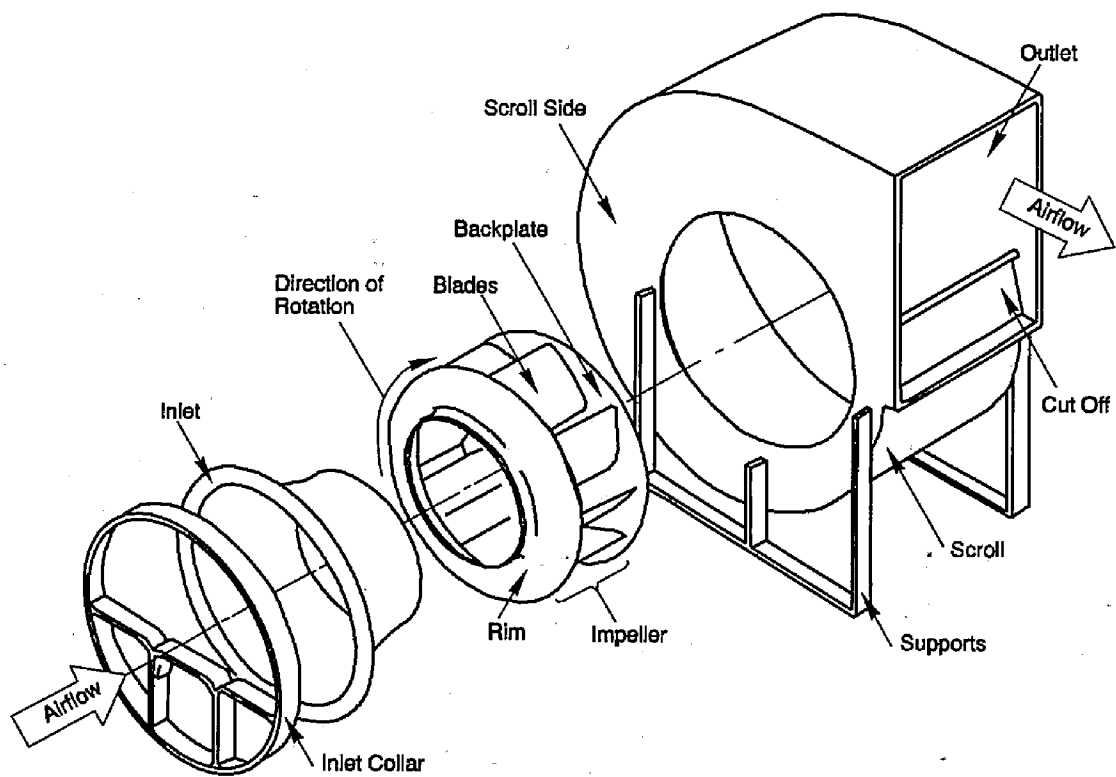


Figure 3. Centrifugal fan components

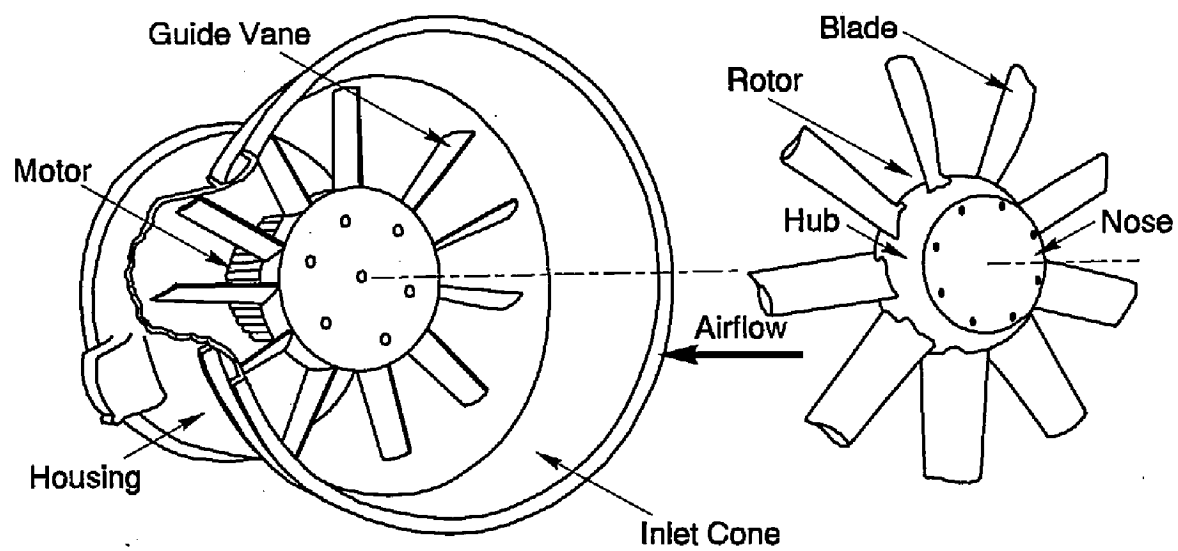


Figure 4. Axial fan components

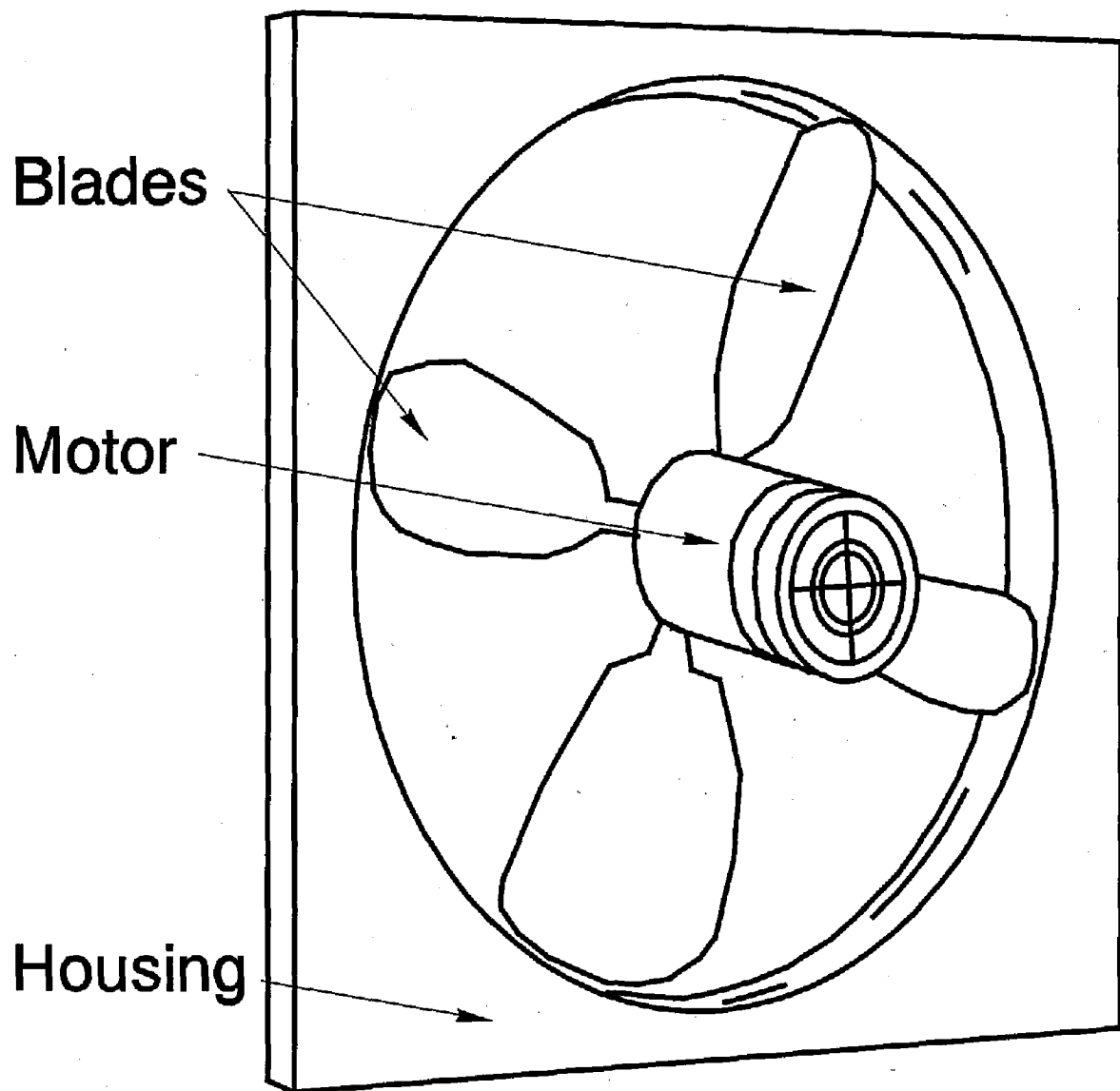


Figure 5. Propeller wall fan

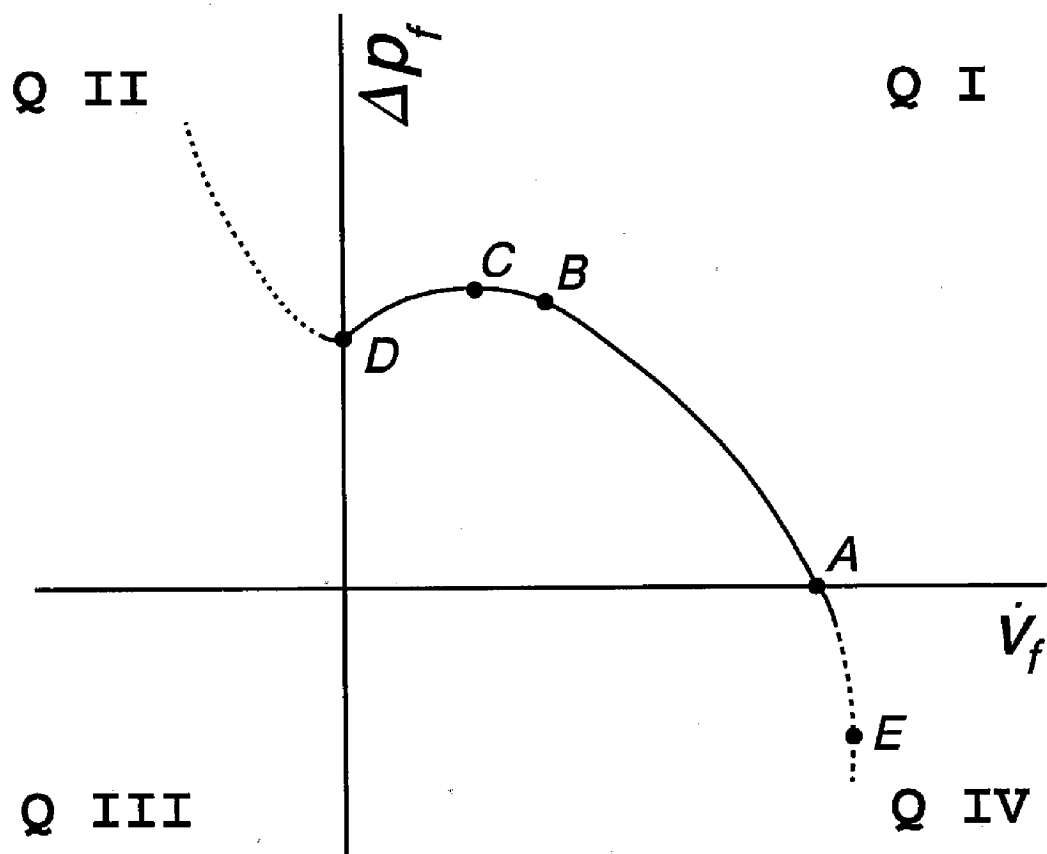


Figure 6. Typical fan performance at constant fan speed

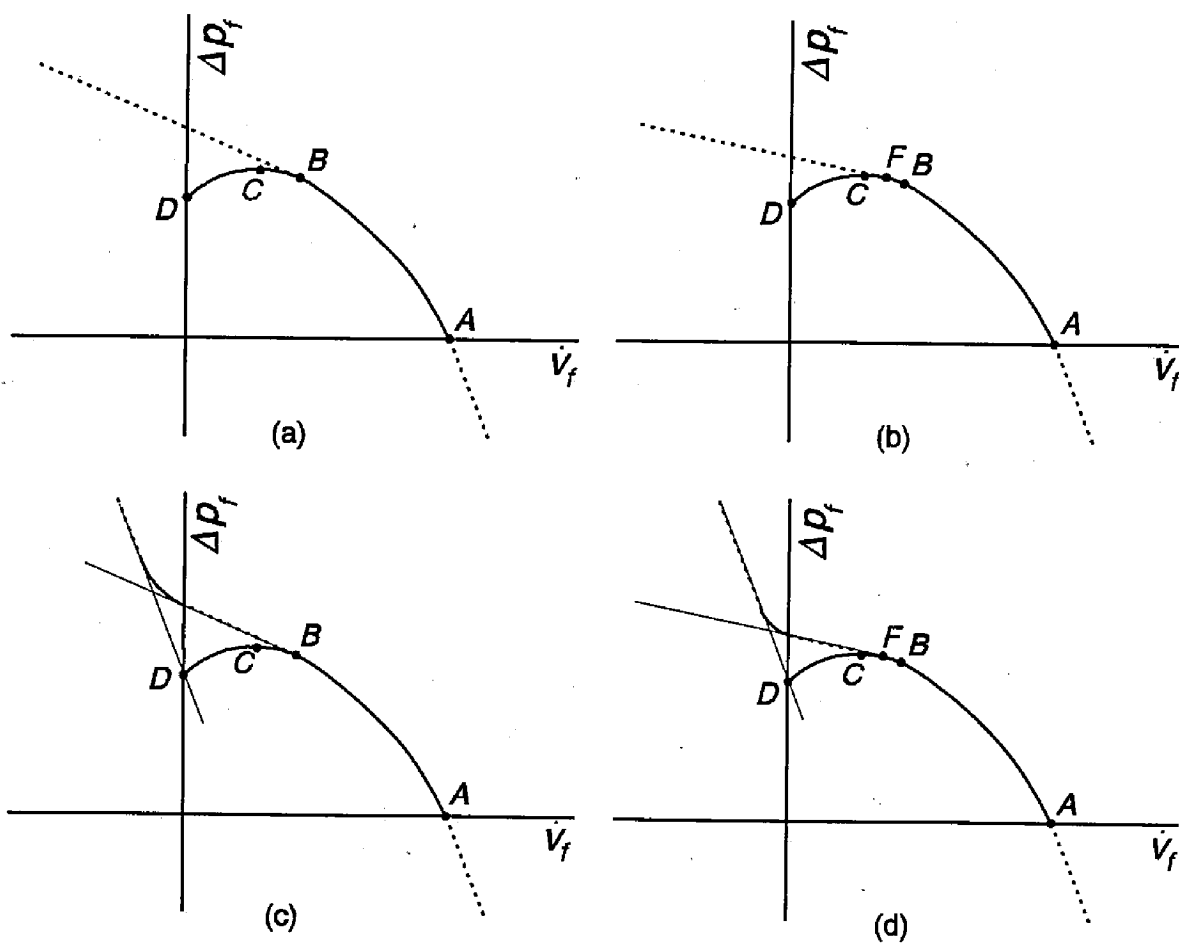


Figure 7. Some approaches to approximation of fan performance for computer simulation

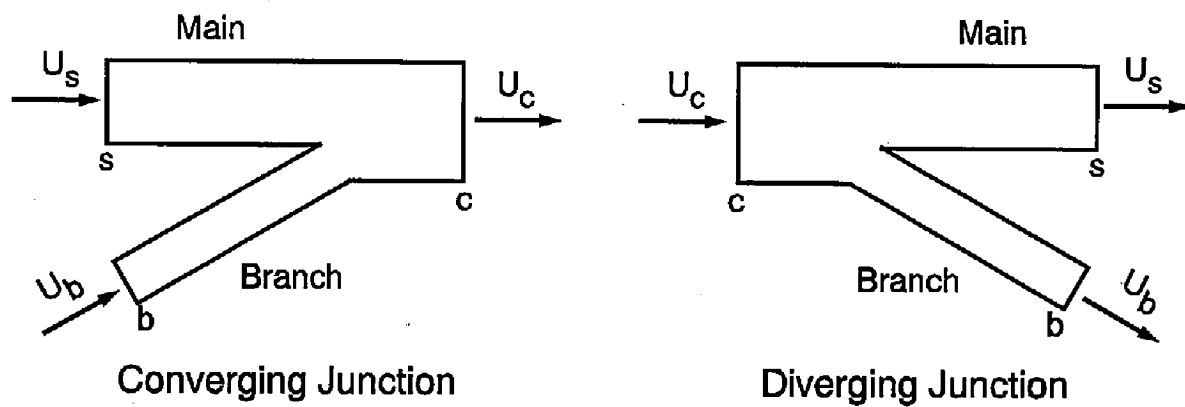


Figure 8. Diagrams of converging and diverging junctions

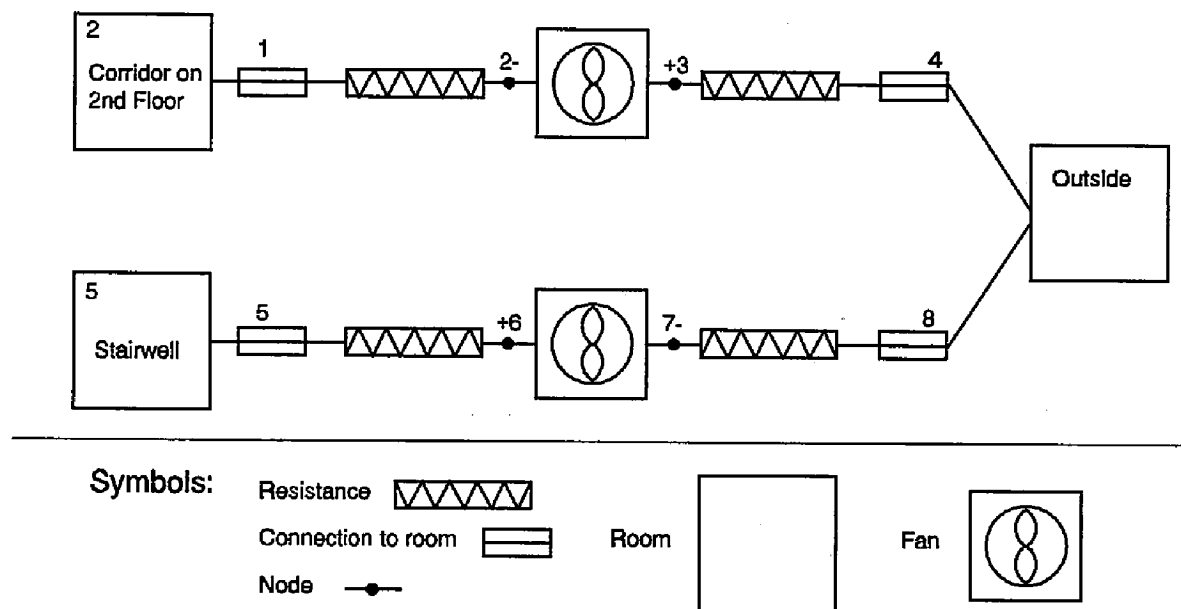


Figure 9. Example fan-duct systems used for simulation of forced flows of the Plaza Hotel smoke control tests

Appendix B: Thermal Properties

Thermal data is read from a file which is in an ASCII format. The default name is THERMAL.DAT. The distributed configuration file (HV1.CF) renames this to THERMAL.DF. An alternative can be used by changing the default with the routine CF_Set, or by using the key word THRMF in the data file that is passed to CFAST.

The relationship is by the name used in specifying the boundary. Any name can be used so long as it is in the thermal database. If a name is used which is not in the database, then CEdit will turn off the conduction calculation, and CFAST will stop with an appropriate error message. The form of an entry in the database is:

material conductivity specific heat density thickness emissivity

and the units are:

material	1 to 8 alphanumeric characters
conductivity	Watts/meter/Kelvin
specific heat	Joules/kilogram/Kelvin
density	kilograms/cubic meter
thickness	meters
emissivity	dimensionless.

The default database that comes with CFAST (THERMAL.DF) includes

Material	Thermal Cond	Specific Heat	Density	Thickness	Emissivity	Description
GYPSUM	0.16	900	790	0.016	0.90	Gypsum Board (5/8")
GYP1/2	0.16	900	790	0.013	0.90	Gypsum Board (1/2")
GYP3/4	0.16	900	790	0.019	0.90	Gypsum Board (3/4")
GYPX5/8	0.14	900	770	0.016	0.90	Type X Gyp (5/8")
GYPPLAST	0.22	1085	1680	0.076	0.90	Type X Gyp (3")
BRICK	1.50	960	2645	0.076	0.90	Clay Brick (3")
FIREBRICK	0.36	750	1040	0.113	0.80	
COMBRICK	0.72	835	1920	0.076	0.90	Common brick (3")
CONCRETE	1.75	1000	2200	0.15	0.94	Concrete, Normal Weight (6")
CEMENTMO	0.72	780	1860	0.025	0.90	Cement mortar (1")
GLASS	1.40	750	2500	0.006	0.10	Plate Glass (1/4")
ALUML/8	231	1033	2702	0.003	0.90	Pure aluminum (1/8")
ALUM2064	186	1042	2770	0.003	0.90	Aluminum alloy 2024-T6 (1/8")
STEEL1/8	48.0	559	7854	0.003	0.90	Plain carbon steel (1/8")
STEELSHT	48.0	559	7854	0.0015	0.90	Plain carbon steel (1/16")
STAIN304	19.8	557	7900	0.003	0.90	304 stainless steel (1/8")
PLYWOOD	0.12	1215	545	0.013	0.90	Plywood building board (1/2")
SHEATHNG	0.055	1300	290	0.013	0.90	Sheathing, regular density (1/2")
ACOUTILE	0.058	1340	290	0.003	0.90	Acoustic tile (1/8")
HARDBDSD	0.094	1170	640	0.013	0.90	Hardboard, siding (1/2")
HARDBDHD	0.15	1380	1010	0.013	0.90	Hardboard, high density (1/2")
PARTBDLD	0.078	1300	590	0.013	0.90	Particle board, low density (1/2")
PARTBDHD	0.170	1300	1000	0.013	0.90	Particle board, high density (1/2")
HARDWOOD	0.16	1255	720	0.019	0.90	Hardwoods (oak, maple) (3/4")
SOFTWOOD	0.12	1380	510	0.019	0.90	Softwoods (fir, pine) (3/4")
WOODSHCM	0.087	1590	350	0.013	0.90	Wood board, shredded/cemented (1/2")
KAGWOOL	0.22	1047	128	0.116	0.97	Mineral fiber insulation
GLASFIBR	0.04	720	105	0.088	0.90	Glass Fiber Insul (3-1/2")
GLASSFB2	0.038	835	32	0.013	0.90	Glass fiber, coated; duct liner (1/2")
GLASSFB3	0.036	795	105	0.013	0.90	Glass fiber, organic bonded (1/2")
GLASSFB4	0.043	835	16	0.013	0.90	Glass fiber, poured or blown (1/2")

VERMICUL	0.068	835	80	0.006	0.90	Vermiculite, flakes (1/4")
URETHANE	0.026	1045	70	0.013	0.90	Urethane insulation, rigid foam (1/2")

The output listing of CFAST, and the thermal database screen for CEdit show a table of "codes." The code is an eight character string whose fields are:

- 1-3 number of nodes if it exceeds 'NN' which is currently 48 (36 for the PC version)
- 4 always blank
- 5 too many slabs - greater than mxslb (S)
- 6 inconsistent number of slabs - all properties must have the same number of slabs (I)
- 7 duplicate names - the first in the list is used (D)
- 8 used in the present calculation (U)

All of the examples shown above represent single layer partitions. The model, however, will handle up to three layers, or slabs, per partition. To specify multiple layers, each property is given one, two or three values separated by slashes. It is important that this be consistent across the whole entry, otherwise CFAST will have an ambiguous situation. The ambiguity is resolved by using the lowest number of layers.

The layers are numbered from the inside to outside. That is, the first material property represents the material on the compartment interior, and the last property is on the outside. There are several examples of this format in the THERMAL.DF file included in this distribution. One example is:

FC1_L003 .15/.03/.22 1500./1042./1047. 790./1.2/128. .016/.24/.019 .9

Since the emissivity applies only to the interior surface, it will always have only a single entry. Other values are ignored. This example represents a three layer assembly taken from Underwriters Laboratory(UL) "Fire Resistance Directory." The code stands for Floor Combustible 1 Hour, and L003 is assigned by UL.

Finally, the HCl coefficients are included for each entry in THERMAL.DF since they pertain to surface effects, and the current algorithm uses a similarity solution for the heat and mass transfer. There are seven coefficients for the HCl absorption. If the first two are zero, the others are not used even though they must be present. These coefficients have only been measured for a few materials. The most commonly used material is:

GYPSUM [0.16 900. 790. 0.016 0.90] 0.0063 191.8 0.0587 7476. 193 1.021 0.431

The numbers in brackets are shown above as the normal properties.

Appendix C: Objects Database

OBJECTS.DF is the database of objects used by CFAST and CEdit. The distributed configuration file (HV1.CF) provides the default name. An alternative is available by changing the default with the routine CF_Set, or for individual data files by using the key word OBJFL.

OBJECTS.DF has a special format to allow both CFAST and CEdit to access the information as quickly as possible. For that reason, a second file, OBJECTS.ORG, has been created. OBJECTS.ORG is designed so that it can be edited with any ASCII text editor. When an entry in OBJECTS.ORG is added or changed, the routine OBJ2DF should be used to convert OBJECTS.ORG to OBJECTS.DF. Failure to do this will prevent CFAST and CEdit from recognizing the changes.

The format of an object entry in OBJECTS.ORG is listed below along with the CFAST variables to which the data is assigned. Each section will first specify the format of that line for the Ith object in the data file using the CFAST variable names. The variables are then listed individually with the appropriate dimensions and units as well as a brief description. The OBJECT key word on line 1 is required in the OBJECTS.ORG file in order to generate an accurate OBJECTS.DF. Note that the default values for flux for ignition and surface temperature for ignition are infinity and the ambient respectively.

```
line 1) OBJECT OBJNAM
        OBJNAM(NUMOBJL) = Name of object (up to 8 characters)

line 2) OBJTYP OBJCRI(2,I) OBJCRI(3,I) OBJMAS OBJGMW OBJVT OBJHC
        OBJTYP(NUMOBJL) = Object type
            1 unconstrained burn
            2 constrained burn
            3 flame spread model (not yet implemented)
            4 pool fire (not yet implemented)
        OBJCRI(2,NUMOBJL) = Flux for ignition (w/m2)
        OBJCRI(3,NUMOBJL) = Surface temperature for ignition (k)
        OBJMAS(NUMOBJL) = Total mass (kg)
        OBJGMW(NUMOBJL) = Gram molecular weight
        OBJVT(NUMOBJL) = Volatilization temperature (k)
        OBJHC(NUMOBJL) = Heat of combustion (J/kg)

line 3) OBJXYZ(1,I) OBJXYZ(2,I) OBJXYZ(3,I) OBJORT(1,I) OBJORT(2,I) OBJORT(3,I)
IOPPOS PNLDS
        OBJXYZ(1,NUMOBJL) = Panel length (m)
        OBJXYZ(2,NUMOBJL) = Panel height or width (m)
        OBJXYZ(3,NUMOBJL) = Panel thickness (m)
        OBJXYZ(4,NUMOBJL) = Surface area of panel element (m2)
        OBJORT(1,NUMOBJL) = Orientation angle PHI
        OBJORT(2,NUMOBJL) = Orientation angle THETA
        OBJORT(3,NUMOBJL) = Orientation angle PSI
        IOPPOS = Double sided panel flag (0 or 1)
        PNLDS = Distance between sides of a panel (m)

line 4) Second panel (ignored for now)

line 5) Third panel (ignored for now)

line 6) Fourth panel (ignored for now)

line 7) OTIME(1,I) to OTIME(TOTJ,I)
        OTIME(NV,NUMOBJL) = Time history (sec)
```

Each OTIME(J,I) represents a point on the objects burn timeline where the variables below are defined exactly. CFAST will interpolate values between any two points. TOTJ is the total number of points on the specified timeline. CFAST automatically assigns an initial time zero for the objects timeline so that there will always be one fewer specified value for the timeline than for the history variables below.

The following lines are the histories for the individual parameters at each of the OTIME points.

```

line 8) OMASS(1,I) to OMASS(TOTJ+1,I)
        OMASS(NV,NUMOBJL) = Pyrolysis rate time history (kg/sec)

line 9) OQDOT(1,I) to OQDOT(TOTJ,I)
        OQDOT(NV,NUMOBJL) = Rate of heat release time history (w)

line10) OAREA(1,I) to OAREA(TOTJ,I)
        OAREA(NV,NUMOBJL) = Area of fire time history (m2)

line11) OHIGH(1,I) to OHIGH(TOTJ,I)
        OHIGH(NV,NUMOBJL) = Height of flame time history (m)

line12) OCO(NV,NUMOBJL) = CO/CO2 time history

line13) OOD(NV,NUMOBJL) = OD or soot time history

line14) OHCR(NV,NUMOBJL) = H/C time history

line15) OOC(1,I) to OOC(TOTJ,I)
        OOC(NV,NUMOBJL) = O/C time history

line16) OMPRODR(1,10,I) to OMPRODR(TOTJ,10,I)
        OMPRODR(NV,10,NUMOBJL) = CT time history

line17) OMPRODR(1,5,I) to OMPRODR(TOTJ,5,I)
        OMPRODR(NV,5,NUMOBJL) = HCN time history

line18) OMPRODR(1,6,I) to OMPRODR(TOTJ,6,I)
        OMPRODR(NV,6,NUMOBJL) = HCl time history

```

Appendix D: Graphics Displays

Card Type	Resolution	Driver	Mode	ID
AST VGA Plus	800x600	AHDPARP	0	PP0
ATI VGA Wonder	800x600	AHDATIP	0	AP0
Everex Viewpoint VGA	800x600 1024x768	AHDEVGP	3 4	EP3 EP4
Genoa 6000 Series VGA	800x600 1024x768	AHDGVGP	1 2	VP1 VP2
Headland/Video-7 VRAM VGA	752x410 720x540 800x600 1024x768	AHDV7VP	0 1 2 3	7P0 7P1 7P2 7P3
Headland/Video-7 VGA 1024i	752x410 720x540 800x600 1024x768	AHDV7VP	0 1 2 3	7P0 7P1 7P2 7P3
IBM EGA	640x350	AHDIBME	2	IE2
IBM Personal System/2 VGA	640x480	AHDIBMV	3	IV3
Orchid Technology Designer VGA or Designer 800	800x600 1024x768	AHDVLIN	2 3	LN2 LN3
Paradise VGA Professional	800x600	AHDPARP	0	PP0
Prism Elan, Elite, or Eclipse VGA	720x540 800x600 1024x768	AHDPSMP	2 3 4	SP2 SP3 SP4
STB VGA Extra/EM	800x600 1024x768	AHDVPLN	2 3	PN2 PN3
Tecmar VGA A/D	800x440 800x600 1024x768	AHDTRIP	1 2 3	TP1 TP2 TP3
Trident TVGA 8900	800x600 1024x768	AHDTRIP	0 1	TP0 TP1
Tseng Labs ET-3000 Extended VGA	800x600 1024x768	AHDVPLN	2 3	PN2 PN3
Tseng Labs ET-4000 Extended VGA	800x600 1024x768	AHDTL4L	2 3	4L2 4L3